UNIVERSITY OF CALIFORNIA
SANTA CRUZ

ANTARCTIC EUPHAUSIIDS IN SPACE AND TIME: BEHAVIOR, DISTRIBUTION, AND GROWTH, WITH IMPLICATIONS FOR PREDATORS

A dissertation submitted in partial satisfaction
of the requirements for the degree of

DOCTOR OF PHILOSOPHY

in

ECOLOGY AND EVOLUTIONARY BIOLOGY

by

Kate E. Richerson

September 2015

The Dissertation of Kate E. Richerson is approved:

Professor Marc Mangel, Chair

Professor Donald Croll

Professor Bruce Lyon

Tyrus Miller
Vice Provost and Dean of Graduate Studies

Table of Contents

List of Figures

List of Tables

Abstract

Kate E. Richerson

Antarctic euphausiids in space and time: behavior, distribution, and growth, with implications for predators

Euphausiids, particularly the Antarctic krill *Euphausia superba,* are a crucial part of the Southern Ocean ecosystem. As the major link between primary production and higher trophic levels, variation in euphausiid abundance has important implications for predators, nutrient cycling, and ecosystem functioning. Climate variability influences euphausiids through multiple pathways, including direct effects on growth and indirect effects on primary production. Increasing ocean temperatures, declining sea ice, and other effects of climate change are likely to negatively affect *E. superba.* In contrast, little is known about the potential impacts of climate change on *Thysanoessa macrura*, a euphausiid with an abundance that likely rivals that of *E. superba.* In this thesis, I explore multiple aspects underlying the spatial and temporal variability of Antarctic euphausiids. In Chapter 2, I use state-dependent life history theory and stochastic dynamic programming to challenge the traditional paradigm of *E. superba* as a passive drifter, and find that accounting for active behavior in this species has important implications for spatial distribution, growth, and survival. In Chapter 3, I use a data-driven approach to quantifying spatial and temporal *E. superba* abundances near the North Antarctic Peninsula. I find that fluctuations in

abundance are tied to lagged indices of climate variability, and that abundance and measures of spatial aggregation are linked in some habitats and seasons. Finally, in Chapter 4, I use temperature-dependent growth models to explore how changing temperatures may differentially affect growth in *E. superba* and *T. macrura.* I find that as ocean temperatures increase, the biomass per recruit of the stenothermic *E. superba* is likely to decline over much of the temperature range in the Southwest Atlantic. In contrast, the eurythermic *T. macrura* is expected to have enhanced growth over much of this range, and increases in *T. macrura* biomass could potentially compensate for some loss of *E. superba* biomass. However, this biomass may not be energetically equivalent from the perspective of a euphausiid predator.

Acknowledgements

Many thanks to my advisor, Dr. Marc Mangel for his invaluable support, expertise, and mentorship.

Thank you to my committee, Drs. Don Croll and Bruce Lyon. Your knowledge, help and guidance was very appreciated.

I am indebted to the United States Antarctic Marine Living Resources Program, especially Drs. George Watters and Christian Reiss, for providing me with data, information, resources, and an opportunity to experience the Southern Ocean first-hand.

Thank you to Dr. Jarrod Santora for his guidance and collaboration, and for sharing his expertise on all things Antarctic.

Thank you to the Mangel lab members, past and present, for being an inspiring, brilliant, and supportive group of scientists. Special thanks to Valerie Brown, Daniel Hively, and Juan Lopez for sharing their mathematical expertise, and Ryan Driscoll for his euphausiid knowledge.

Many thanks to the Raimondi-Carr lab for letting me use their equipment and laboratory space.

I am very grateful to the National Science Foundation and the Center for Stock Assessment and Research at UC Santa Cruz for funding.

Thank you to my friends and family for their continued support, encouragement, and love.

Chapter 1. Introduction

The Southern Ocean

With an area of ~34.8 million km^2, the Southern Ocean is perhaps the largest marine ecosystem on earth (Knox 2006, Griffiths 2010). The Antarctic Treaty defines the Southern Ocean as the waters surrounding the Antarctic continent as far north as 60°S. A more biologically meaningful definition, however, is the ocean between the continent and the Polar Front (PF), which is the strongest of three eastward-flowing jets in the Antarctic Circumpolar Current (ACC; Fig. 1.1). The PF forms a barrier between north-south water movement and is therefore thought to delineate the Antarctic biogeographic region (Clarke et al. 2005). Within the ACC, the sub-Antarctic Front lies north of the PF and the Southern Antarctic Circumpolar Front south, each separating distinct water masses (Orsi et al. 1995). The ACC, driven by westerly winds, is the strongest current in the world and is unique in that it flows in a complete circle, unbroken by large landmasses and connecting the Pacific, Atlantic, and Indian Ocean basins. Closer to the Antarctic Continent, easterly winds drive the westward-flowing Antarctic Coastal Current, which forms a series of large clockwise gyres, most notably in the Ross Sea and Weddell Sea (Knox 2006).

The importance of euphausiids

There are 86 species of pelagic crustaceans in the family Euphausiidae distributed across oceans worldwide. In the Southern Ocean, six species live south of the Polar Front: *Euphausia crystallorophias, Euphausia frigida, Euphausia superba, Euphausia triacantha, Thysanoessa macrura,* and *Thysanoessa vicina* (Cuzin-Roudy et al. 2014). All are consumed by vertebrate predators, forming an important link between primary productivity and higher trophic levels. However, as the primary prey source of many fish, squid, seabirds, and marine mammals, *E. superba* (the "superb krill") is generally considered to be the most important (Smetacek and Nicol 2005). *E. superba* is relatively large (up to 6 cm) and long-lived (up to 7 years), with a circumpolar distribution that is concentrated mainly in the Southwest Atlantic region (Atkinson et al. 2008). This species forms swarms that can be as dense as 1000 individuals/m^3 and span several kilometers (Miller and Hampton 1989), and is one of the most abundant species on earth, with biomass estimated at 379 million tons (Atkinson et al. 2009). The life cycle of this species is closely tied to sea ice (Wiedenmann et al. 2009), and declining densities in the Southwest Atlantic have been correlated with declining sea ice around the Antarctic Peninsula (Atkinson et al. 2004).

In contrast to *E. superba*, the omnivorous *T. macrura* depends less on phytoplankton and is not associated with sea ice habitat (Kattner et al. 1996, Hagen et

al. 2001, Flores et al. 2012b). This species is the most abundant and widespread euphausiid in the Southern Ocean, outnumbering *E. superba* in many locations. For example, near the North Antarctic Peninsula, long-term (1992-2009) data show mean *T. macrura* densities being 2-3 times higher than mean *E. superba* densities across the summer season (Loeb and Santora 2015). Though it reaches a smaller adult size (~40 mm; Haraldsson and Siegel 2014), *T. macrura* is an important component in some predator diets (Nemoto and Nasu 1958, Kock et al. 1994, Deagle et al. 2007), and some have suggested that the trophic importance of this species may be underappreciated (Nordhausen 1992). With the widest latitudinal and thermal ranges of all Southern Ocean euphausiids (Cuzin-Roudy et al. 2014), this eurythermic species may be better able to tolerate warming sea temperatures than more stenothermic species like *E. superba* (Driscoll 2013).

Seasonality and climate cycles

The Southern Ocean system is characterized by strong seasonality in sea ice cover, with maximum coverage in late winter (September-October), minimum cover in late summer (February-March), and rapid formation and retreat in fall and spring, respectively. Across the year, total sea ice cover may vary by a factor of 5, from $20x10^6$ km^2 in late winter to about $4x10^6$ km^2 in late summer (Zwally et al. 1983). Both the extent and temporal dynamics of sea ice are important in structuring the ecosystem through multiple pathways, including light availability, temperature regulation, habitat, and nutrient availability (Eicken 1993). Though the Southern

Ocean is generally considered to be a high-nutrient, low-chlorophyll system (Martin et al. 1990), sea ice dynamics contribute to the strong seasonality of primary production, with large phytoplankton blooms typically following the retreat of sea ice in the spring and summer. This is attributed to increased stability and reduced depth of the mixed layer associated with the ice edge, creating a high-irradiance stable environment conducive to phytoplankton growth (Smith and Nelson 1985). In addition, melting sea ice may enhance blooms by releasing iron and other nutrients into the water column (Sedwick and DiTullio 1997). Productivity is particularly high on the continental shelf, in polynyas, and/or near coastlines, islands, and ice edges, while the open ocean tends to have lower productivity (Smith and Nelson 1985, Moore and Abbott 2000, Arrigo and van Dijken 2003). The structure of the Southern Ocean food web has traditionally been considered relatively simple, with diatoms sustaining large populations of macrozooplankton (particularly euphausiids), which are then consumed by vertebrate predators (e.g. El-Sayid 1978, but see Ducklow et al. 2006). Thus, the spring and summer blooms are important determinants of the success of primary consumers, and consequently, the success of organisms at higher trophic levels (e.g. Marrari et al. 2008).

Sea ice dynamics in many parts of the Southern Ocean are tied to the El Niño-Southern Oscillation (ENSO) and, to a lesser extent, the Southern Annular Mode (Stammerjohn et al. 2008b). Sea ice and ENSO dynamics have been linked to population-level changes in a variety of species, including seabirds (Croxall et al. 1988, Chastel et al. 1993), penguins (Forcada et al. 2006) and fur seals (Croxall et al.

1988, Forcada et al. 2005). Some of these responses are linked to ENSO-driven changes in prey populations, particularly the Antarctic krill *E. superba.* ENSO influences sea ice duration and extent as well as sea surface temperature, which modulate the timing and magnitude of phytoplankton and algae availability, thus driving variability in Antarctic krill populations (Siegel and Loeb 1995, Quetin et al. 1996, Quetin and Ross 2001, Atkinson et al. 2004, Loeb et al. 2009a, Wiedenmann et al. 2009). In addition, the larvae and juveniles of *E. superba* are ice-associated, suggesting that sea ice may form important habitat for this species (Flores et al. 2012b). Fluctuations in prey availability are tied to variation in reproductive success in vertebrate predators such as seals, penguins, and seabirds (Croxall et al. 1999, Reid and Croxall 2001). Thus, the interaction of seasonality and climate cycles have profound influences on the Southern Ocean food web.

Climate change

Climate change, along with other anthropogenic stressors such as exploitation, habitat destruction, and pollution act on marine ecosystems in complex ways (Crain et al. 2008). These changes have implications for ecosystem structure, function, and services. Anthropogenic climate change has been affecting the Southern Ocean for at least the past several decades (reviewed in Constable et al. 2014). Reductions in stratospheric ozone have been linked to altered wind patterns, resulting in shifts in circulation, increased eddy kinetic energy, and changes in sea ice (Marshall et al. 2006, Stammerjohn et al. 2008b, Thompson et al. 2011). Ocean waters have been

warming (Turner et al. 2009, Schmidtko et al. 2014), freshening (Rintoul 2007, Hellmer et al. 2011), and acidifying (Orr et al. 2005). Increases in sea surface temperature have been particularly apparent in the Southwest Atlantic, with an increase of ~1.3 ºC around the Antarctic Peninsula since the 1950s (Meredith and King 2005) and ~2.3ºC around South Georgia since the 1920s (Whitehouse et al. 2008a). There has been a recent net total increase in sea ice across the Southern Ocean driven by increasing sea ice duration and extent in the Ross Sea (Parkinson and Cavalieri 2012). However, sea ice is declining rapidly around the Antarctic Peninsula, and total sea ice extent is projected to decrease by a third over the twenty-first century (Bracegirdle et al. 2008). Reductions in sea ice extent and duration have been implicated in a multidecadal decline in *E. superba* concentrations in the Southwest Atlantic (Atkinson et al. 2004). Warming temperatures are likely to reduce the growth habitat in this area (Hill et al. 2013), and acidification is projected to negatively affect krill reproduction across broad swaths of the Southern Ocean (Kawaguchi et al. 2013).

History of exploitation

In spite of its image in the popular consciousness as a pristine wilderness virtually untouched by humans, the Southern Ocean ecosystem bears the fingerprint of both historic and contemporary anthropogenic forces. Serious exploitation began in the early 1800s with the harvest of fur seals (*Arctocephalus gazella*), leading to near-extinction in South Georgia and the South Shetland archipelago within a few decades

(Hucke-Gaete et al. 2004, Mori and Butterworth 2006). Whaling soon followed, beginning around 1900 and leading to the sequential depletion of Antarctic blue (*Balaenoptera musculus*), fin (*Balaenoptera physalus*), sperm (*Physter macrocephalus*), humpback (*Megaptera novaengliae*), and sei whales (*Balaenoptera borealis*) (Mori and Butterworth 2006). Many of these species were hunted to near-extinction; for example, Antarctic blue whales were reduced to 0.5% of their pre-exploitation population by the beginning of World War II (Branch et al. 2004). Whaling on some species continued until the 1970s, but today some populations appear to be increasing (Branch et al. 2004). Commercial harvest of finfish began in the 1960s, leading to the depletion of several species including marbled rockcod (*Notothenia rossii*), mackerel icefish (*Champsocephalus gunnari*), grey rockcod (*Lepidonotothen squamifrons*) and humped rockcod (*Gobionotothen gibberifrons*) (Ainley and Pauly 2014). Some of these stocks are slowly recovering (Marschoff et al. 2012); however, concerns remain over the health of other stocks such as the Antarctic toothfish (*Dissostichus mawsoni*) and Patagonian toothfish (*Dissostichus eleginoides*) (Ainley et al. 2012).

The fishery for *E. superba* was established in the 1970s and is currently the largest by tonnage in the Southern Ocean (Ichii and Everson 2000, Dietrich et al. 2011). Harvest peaked in the 1980s, but catches have been steadily increasing over the past decade, and there is predicted that increased demand for krill products, such as nutritional supplements and aquaculture feed, along with new harvesting technologies will lead to increased harvests (Nicol et al. 2000, Nicol and Foster

2003). Fishing may compound the effects of climate change on *E. superba* populations and their predators; for example, Trivelpiece et al. (2011) implicated the combined effects of harvest and warming in the declines of two krill predators, the Adélie penguin (*Pygoscelis adeliae*) and chinstrap penguin (*Pygoscelis antarctica*).

Current management of Southern Ocean fisheries

Except for seals and whales, all harvested species in the Southern Ocean are managed by the Commission for the Conservation of Antarctic Marine Living Resources (CCAMLR). CCAMLR was established by a 1980 international treaty known as the Convention on the Conservation of Antarctic Marine Living Resources and manages the fisheries for Patagonian toothfish, Antarctic toothfish, mackerel icefish, and Antarctic krill. The Convention entered into force in 1982 following the depletion of a number Southern Ocean species and was motivated in part by concerns over the impact that the krill harvest might have on the Antarctic ecosystem, particularly krill-dependent predators. CCAMLR is unique in that its convention was designed around Ecosystem-based Fishery Management (EBFM), rather than beginning with single-species management and attempting to make the transition to EBFM (Constable 2011). Under this precautionary, ecosystem-based approach, Article II of the Convention requires that 1) harvested populations should not fall below levels that ensure stable recruitments; 2) ecological relationships between harvested populations, predators, and other associated species must be maintained and depleted populations restored; and 3) the risk of ecosystem changes that are not

reversible on the scale of two to three decades should be minimized (CCAMLR 1982). The area managed by CCAMLR is currently divided into three broad statistical areas: Area 48 (the South Atlantic), with an annual krill catch limit of 4 million tons, Division 58.4.1 (southeast Indian Ocean), with an annual catch limit of 440,000 tons, and Division 58.4.2 (south-west Indian Ocean) with an annual catch limit of 450,000 million tons (Croxall and Nicol 2004). These catch limits are currently well below the estimated krill biomass in each area (44.3 million tones, 4.83 million tones, and 3.9 million tones, respectively); however, the fishery operates near the breeding grounds of many krill-dependent predators, leading to concerns that localized krill depletions could impact these populations (Hewitt et al. 2004). In response to such concerns, CCAMLR has defined fifteen Small Scale Management Units (SSMUs) in the Scotia Sea region, in order to facilitate management on a scale more relevant to land-based predators (Constable and Nicol 2002, Hewitt et al. 2004). Figure 1.2 shows the location of the SSMUs, all located within Area 48.

Multiple options have been proposed for the allocation of catch limits among the SSMUS, including limits based on 1) historical catches in the SSMU; 2) estimated predator demand in the SSMU; 3) the standing stock of krill in the SSMU; 4) standing stock minus predator demand in the SSMU; and 5) dynamic allocation based on predator surveys conducted each year before the fishing season (Hewitt et al. 2004). Several models are currently being used to weigh these options. Chief among them is the Krill Predator Fishery Model (KPFM; Watters et al. 2005, 2006, Hill et al. 2007, Watters et al. 2013), which models the interactions between krill, fishing, and

krill-dependent predators. In this model, the number of krill $K_{i,t}$ in SSMU i at time t is described by

$$K_{i,t} = K_{i,t-1}\exp\left(-Z_{i,t-1} - \sum_{j\neq i}\nu_{i\to j}\right) + \sum_{j\neq i}\left(K_{j,t-1}\frac{\nu_{j\to i}}{Z_{j,t-1}+\nu_{j\to i}}\left(1-\exp\left(-Z_{j,t-1}-\sum_{j\neq i}\nu_{j\to i}\right)\right)\right) + R_{i,t} \quad (1.1)$$

where Z represents total (fishing and natural) mortality, $\nu_{i\to j}$ represents the transport rate between SSMU i and j, and $R_{i,t}$ is the recruitment to the SSMU. Recruitment is given by a Beverton-Holt stock-recruitment relationship

$$R_{i,t} = \frac{\alpha_i K_{i,t-\rho}}{1+\beta_i\alpha_i K_{i,t-\rho}}\exp\left(\phi_i X_t + \varepsilon_t\right) \quad (1.2)$$

where ρ is a lag determined by the age at which krill recruit to the adult stock, α_i is maximum per-capita recruitment in SSMU i, β_i is a measure of density dependence, X_t is a time-varying environmental anomaly affecting all SSMUs that is modulated by the SSMU-specific scaling parameter ϕ_i, and ε_t is a normally-distributed time-varying error term.

In this thesis, I explore several aspects of euphausiid ecology that may be important to consider in the Krill Predator Fishery Model. In Chapter 2, I use state-dependent life-history theory to model *E. superba* movement and thus give higher fidelity to the movement rates $\nu_{i\to j}$ in Eqn 1.1. I find that active behavior can have important consequences for movement between SSMUs. Thus, as the movement rates between SSMUs in KPFM are based on passive drift, accounting for active behavior

may be an important missing component in this model. In Chapter 3, I explore the environmental effects on recruitment (the X_t). I find correlations between krill abundance around the North Antarctic Peninsula (NAP) and measures of ENSO influence. This indicates that including an index of the ENSO cycle in the recruitment anomaly for SSMUs in the NAP area is likely important and that the right hand side of Eqn 1.2 should likely be modified to include a lag at a possibly different time scale than ρ, in contrast to other areas where krill abundance is not linked to ENSO (Fielding et al. 2014, Saba et al. 2014). Finally, in Chapter 4, I explore how changing temperatures may alter the relative availability of *E. superba* and *T. macrura* to predators. I find that *T. macrura* has the potential to become an increasingly important prey in a warming ocean, indicating that other euphausiid species should be considered when modeling the availability of krill to predators. Thus, the $K_{i,t}$ described by KPFM could perhaps be better modeled as a multispecies measure of euphausiid abundance.

The Antarctic Peninsula

Much of the work in this thesis focuses on the *E. superba* population in the northern part of the West Antarctic Peninsula (WAP; Figure 1.3). The WAP ecosystem is particularly important for several reasons. First, as one of the fastest-warming places on the planet, the effects of climate change are especially apparent on this area and its biota, particularly *E. superba* (Atkinson et al. 2004). Second,

Antarctic krill recruited near the WAP are thought to sustain much of the large populations of krill found across the Scotia Sea and South Georgia (Siegel 1992, Thorpe et al. 2007). Third, the northern region in particular is home to large numbers of krill-dependent predators (Santora and Veit 2013) as well as a major krill fishing ground (Jones and Ramm 2004). It is also worth noting that *T. macrura* is abundant in this area, outnumbering *E. superba* by a factor of 2-3 on average (Loeb and Santora 2015). Thus, climate and euphausiid dynamics in this area have important implications for predators, fisheries, and the larger Southwest Atlantic ecosystem.

Aims

In this thesis, my goal was to expand on my interest and previous experience in policy-relevant science, particularly in fisheries and EBFM (e.g. Richerson et al. 2010, Reardon et al. 2013). To that end, I use a combination of modeling and data-driven approaches to explore aspects of euphausiid dynamics in the Southern Ocean, with emphasis on consequences for predators and management. In Chapter 1, I use state-dependent life history theory and stochastic dynamic programing to investigate the potential consequences of krill behavior on growth, mortality, and spatial distribution. In Chapter 2, I use a long-term acoustic data set to explore both inter- and intra-annual changes in Antarctic krill abundance and spatial distribution. I link these measures to lagged indices of ENSO influences. In Chapter 3, I develop a temperature-dependent model of *T. macrura* growth and contrast potential changes in biomass available to predators with that of *E. superba* in a warming ocean. I also

investigate the reproductive status of *T. macrura* during the spawning season, and find mature individuals at sizes smaller than previously reported. Such early maturation may have important implications for the population dynamics of this species.

Figures

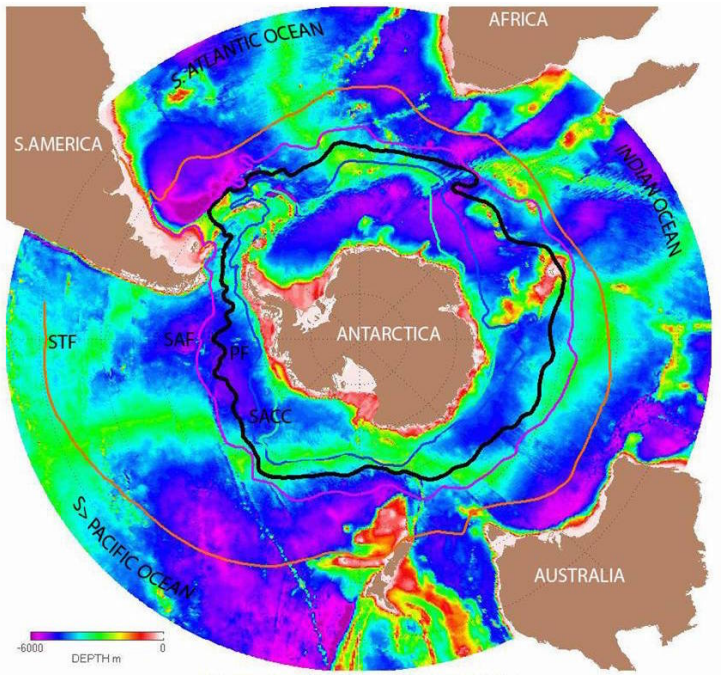

Figure 1.1. Major fronts and bathymetry of the Southern Ocean, including the sub-Antarctic Front (SAF), Polar Front (PF), and Southern Antarctic Circumpolar Front (SACC). Fronts from Orsi et al. 1995; image courtesy of NASA/JPL-Caltech.

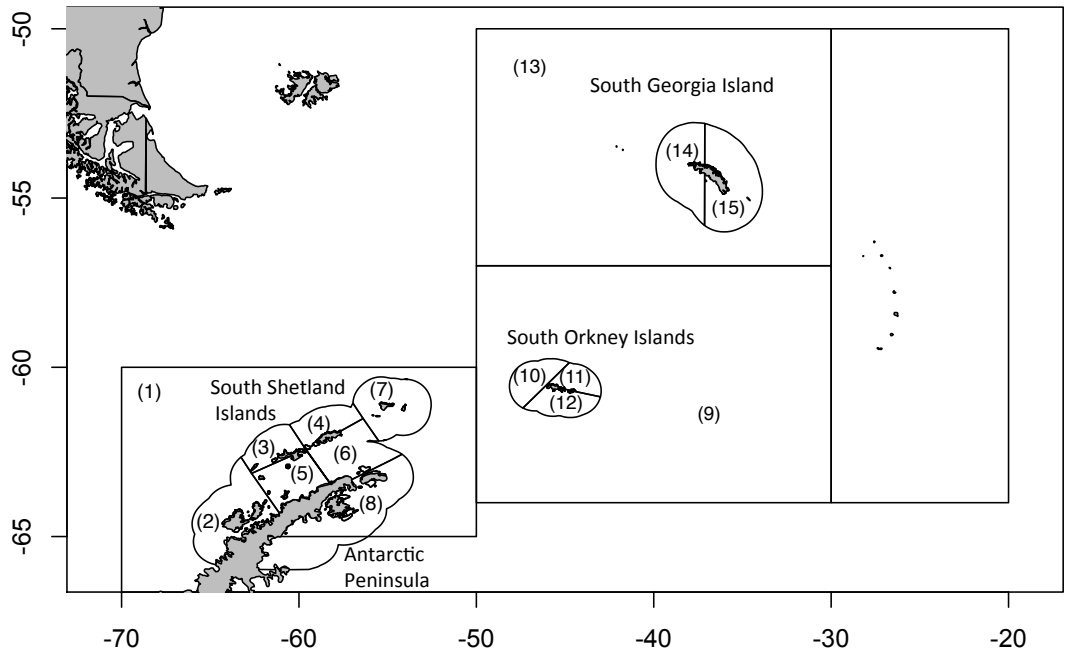

Figure 1.2. Small Scale Management Units (SSMUs) in the Southwest Atlantic Ocean.

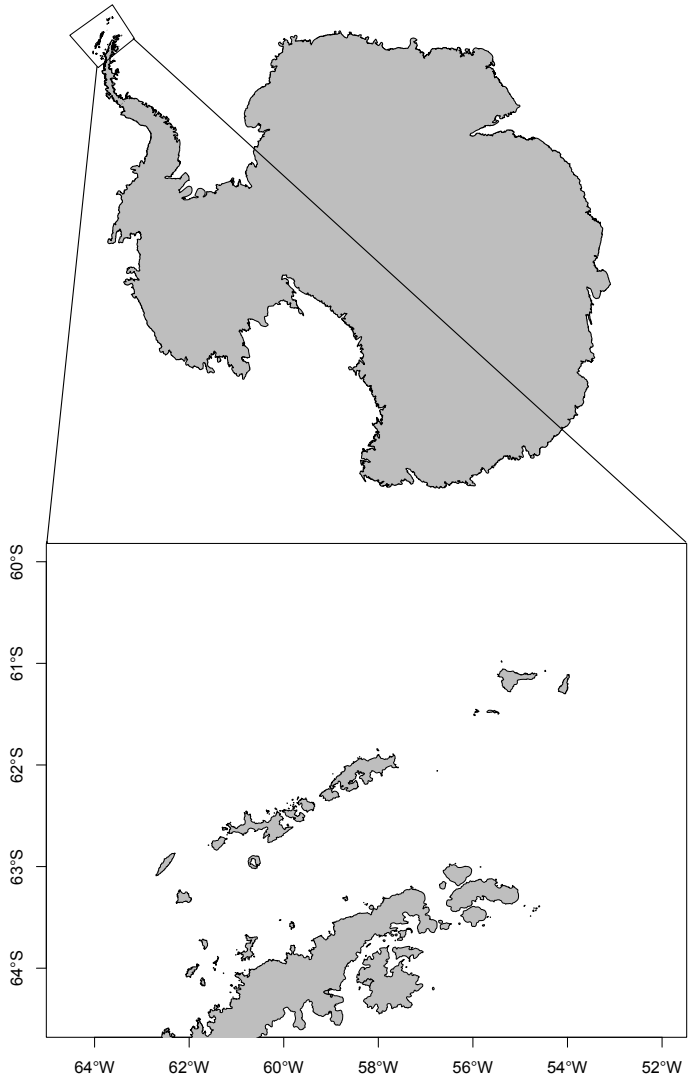

Figure 1.3. The northern section of the West Antarctic Peninsula.

Chapter 2. More than passive drifters: a stochastic dynamic model for the movement of Antarctic krill[1]

Abstract

Antarctic krill (*Euphausia superba*) are a key part of the marine food web and are the target of the largest fishery in the Southern Ocean. Though ecosystem and management models typically assume that krill are passive drifters, their relatively large size and strong swimming ability suggest their active movement may play an important role in the spatial distribution of krill. Thus, active swimming behavior by krill may influence spatial structure of food web interactions (e.g., feeding behavior of seabirds and marine mammals) and regional commercial fishery activity. The objective of this work is to model the potential for active movement to affect krill distribution, and consequently, growth, reproductive success, and survival. We use state-dependent life history theory, implemented by stochastic dynamic programming, in combination with spatial information on food availability, current velocity,

[1] This chapter published as Richerson, K., G. Watters, J. Santora, I. Schroeder, and M. Mangel. 2015. More than passive drifters: a stochastic dynamic model for the movement of Antarctic krill. Marine Ecology Progress Series 529:35-48.

temperature, and predation risk, to predict krill swimming behavior near the northern Antarctic Peninsula. We find that including active krill behavior results in distribution patterns that are associated with increased survival, growth, and reproductive success compared to a model that treats krill as passive drifters. The expected reproductive success of actively behaving krill is about 70 percent greater than that of passively diffusing krill, suggesting that there are strong selective pressures for active behavior along oceanic drift trajectories. This modeling framework will benefit assessment of new catch limits as krill fishing grounds are partitioned into smaller spatial management units.

Introduction

Antarctic krill (*Euphausia superba*, hereafter krill) play a fundamental role in the trophodynamics of the Southern Ocean ecosystem (Nicol and de La Mare 1993). They are a crucial link in the transfer of nutrients and energy to higher trophic levels and are a major prey source for many species of fish, squid, seabirds, and marine mammals (Smetacek and Nicol 2005). Fluctuations in krill biomass availability can have important consequences for predator reproductive success (Croxall et al. 1999, Reid and Croxall 2001, Lynnes et al. 2004, Trivelpiece et al. 2011), though the relationships between krill biomass and predator reproductive performance are complex (Croxall et al. 1999).

Effective management of human impacts on krill stocks is a matter of great concern for the Southern Ocean ecosystem. A commercial krill fishery has been

operating in the Southern Ocean since the 1970s, and catches have been increasing over the past two decades (Nicol et al. 2012). The increased demand for krill products, such as nutritional supplements and aquaculture feed, along with new harvesting technologies may lead to increased fishing activity and the potential for localized depletion in the vicinity of land-based predator colonies, particularly during the breeding season (Nicol et al. 2000, Nicol and Foster 2003, Hewitt et al. 2004, Nicol et al. 2012). In addition, krill recruitment is correlated with the extent and duration of winter pack ice, leading to concerns that climate change and declining sea ice could negatively impact krill populations (Atkinson et al. 2004, Wiedenmann et al. 2009).

Though most management models treat krill as passively drifting along ocean currents, krill are a schooling species with strong swimming abilities, perhaps more akin to small fish than plankton. They can swim at a steady cruising speed of up to 15 cm s^{-1}, move at 40-50 cm s^{-1} for short periods (Kils 1982), perform diel vertical migrations (Kils 1982, Godlewska 1996, Hernández-León et al. 2001), exhibit schooling behavior (Hamner and Hamner 2000), undertake sustained directed movement (Marr 1962, Kanda et al. 1982), and actively migrate, especially in regions with lower current velocities (Siegel 1988, Trathan et al. 1993). While it is unlikely that krill make large-scale directed migrations in the open ocean where current velocities are high, localized responses to small-scale cues may affect the broad-scale distribution of krill (Lascara et al. 1999a, Murphy et al. 2004). In addition, modeling studies indicate that behavior can influence local-scale krill distributions (Cresswell et

al. 2007). Thus, accounting for krill behavior may have important implications for our understanding of krill population dynamics at local to regional scales, their interactions with predators, and ultimately the effective management of krill fisheries.

The Southern Ocean krill fishery is managed by the Commission for the Conservation of Antarctic Marine Living Resources (CCAMLR). Due to concerns over localized fishing impacts on krill-dependent predators, CCAMLR established fifteen small-scale management units (SSMUs) in the Scotia Sea region in order to facilitate spatial management on a scale more relevant to land-based predators and avoid localized depletion (Constable and Nicol 2002, Hewitt et al. 2004). Options for allocation of catch limits within SSMUs include limits based on 1) historical catches in the SSMU; 2) estimated predator demand (the estimated annual demand by Adélie, chinstrap, gentoo and macaroni penguins, lactating female Antarctic fur seals, baleen whales and fish) in the SSMU; 3) the standing stock of krill in the SSMU; 4) standing stock minus predator demand in the SSMU; and 5) allocation based on predator surveys conducted each year before the fishing season (Hewitt et al. 2004). Several modeling tools are currently being used to assess these potential strategies (Watters et al. 2005, Hill et al. 2007, Watters et al. 2008, Watters et al. 2009, Plagányi and Butterworth 2012, Watters et al. 2013). In these models, krill are assumed to either stay in the SSMU of their birth for their entire lives, or to move passively with ocean currents. Thus, these models do not account for the possibility of active behavior by krill, and may therefore miss an important component of krill movement and consequent spatial distribution. In addition, spatial location is likely to influence the

growth, mortality, and reproductive success of krill (Siegel and Nicol 2000, Hofmann and Hüsrevoğlu 2003, Atkinson et al. 2006). By accounting for the influence of krill behavior on spatial distributions, we can make further inferences about the importance of behavior in krill dynamics.

Dynamic state variable models (Mangel and Clark 1986, Houston et al. 1988, Clark and Mangel 2000, Mangel 2015) provide a useful tool for exploring krill behavior across space and time because krill must balance the energetic costs of movement with feeding, growth, reproduction, and the risk of predation. These models use state-dependent life history theory, implemented through stochastic dynamic programming (SDP) to predict optimal behavioral decisions within a set of constraints. Dynamic state variable models allow organisms to make decisions about growth, maturation, and behavior based on both their own internal state as well as external cues such as environmental factors or time to some reproductive event.

Here, we use a dynamic state variable model to predict krill swimming speed and movement direction near the North Antarctic Peninsula (NAP). We then use forward simulations to explore how the spatial distribution, growth, survival, and reproductive success of krill vary relative to active and passive transport behaviors. In particular, we investigate the following: i) krill swimming speed and movement direction (our overarching research question); ii) conditional on i), how does the spatial distribution of krill vary relative to active and passive transport behaviors; and iii) how does active swimming influence growth, egg production, and survival?

Methods

Our modeling study focuses on the vicinity of the South Shetland Islands, near the NAP (Figure 2.1). We chose this area because: 1) it is home to a large number of krill and krill-dependent predators (Reiss et al. 2008, Santora and Veit 2013); 2) it is a major krill fishing ground (Jones and Ramm 2004) and there is potential for competition between krill predators and the fishery (Croll and Tershy 1998); and 3) observed patterns of krill distributions have been theorized to arise in part because of active krill migration (Siegel 1988, Watkins et al. 1992, Trathan et al. 1993). Circulation in this area is complex, with contributions from the Antarctic Circumpolar Current, the Weddell Gyre, and the Antarctic Coastal Current (Thompson et al. 2009a). The bathymetry of the region is varied, including the continental shelf around the islands as well as deeper waters in the Bransfield Strait and Drake Passage (Figures 2.1, 2.2c). We focus our model on January of the austral summer, when most spawning in the vicinity of the Antarctic Peninsula begins (Quetin and Ross 2001). During this late summer period, observed spatial segregation of adults and juveniles, with aggregations of spawning adults in oceanic regions and the continental shelf, are hypothesized to be the result of active movement by adult krill (Siegel 2000).

Environment

Though krill are omnivorous, their summer diet consists mainly of phytoplankton (Falk-Petersen et al. 2000). Across the Southern Ocean, krill densities are positively correlated with chlorophyll *a* (Atkinson et al. 2008), though the relationship is complex and may be complicated by depletion at smaller scales due to grazing (Wright et al. 2010). However, chlorophyll *a* is a significant predictor of growth rate (Atkinson et al. 2006). Thus, we use satellite estimates of chlorophyll *a* from the GlobColour Project (www.globcolour.info/), which combines information from the MERIS, MODIS, and SeaWifs sensors, as a proxy for food abundance. For all available years (1998-2013), we obtained the 8-day mean chlorophyll concentrations across the study area at the 4 km scale and averaged across years to produce a mean chlorophyll *a* field for each 8-day period in January.

Surface currents were calculated from geostrophic velocities derived from mean sea level measured by satellite altimetry. The mean sea level data used to calculate the geostrophic velocities is the merged sea level product created by Archiving, Validation, and Interpretation of Satellite Oceanographic data (AVISO; http://www.aviso.altimetry.fr). From AVISO's Maps of Absolute Dynamic Topography (MACT, 7 day intervals) we calculated geostrophic velocities by assuming geostrophy and using centered finite differencing on the MACT product to obtain u_g and v_g (Sudre et al. 2013, equations 1a and 1b). Monthly means of u_g and v_g for January were calculated and a final climatology was constructed from the monthly

means for the years 2003-2011. The MACT product we used was based on the older AVISO product and not the product introduced in April 2014 (http://www.aviso.altimetry.fr/fileadmin/documents/data/duacs/Duacs2014.pdf). The resulting surface velocity vectors derived from the older AVISO product have better coherence with observed drifter buoys (Thompson et al. 2009) and circulation models (Jiang et al. 2013), particularly around the islands and the Shackleton Fracture Zone. We suspect that the new optimal interpolation method used in creating the more recent product may be smoothing out some of the circulation features that are present in the older data and that appear in drifter studies and circulation models; thus we chose to use the older product.

Krill are ectotherms, with a dome-shaped growth rate/temperature profile and maximum growth rates occurring around 0.5 °C (Atkinson et al. 2006, Wiedenmann et al. 2008). In addition, krill densities are negatively correlated with sea surface temperature (SST), although this may simply reflect krill responses to temperature correlates such as food availability (Trathan et al. 2003). To characterize the temperature environment experienced by krill in our model, we use ¼ degree resolution mean January SST data averaged over 2003-2011 from the Group for High Resolution Sea Surface Temperature at the NOAA National Climatic Data Center (Reynolds et al. 2007, obtained from http://coastwatch.pfeg.noaa.gov/erddap/griddap/).

We obtained bathymetry data at the 30-arc second scale from the General Bathymetric Chart of the Oceans (GEBCO, http://www.gebco.net/). We obtained coastline polygons from the SCAR Antarctic Digital Database (http://www.add.scar.org/). We gridded all data at the 1 km scale and linearly interpolated when necessary using the Akima package version 0.5-11 (Akima et al. 2013) in R 3.0.2 (R Development Core Team 2013). In Figure 2.2 we show sample current, chlorophyll *a*, temperature, and bathymetry landscapes.

Growth and the cost of movement

In order to estimate baseline growth (*i.e.* growth that does not include the cost of active movement), we use the model of Atkinson et al. (2006; also see Wiedenmann et al 2009), in which instantaneous growth is used to predict krill growth as a function of size, temperature, and chlorophyll *a* concentration. We use a parameterization for all age and sex classes combined where daily growth rate (DGR) for a krill of size L (mm) experiencing chlorophyll *a* concentration F (mg m^{-3}) at temperature T ($^{\circ}C$) is

$$DGR(L,F,T) = -0.066 + 0.002L - 0.000061L^2 + 0.385\frac{F}{0.328+F} + 0.0078T - 0.0101T^2 \quad (2.1)$$

Thus, for a non-swimming krill of length L_0 at time t, the new length at time $t+\Delta t$ is

$$L_0(t+\Delta t) = L_0 + DGR \cdot \Delta t \qquad (2.2)$$

We convert length to dry weight $DW_0(t)$ and then carbon weight $CW_0(t)$, both measured in mg, using the allometric relationships in Table 2.1.

Swadling et al. (2005) found a linear relationship between current speed S (in cm s^{-1}) and krill respiration rate R (in mg O_2 hr^{-1} g_{DW}^{-1}),

$$R=2.16+0.35S \qquad (2.3)$$

This relationship holds true for speeds from 5 to 18 cm s^{-1}, and Swadling et al. (2005) hypothesize that krill are not strongly influenced by the current below 3 cm s^{-1}. Though the authors suggest a nonlinear relationship between respiration rate and speed at low velocities, for simplicity we assume that krill expend the same energy swimming 0-3 cm s^{-1}, and that at speeds above 3 cm s^{-1}, respiration rises linearly with a slope of 0.35 (Figure 2.3). This is a reasonable assumption because at 3 cm s^{-1} krill appear to be operating at their routine metabolic rate and are likely maintaining the minimum pleopod rate required to keep them from sinking (Swadling et al. 2005). Thus, using a respiratory quotient of 0.72 (following Lowe et al. 2012) and the molar masses of carbon and oxygen, we estimate the additional carbon C lost due to swimming at speed S as

$$C(S)=0.35S \cdot \frac{12.011}{32.0} \cdot 0.72 = 0.0946 \cdot S \qquad (2.4)$$

if S is greater than 3 cm s^{-1}, or

$$C(S)=0 \qquad (2.5)$$

if S is less than or equal to 3 cm s^{-1}.

In order to estimate the change in size of a krill swimming at speed S over Δt, we calculate the baseline growth using Eqn 2.2, convert the new length to carbon weight, and decrement the cost of swimming, such that the new carbon weight is

$$CW(t+\Delta t)=CW_0-C(S)\cdot 24\Delta t\cdot DW_0\cdot 10^{-3} \qquad (2.6)$$

We then reconvert carbon weight to length using the relationships in Table 2.1. Thus, we are able to predict the change in length each time step given length, environmental conditions and swimming behavior.

Mortality

Estimates of krill mortality rates vary widely, perhaps due in part to spatial and interannual variability in mortality (Siegel and Nicol 2000). There is considerable predation pressure from land-based krill predators, which are more abundant on the continental shelf (Croll and Tershy 1998). Thus, following Cresswell et al. (2007), we separate mortality into on-shelf, shelf slope, and off-shelf zones. We let average mortality $\overline{\beta}$ =0.0025 d^{-1}, an intermediate value from the range reported for the

Antarctic Peninsula that translates to an approximate 40% annual survival rate (Siegel and Nicol 2000). Mortality in cell *x* is

$$\beta(x)= \frac{10^{\alpha}}{1+10^{\alpha}} \qquad (2.7)$$

We scale α by zone (on-shelf, shelf break, and off-shelf), such that

$$\alpha = \bar{\alpha} + \alpha_z \qquad (2.8)$$

where α_z represents the mortality of a habitat relative to the mean mortality. Here, we let α_z=0.5 on-shelf, α_z=0 on the shelf break, and α_z=-0.5 off-shelf (Cresswell et al. 2007). We let

$$\bar{\alpha} = \log_{10}\left(\frac{\bar{\beta}}{1-\bar{\beta}}\right) \qquad (2.9)$$

so that in the absence of a scaling parameter α_z (i.e. α_z=0), mortality is equal to mean mortality $\bar{\beta}$.

The krill movement model

We grid the entire study area (-63 to -60 latitude, -63 to -53.5 longitude) into ~1 km^2 cells and let $\vec{x}$ denote the position of the center of a cell. We let $F(l, \vec{x}, t)$ denote the maximum expected reproductive success (measured in terms of viable eggs – those laid in water sufficiently deep for their survival) at time *T* for a krill with

current length $L(t)=l$ and in cell $\vec{x}$. Here, the maximum is taken over the behavioral choices concerning swimming. We determine the fitness function as follows.

a. End Condition

Stochastic dynamic programming models begin at the final time step and iterate backwards in time to solve for the behavior that maximizes expected future fitness given current conditions and time to the terminal timestep. Thus, it is necessary to define a measure of Darwinian fitness at the last time step, called the end condition. Here, we assume that female krill spawn their eggs in the final timestep and that this represents the terminal fitness reward. Following Nicol et al. (1995), we assume that a krill of length l releases $E(l)$ eggs given by

$$E(l)=max(0,-5293.1+144.84l) \qquad (2.10)$$

Krill eggs are released in the upper water column, where they sink to 700-1000 m before hatching into free-swimming larvae and beginning their ascent back towards the surface (Quetin and Ross 1984). Therefore, eggs released on the continental shelf are unlikely to develop, because they will reach the ocean floor before hatching (Hofmann and Murphy 2004). However, in many areas near the Antarctic Peninsula, krill eggs are predicted to successfully hatch well within the 1000-m isobath (Hofmann and Hüsrevoğlu 2003). Thus, we set the egg-survival threshold to 500 m, such that eggs deposited in water shallower than 500 m are lost and eggs released in deeper water are expected to survive. Clearly, a less-sharp egg-survival/bathymetry relationship can be used when such data are available.

Therefore, the fitness F of a krill of length L in cell $\vec{x}$ at the final timestep T is

$$F(l,\vec{x},T)=-5293.1+144.84L \qquad (2.11)$$

if bottom depth is greater than 500 m, or

$$F(l,\vec{x},T)=0 \qquad (2.12)$$

if bottom depth is less than 500 m. Thus, the fitness accrued by a krill in the final timestep of the model depends on both its size and location; although being bigger leads to more eggs, getting bigger (for example, by feeding in high-chlorophyll areas close to land) has associated risks (*i.e*. predation by land-based predators) that lead to a growth-survival trade-off.

b. The dynamic programming equation

After setting the end condition, we iterate backwards with timesteps of Δt=12h (0.5d) to solve for the optimal behavioral choice using the Dynamic Programming Equation (DPE). The DPE is an algorithm that solves for the behavior that maximizes expected future fitness given the organism's current state and the time to the final time step, when it will gain an increment in fitness as defined by the end condition described above. We solve the DPE for krill size varying from 40 to 50 mm over 28 days (January 1 to 28) in the entire study area. At each timestep t, we allow krill to choose from 6 swimming speeds (0 to 15 cm s^{-1}) and 8 directions of movement (0 to 7π/4 radians), giving 41 swimming velocity $\vec{m}$ choices (Figure 2.4).

A krill swimming at velocity $\vec{m}$ beginning in cell $\vec{x}$ with current velocity $\vec{v}(\vec{x})$ (km hr^{-1}) will have a new location $\vec{x}'$,

$$\vec{x}' = x + \vec{m}\Delta t + \vec{v}\Delta t \qquad (2.13)$$

and a new length *l*', calculated from Eqn 2.6 and the conversions in Table 2.1. We leave assigning a probability distribution on $\vec{x}'$ to future work.

Thus, for a krill in cell $\vec{x}$ with current velocity $\vec{v}(\vec{x})$, the DPE is

$$F(l,\vec{x},t) = \max_{\vec{m}}\left(e^{-\beta(x)} \cdot F(l',\vec{x}',t+1)\right) \qquad (2.14)$$

The movement velocity choice $\vec{m}^*(l,\vec{x},t)$ that results in maximum expected fitness can then be used in forward simulations of krill behavior.

c. Forward simulations

The DPE produces a set of predicted behaviors $\vec{m}^*(l,\vec{x},t)$ for a female krill given its size, location, and the time to the terminal timestep, when it will release eggs. Using these behavioral rules, we can run forward Monte Carlo simulations for large numbers of krill to explore how krill spatial distribution will change through time as krill behave according to the rules set up by the DPE. We can also compare these distributions to simulations where krill act as passive drifters (*i.e.* in the model, a swimming speed of 0).

In order to illustrate the potential for active movement to influence krill distributions, we conducted 61 simulations of 10,000 45-mm krill beginning near King George Island and Livingston Island (see Figure 2.7 for starting locations). We chose these starting locations because krill are relatively abundant in much of this area during summer (Reiss et al. 2008) and because it allowed us to follow krill trajectories for most or all of the simulation time window without leaving the study area. We begin with krill of 45 mm because this is a common size class in the area (Reiss et al. 2008). We then iterated forward through time for 28 days, with change in size each time step calculated according to Eqn 2.6 and predicted behavior at each timestep drawn from the solution to the DPE. Following Thorpe et al. (2004) we add a stochastic component to the advective current flow, such that for the *i*th simulated krill

$$\vec{X}_i(t+\Delta t) = \vec{X}_i + \vec{m}(L_i, \vec{X}_i, t)\cdot\Delta t + \vec{V}\cdot\Delta t + \vec{W} \qquad (2.15)$$

where $\vec{w}$=(d cos(τ), d sin(τ)) is a random walk mimicking eddy diffusivity, with $d = \sqrt{12\Delta t D_h R_1}$ and $\tau = 2\pi R_2$. D_h is the horizontal diffusion coefficient (set to 100 $m^2\ s^{-1}$), and R_1 and R_2 are random numbers between 0 and 1 drawn from the uniform distribution (Hilborn & Mangel 1997). We ran each simulation twice, once for "active" krill, where $\vec{m}\,(L(t), \vec{X}(t), t)$ is taken from the solution to the DPE, and once for "passive" krill, where $\vec{m}\,(L(t), \vec{X}(t), t)$=0. Varying D_h by +/-50% does not change the general pattern of results.

Results

We consider

(i) krill swimming speed and movement direction

(ii) conditional on (i), how does the spatial distribution of krill vary relative to active and passive transport behaviors; and

(iii) how does active swimming influence growth, egg production, and survival?

Predicted behavior

Based on the backwards algorithm, we predict that krill swim an average of 3.65 (±2.62) cm s^{-1}, or about 3.15 km d^{-1}. Mean swimming speeds were similar across size classes (Figure 2.5). Mean swimming speeds show an increase, then sharp decrease close to the terminal time, likely indicating a critical window when krill inside the 500m isobath must move quickly in order to be in a favorable area for releasing eggs by the final timestep. After this critical window, many krill are close enough to the final time that swimming in the last few timesteps is unlikely to greatly alter their reproductive outcome, so mean speeds decrease near the terminal time.

Predicted swimming behavior also varied across space and time, reflecting the differing environmental conditions and the effect of time to the terminal fitness

reward in the model. In Figure 2.6, we show predicted swimming velocities for 45 mm krill at several sample timesteps.

After running the forward simulations of 10,000 45-mm female krill with and without behavior over 28 days, we found that by the final timestep (or when krill reached the edge of the study area), the mean distance between an active krill and a passive krill with the same point of origin ranged from 7.73 to 168.51 km (mean 67.50 km). In 27 of 61 simulations, the average locations of passive and active krill were in different SSMUS by the end of the simulation.

Although overall actively behaving and passively drifting krill reached similar mean sizes (mean 47.88±1.34 mm for active krill, 47.07±1.77 mm for passive krill; Figure 2.8a), actively behaving krill produced on average more viable eggs per individual in all simulations (mean 1602.31±215.78 for active 944.39±655.97 for passive krill; Figure 2.8b). Predicted mean eggs across passive simulations ranged from 0 to 1737.10±10.72 and across active simulations from 1124.16±10.96 to 1868.44±24.99. Survival rates for active krill were higher than for passive krill in 36 of 61 (mean 93.8% for active krill, 91.4% for passive krill; Figure 2.8c). A measure of the strength of natural selection on active swimming behavior is the ratio of these expected reproductive successes, *i.e.* $0.938 \cdot 1602/(0.914 \cdot 944)=1.74$. With multiple reproductive bouts per year, the strength of natural selection is magnified. See Appendix A for individual results from all simulations.

Though tests of statistical significance are not appropriate for model simulation data (White et al. 2014), we report a measure of effect size (Cohen's *d*) for both length and egg production. Cohen's *d* is a measure of the difference between two sample means as multiple of their weighted standard deviation; values of 0.2, 0.5 and 0.8 are considered small, medium or large effect sizes (Cohen 1988). In our studies, effect sizes varied between simulations, from 0.8 to 35.5 for length and from 0.67 to 176.1 for egg production (see Appendix A for all values).

Discussion

Our results indicate that active krill movement plays an important role in determining the spatial distribution of krill in the vicinity of the northern Antarctic Peninsula. This accords with field observations that have found spatial distributions of krill in this area unlikely to result from advective processes alone (Siegel 1988; Watkins et al. 1992, Trathan et al. 1993, Lascara et al. 1999). Those studies find a clear segregation of size and maturity stages, suggesting that ontogenetic migrations may in part explain observed spatial patterns. In our study, reproductive females appear to actively move in order to release eggs in more favorable areas, suggesting one possible mechanism for the segregation of sex and age classes. Though our forward simulations only tracked krill for a single month, if the pattern we observed here continued over the course of a season, for some locations active krill could be on the order of hundreds of kilometers away where they would be predicted to be using a passive drift model of krill transport. Clearly, model predictions are unlikely to be a

perfect reflection of behavior in the field, and krill may not always act according to the optimal swimming trajectories in our model. However, this result underscores the potential for behavior to alter our conceptions of krill distributions across space and time.

Since SSMUs are relatively small (10,800-927,400 km^2; Hewitt et al. 2004), and current management models resolve on a bi-annual timescale (Plagányi and Butterworth 2012, Watters et al. 2013), the predicted movement of krill between SSMUs could be very different if behavior were included in the management models. These models either assume no movement or use transport rates based on passive particle tracking models. Including some assumptions about active movement into estimates of transport rates could provide an opportunity to include more biological realism in these models. Furthermore, our work shows that movement behavior may play an important role in reproductive success and avoidance of predators.

Our simulations suggest that for some other areas near the South Shetland Islands, krill distributions (whether assumed to be passive or active) may be locations that accumulate krill and therefore, catch limits based on the assumption that krill are quickly advected past these islands may be overly optimistic. In some areas near the Antarctic Peninsula, there is evidence of quasi-resident krill populations (Wiebe et al. 2011, Piñones et al. 2013). Krill tend to be concentrated in areas with moderate levels of eddy kinetic energy (Santora et al. 2012) and may be associated with gyres that

link the Antarctic Circumpolar Current and the Antarctic Coastal Current (Nicol 2006), suggesting krill may use current features to stay in favorable habitats.

Although previous modeling studies have investigated krill behavior (Alonzo and Mangel 2001, Alonzo et al. 2003, Cresswell et al. 2007), ours is the first to explicitly account for the metabolic cost of active movement and its potential to affect growth and reproduction. Because swimming costs may represent a significant fraction of daily energy expenditure (13% to 73%; Swadling et al. 2005), a detailed understanding of krill energy budgets, swimming cost, and growth would best inform our model. However, to our knowledge, only one laboratory study (Swadling et al. 2005) has attempted to quantify the cost of movement for Antarctic krill. This experiment may not be directly applicable to krill under the natural conditions of our study area, in particular because it did not account for swarming behavior, which is thought to decrease oxygen consumption (Ritz 2000). In addition, it did not distinguish between size classes and was conducted at $1\ ^{\circ}C$, while temperatures in our model ranged from -0.84 to 2°C. Because krill metabolism is strongly influenced by both temperature and size (Buchholz and Saborowski 2000), the cost of active swimming in our study should only be considered an approximation.

The growth model of Atkinson et al. (2006) is based on field measurements in the southwest Atlantic, meaning it may already reflect the metabolic cost of some average level of active movement, especially because krill make daily vertical migrations and have been observed undertaking directed movement (Godlewska

1996, Hernández-León et al. 2001, Marr 1962). However, while other energetics models, such as that of Hofmann and Lascara (2000), do not include the cost of active movement, they predict considerably lower growth rates at the levels of chlorophyll *a* found in our study area compared to those found by Atkinson et al. (2006). Atkinson et al. (2006) suggest that ingestion of protozoans in areas of low chlorophyll *a* may in part explain the higher growth rates compared to those predicted by Hofmann and Lascara (2000). Therefore, because this model is based on growth rates of krill experiencing field conditions similar to those in our study area, we consider it the best available estimate of baseline growth in the absence of movement, although it may already account for some energy expended on swimming. Thus, our estimates of growth, and consequently, predicted swimming speeds for actively-swimming krill may be conservative, and our estimates of growth for slowly- or non-swimming krill may be overestimated.

We use surface currents in our model, but krill perform diel vertical migrations (Godlewska 1996, Hernández-León et al. 2001), where temperature, current velocity, predation risk, and food availability at depth differ from those at the surface. Krill may use these differing conditions to avoid predation and alter transport trajectories (De Robertis 2002, Hofmann and Murphy 2004). However, vertical migration behavior in krill has already been explored in modeling studies (Alonzo and Mangel 2001, Alonzo et al. 2003, Cresswell et al. 2007, Cresswell et al. 2009), one of which suggests that vertical movement does not strongly influence location (Cresswell et al. 2007). Therefore, we assume that including diel migration would not

alter the qualitative patterns in spatial distribution we predict here. However, because diel migration likely affects growth and predation risk (Alonzo and Mangel 2001, Alonzo et al. 2003), vertical movement may modulate our predicted impacts of active krill movement on growth and mortality.

Modeling can serve as an important tool for guiding future empirical studies (Hilborn and Mangel 1997, Clark and Mangel 2000), and much remains unknown about active krill movement under field conditions. Krill are not well-suited to mark-recapture studies (Nicol 2000); however, acoustic studies have the potential to provide a variety of information about krill. Several studies have used acoustics to examine krill swarm behavior in the field (e.g. Cox et al. 2009, Brierley and Cox 2010, Tarling and Thorpe 2014), and acoustics have been used to explore the details of swimming behavior in other euphausiids (e.g. De Robertis et al. 2003, Klevjer and Kaartvedt 2006). Tarling and Thorpe (2014) found that flow regime, salinity, distance to ice edge, and fluorescence alter krill swarm characteristics, and further acoustic studies of krill in the field may allow us to relate krill swimming behavior to further physical and biological features across the seascape. In addition to acoustic studies, videographic techniques (summarized in Hamner & Hamner 2000) could allow the collection of data on the fine details of krill swimming behavior, such as pleopod beating rate and turning frequency. Though krill appear to respond to a number of environmental features (e.g. Marr 1962, Kanda et al. 1982, Tarling and Thorpe 2014), much remains to be understood about the proximate cues that elicit krill behavior. Krill respond to chemical and visual cues (Strand and Hamner 1990), alter their

behavior in response to phytoplankton (Kawaguchi et al. 2010), and show spatial segregation based on maturity (Siegel 2000), indicating that krill likely respond to physical, chemical, and biological elements of the environment. Further, these responses are likely to depend on the size, stage, condition, and location of the organism. Our model underlines the fact that there is likely strong selective pressure to evolve behavioral responses to the environment, and that these are likely to be complex and nuanced, representing tradeoffs between survival, growth, and reproduction.

In conclusion, our model suggests that krill are more than simply passive drifters, and that their predicted behavior will vary across space and time, resulting in more complex movement and distribution patterns than might be predicted by simple advection. In addition, these altered distributions can affect reproductive success and mortality. Though more work remains to be done in elucidating the degree to which active movement may affect krill populations, this model can serve as proof of concept for the importance of behavioral modeling in the management of krill fisheries.

Tables and Figures

Table 2.1. Conversions for length (L, mm) to dry weight (DW, mg) and dry weight to carbon weight (CW, mg).

Equation	Source
$DW=6.46\bullet10^{-5}L^{3.89}$	Atkinson et al. (2006)
$CW=0.366DW^{1.037}$	Hofmann & Lascara (2000)

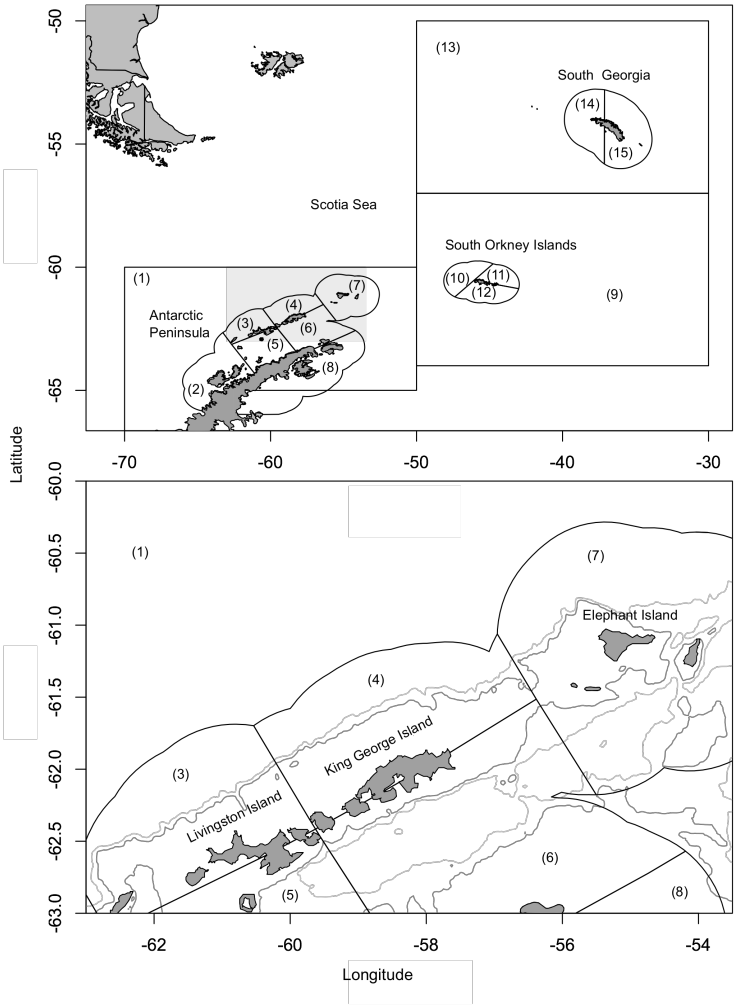

Figure 2.1. Top panel: Map of the Southwest Atlantic Ocean showing locations of the fifteen small-scale management units (SSMUs), with the area of focus shaded. Bottom panel: The area of focus, including SSMUs, 500-m isobath (dark gray) and 1000-m isobath (light gray).

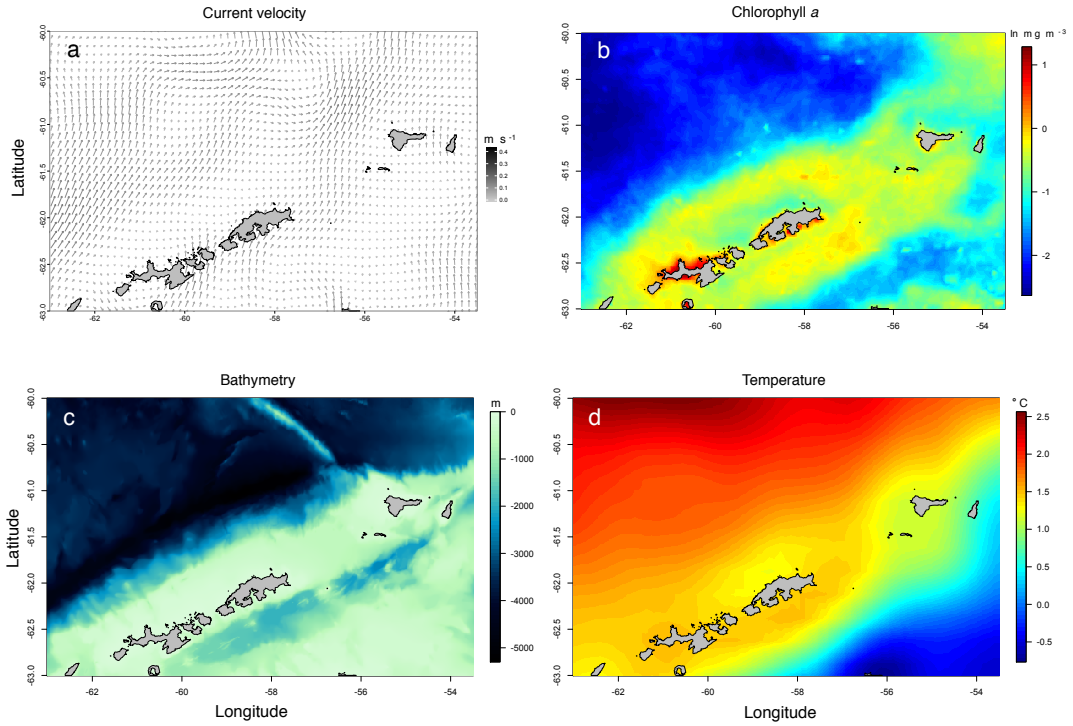

Figure 2.2. The environment: (a) Mean January current vectors (m s^{-1}), 2003-2011. (b) Log mean January chlorophyll *a* concentrations (mg m^{-3}), 1997-2013. (c) Bathymetry (m). (d) Mean January temperature (°C), 2003-2011.

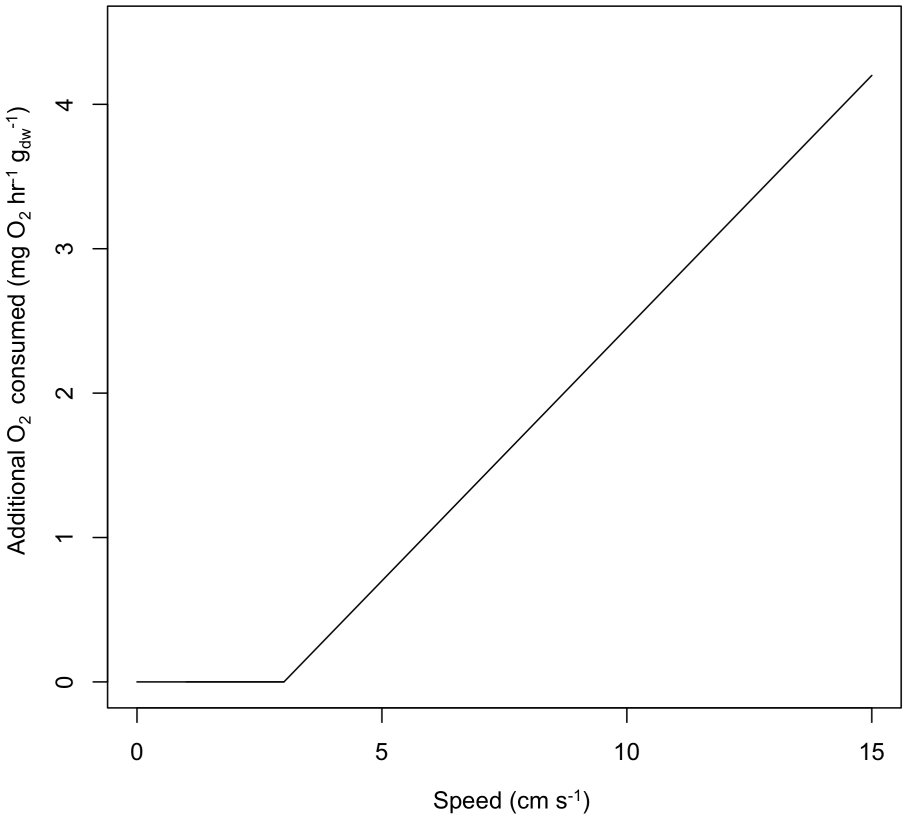

Figure 2.3. Additional metabolic cost (mg O_2 hr^{-1} g_{DW}^{-1}) as function of swimming speed (cm s^{-1}), based on Swadling et al. (2005).

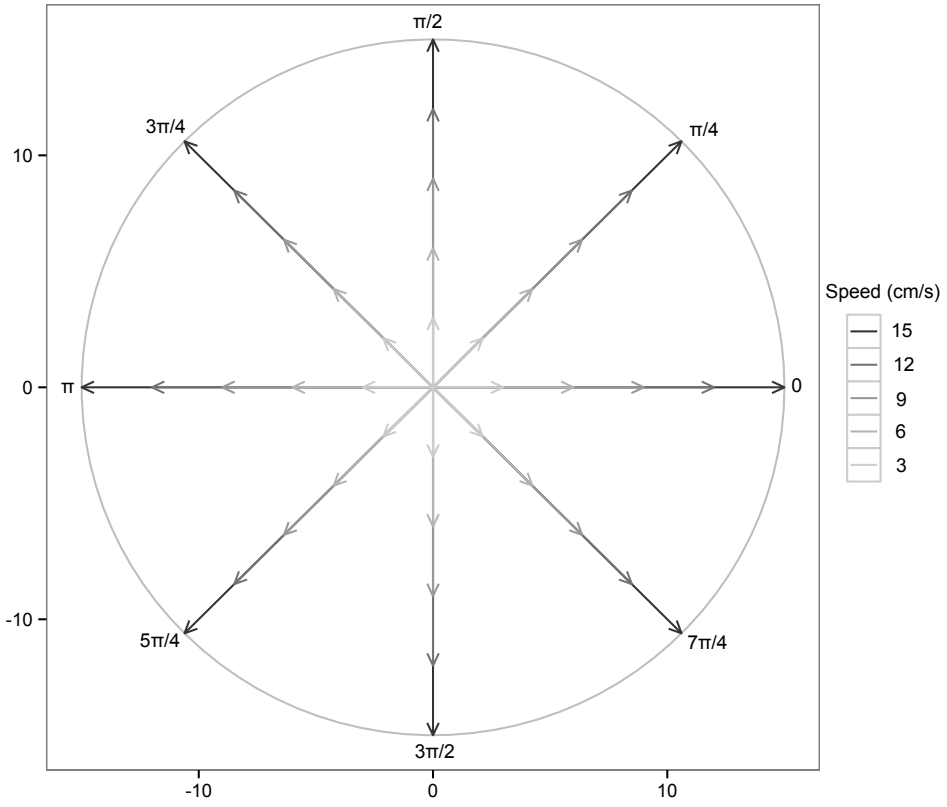

Figure 2.4. Potential swimming velocity choices in the model.

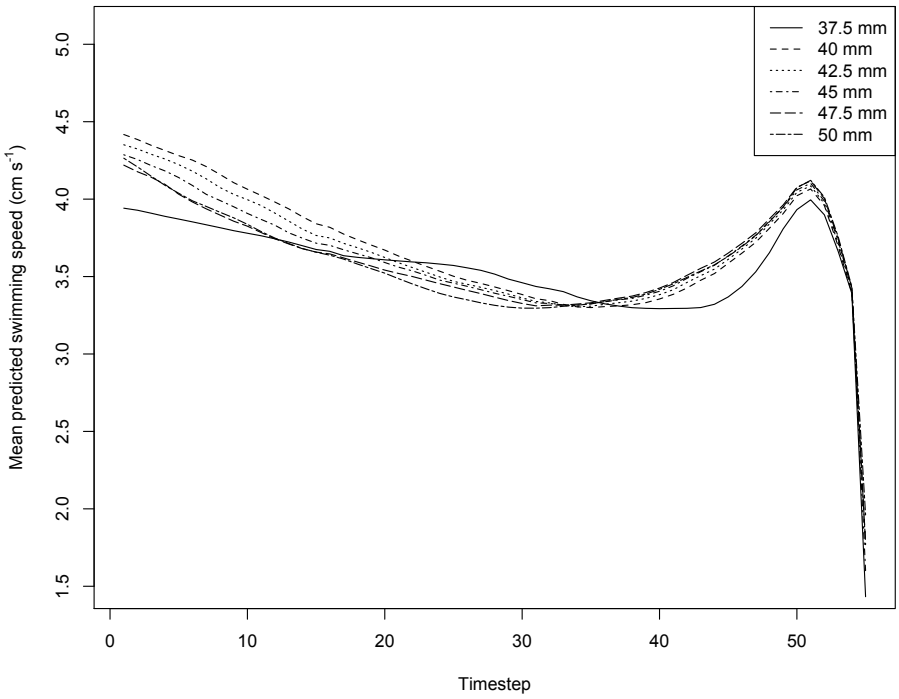

Figure 2.5. Mean predicted swimming speed (cm s^{-1}) for krill of different sizes.

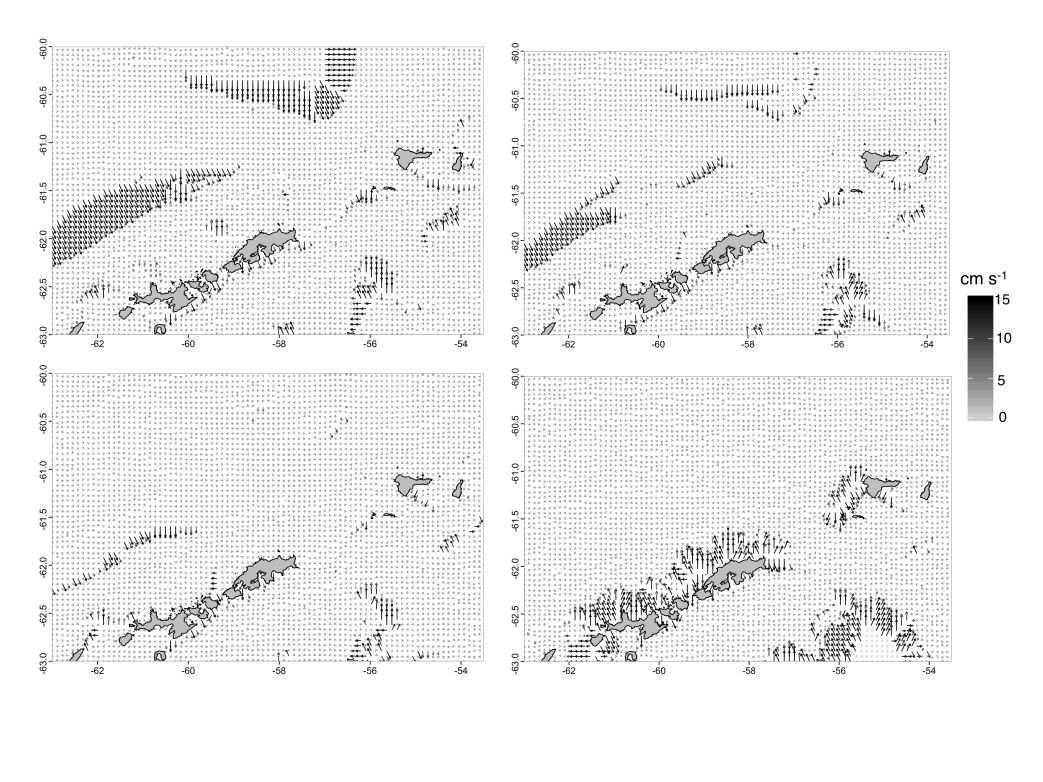

Figure 2.6. Predicted swimming velocities (cm s^{-1}) for 45 mm krill at t=1 (top left), t=15 (top right), t=30 bottom left), and t=50 (bottom right).

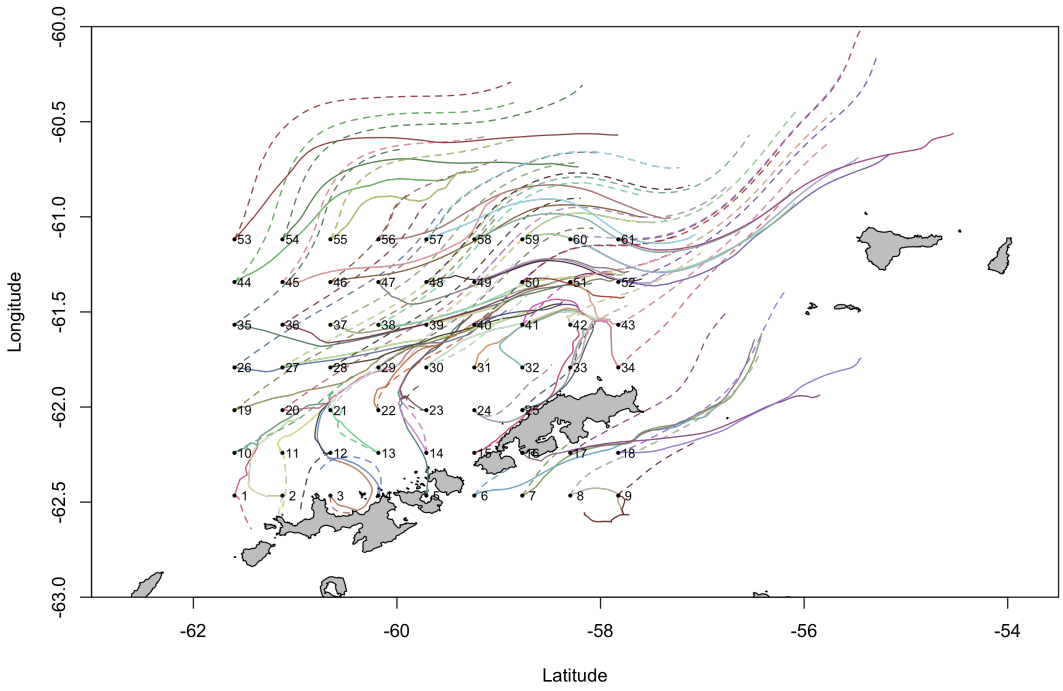

Figure 2.7. Mean trajectories of simulated active (solid line) and passive (dashed line) krill released at numbered starting points.

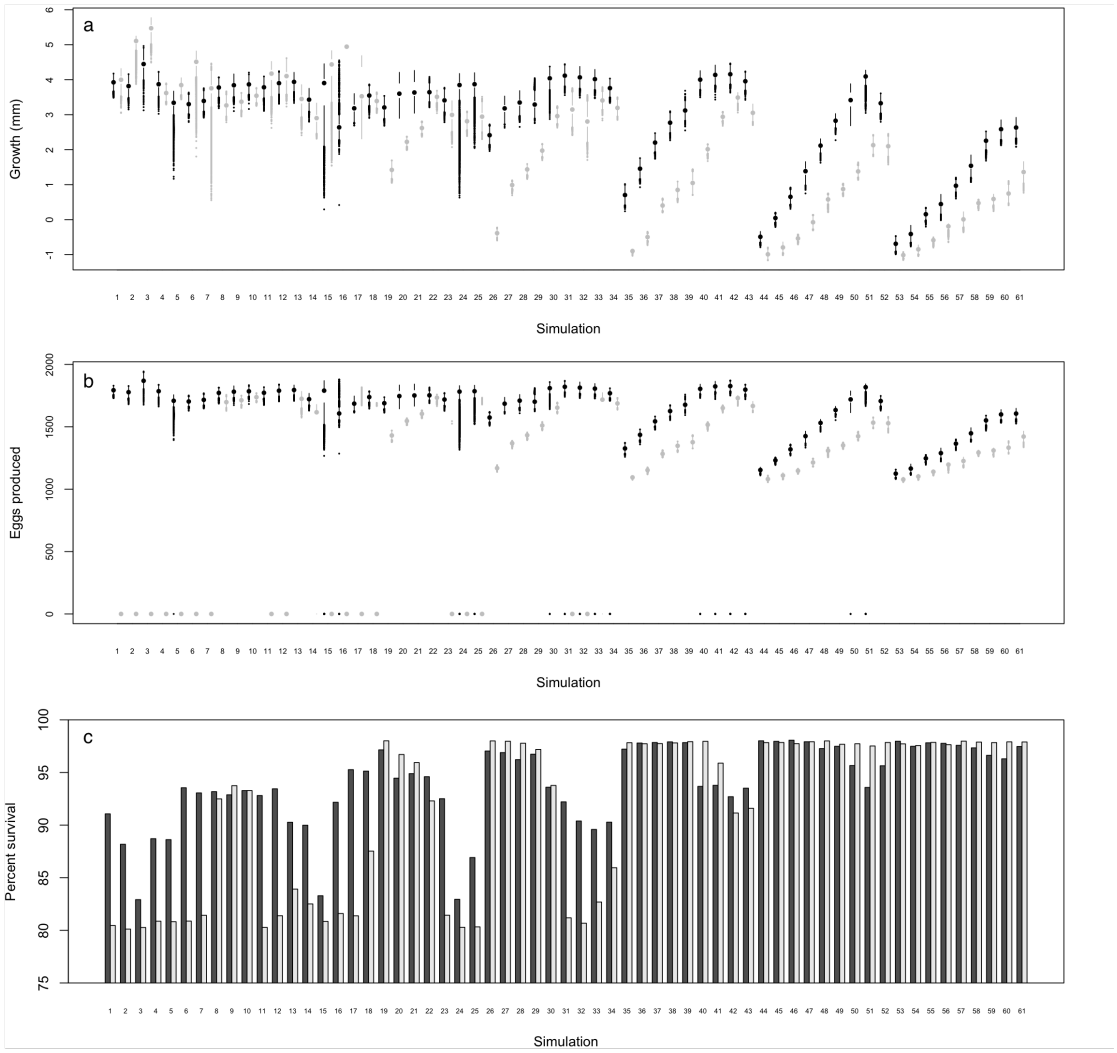

Figure 2.8. Results from forward simulations of active (black) and passive (gray) krill. (a) Growth (mm) over the simulation window. Large dots represent the median, vertical bars represent upper and lower quartiles, small dots represent outliers. (b) Eggs released outside the 500 m isobath. (c) Percent survival over the simulation.

Chapter 3. Inter- and intra- annual variability of Antarctic krill distributions near the North Antarctic Peninsula as revealed by acoustics

Abstract

Antarctic krill (*Euphausia superba*) densities vary in space and time across multiple scales, with consequences for krill predators, the krill fishery, and management decisions. I use acoustic data collected 1997-2011 (15 yrs) around the South Shetland Islands near the northern Antarctic Peninsula to quantify spatiotemporal patterns in krill biomass, distribution and patchiness both within and across years. Moreover, I evaluate potential climate drivers of krill biomass and spatial organization by through comparison with seasonally-lagged climate indices. Krill abundance varied by an order of magnitude throughout the 15 year period, with mean concentration ranging from a high of 171.9 g m^{-2} in 1997 to a low of 9.4 g m^{-2} in 2002. I find that across years krill abundance and variability are correlated with seasonally averaged measures of El Niño-Southern Oscillation (ENSO) influence at lags of approximately 2-2.5 years, which may correspond to strong reproduction and recruitment events. Acoustic measures of krill show generally weak spatial autocorrelation, with higher patchiness in years with higher abundances in some habitats. Within years, there was an overall trend of declining krill abundance and

contracted spatial distribution between mid- and late summer, but this pattern was not consistent across all years. This synthesis may be used to model krill preyscapes to better understand regional foraging ecology of krill predators and fishery performance.

Introduction

Antarctic krill (*Euphausia superba*, hereafter krill) are a keystone species in the Southern Ocean ecosystem, and a major prey source for many species of fish, squid, seabirds, and marine mammals (Smetacek and Nicol 2005). Krill are the focus of the Southern Ocean's largest fishery by tonnage, leading to concerns that harvesting, as well as climate-induced changes in distribution and abundance, may lead to decreased availability to predators (Hewitt et al. 2004, Flores et al. 2012a). Krill are patchily distributed and their abundance varies across a range of temporal and spatial scales, ranging from population-wide fluctuations that occur on the scale of years and thousands of kilometers, to variation at the concentration level that occur at the scale of months and hundreds of kilometers, to patch dynamics that occur at the scale of weeks and tens of kilometers (Murphy et al. 1988, Miller and Hampton 1989). These multi-scale levels of variation have important consequences to predators at various levels. For example, interdecadal changes in krill biomass have been linked to changing population trajectories of chinstrap and Adélie penguins breeding on the South Shetland Islands (Trivelpiece et al. 2011). At smaller temporal and spatial scales, krill availability during the breeding season has been linked to the

reproductive success of multiple predators (Croxall et al. 1999, Boyd and Murray 2001, Reid and Croxall 2001, Murphy et al. 2007), and spatial/seasonal overlap between the krill fishery and predator foraging has raised concerns that harvest may reduce the availability of krill to predators (Croll and Tershy 1998). Thus, understanding the factors that underlie krill variability across space and time is important in the management of krill fisheries and for the Southern Ocean ecosystem as a whole. For example, fishing vessels and predators such as blue whales may operate on similar spatiotemporal scales (Wiedenmann et al. 2011), raising the possibility of conflicts between human extraction and predator foraging needs, which can only be quantified with knowledge of the dynamics of the exploited stock. This study uses a long-term acoustic data set collected from 1997-2011 around the South Shetland Islands (Figure 3.1) to elucidate intra- and inter-annual patterns in krill abundance and spatial organization and possible consequences for krill-dependent predators.

As revealed by acoustic and net data, krill populations exhibit interannual and decadal fluctuations in biomass and demography. In the Northern Antarctic Peninsula (NAP) region, periodic strong year classes produce cyclical patterns of krill biomass (Hewitt et al. 2003). Krill recruitment is tied to climatic factors, particularly the extent and duration of winter sea ice and El Niño-Southern Oscillation variability (Loeb et al. 1997, Quetin et al. 2007, Loeb et al. 2009b). Although krill abundance and demography have been tied to climate, the consequences for both interannual and intraseasonal spatial distributions have not been fully quantified. In addition,

previous work linking krill abundance and climate in this area have focused solely on net haul data (Loeb and Santora 2015). Indices of biomass based on net tows appear uncorrelated with acoustic data (Kinzey et al. 2015), raising the possibility that acoustic estimates of abundance may reveal different information about the influence of climate on the abundance and spatial organization of krill populations.

Krill abundance varies across space as well as across time. Advective processes such as the southern Antarctic Circumpolar Current (ACC) are thought to dominate in the open ocean, but small-scale behavioral responses to environmental cues (e.g. food availability) may alter krill advective trajectories (Lascara et al. 1999b, Murphy et al. 2004). In addition, active krill migration may play an important role in krill distributions, particularly in areas with lower current velocities (Murphy et al. 2004). Krill distributions near the Antarctic Peninsula show patterns unlikely to result from advection alone, with clear segregation of size and maturity stages suggesting that ontogenetic migrations may in part explain observed spatial patterns (Siegel 1988, Watkins et al. 1992, Trathan et al. 1993, Lascara et al. 1999b, Richerson et al. 2015). Krill also exhibit seasonal changes in habitat use, suggesting that behavior is responsible for seasonal variations in distribution (Lascara et al. 1999b); however, a baseline of fine-scale changes in acoustically-derived krill distribution has yet to be quantified.

Acoustic data from the United States Antarctic Marine Living Resources (US AMLR) Program collected around the South Shetland and Elephant Island areas

provides an opportunity to investigate how krill distributions vary across both long (interannual) and short (monthly) time scales. The data were collected during the austral summers of 1997-2011, with sampling repeated twice in 11 of 16 years, allowing comparisons of krill distributions early (January) and later (February) in the spawning season. In particular, I examine 1) interannual patterns in abundance and distribution; 2) intraseasonal changes in abundance and distribution; 3) statistical descriptions of krill spatial aggregation and organization 4) connections between krill abundance and variability with indices of environmental forcing (ENSO and Southern Annular Mode or SAM). I conclude that climate fluctuations influence interannual fluctuations in krill abundance and aggregation, while factors such as behavior and advection may drive intra-annual changes in krill abundance and distribution.

Methods

Survey area

The US AMLR Program study area is located around the South Shetland Islands, near the NAP (Figure 3.1). This is an area of complex bathymetry and circulation, with contributions from the Antarctic Circumpolar Current, the Weddell Gyre, and the Antarctic Coastal Current (Thompson et al. 2009b). The varied bathymetry of the area includes the continental shelf around the islands as well as deeper waters in the Bransfield Strait and Drake Passage. This area is also a major krill fishing ground (Jones and Ramm 2004) and home to large numbers of a variety

of krill predators (Reiss et al. 2008, Santora and Veit 2013), making it of particular concern to management.

Survey methods

The US AMLR Program conducted annual surveys in the pelagic and coastal waters near the South Shetland Islands during the austral summers (January to March) of 1988-2011. These surveys occurred in a fixed sampling grid and collected a variety of oceanographic, biological, and acoustic data, with a focus on krill demographics, abundances, and distributions. Through 1996, all surveys were performed in the Elephant Island strata, covering an area of 43,865 km^2. In 1997, the survey grid was expanded to two other strata: West (38,542 km^2 in area located north of north of King George and Livingston Island) and South (24,479 km^2 in the Bransfield Strait) (Figure 3.1); thus, I focus the analyses on the years from 1997-2011. In 2002, a fourth area, Joinville Island (18,151 km^2 located northeast of Joinville Island) was added; however, total survey effort was low here. Transects in the Elephant Island and Joinville Island areas run north-south, while transects in the West and South areas run northwest-southeast (Figure 3.1). In most years, two survey legs were completed approximately a month apart, with one in mid-summer (typically January to early February) and one in late summer (typically February to early March). However, in 1997, 2006, 2007, and 2009 only the first leg was completed, and in 2000 only the second leg was completed; see Table 3.1 for a summary.

The AMLR program uses multifrequency echosounders (38, 120, and 200 kHz) to survey the abundance and spatial distributions of krill in the upper 200 m of the water column within the study area (for full details of the acoustic survey see Hewitt et al. 2003 and Reiss et al. 2008). Briefly, volume-backscattering strengths (S_v, Db) were recorded during daylight hours along survey tracklines. These data were converted into the integrated volume–backscattering coefficient (Nautical Area Scattering Coefficient or NASC, m^2 nautical $mile^{-2}$) associated with krill, providing an index of krill abundance. These values are then further processed into a depth-integrated estimate of krill biomass concentration (g m^{-2}) using krill target strength and a weighted mean estimate of krill mass.

Krill time series and spatial variability indices

Both spatial organization and abundance of prey affect predator foraging success; thus, I focused this analysis of the krill preyscape on measures of krill abundance (*ie* mean and standard deviation of biomass) and patchiness (*ie* spatial autocorrelation and aggregation). Because krill tend to show spatial segregation during the summer with juveniles concentrated on the continental shelf, adults near the shelf slope, and spawning females off-shore (Nicol 2006), I grouped observations by habitat type (on shelf, <500 m depth, shelf slope 500-1000 m and off shelf >1000 m). I calculated mean, variance, and standard deviation of krill density in mid and/or

late summer in each habitat, as well annual values across the entire study area. I define a standardized abundance anomaly Z_y as

$$Z_y = \frac{x_y - \bar{x}}{s} \qquad (3.1)$$

where x_y is the mean density in year y, $\bar{x}$ is the long term mean density, and s is the long term standard deviation of density. These calculations, and all other calculations below were done in R version 3.0.2 (R Development Core Team 2013).

To assess the interannual spatial organization of the krill preyscape, I calculated two measures of spatial krill distribution each year: global Moran's I and the negative binomial $\hat{k}$. Moran's I (Moran 1950) is a measure of spatial autocorrelation and can take values between -1 and 1, with positive values indicating a clustered distribution, negative values indicating dispersion, and values near zero indicating random distribution. The statistic is calculated as

$$I = \frac{b}{\sum_i \sum_j w_{ij}} \frac{\sum_i \sum_j w_{ij}(X_i - \bar{X})(X_j - \bar{X})}{\sum_i (X_i - \bar{X})} \qquad (3.2)$$

where b is the number of spatial units (indexed by i and j), X_i is the variable of interest at location i, and $\boldsymbol{w}$ is the spatial weights matrix such that w_{ij} is the spatial weight between locations i and j. I used the *ape* package (Paradis et al. 2004) to calculate this statistic in mid- and/or late summer of each year. This package uses an inverse distance weighted spatial weights matrix, so I used the *spdep* package (Bivand and Piras 2015) to compare the results to values of Moran's I calculated

using binary and variance-stabilizing weighting methods. These results were very similar to values produced using the inverse distance weighted matrix, so I did not report them here.

The Negative Binomial Distribution (NBD) is commonly used to describe observations that are overdispersed in space or time. If a discrete random variable N (for example, the number of krill swarms) follows the NBD then

$$\Pr\{N = n\} = \frac{\Gamma(k+n)}{n!\Gamma(k)}\left(\frac{k}{k+m}\right)^{k}\left(\frac{m}{k+m}\right)^{n} \qquad (3.3)$$

where m is the mean and k is the overdispersion parameter (Mangel 2006). The NBD can also be thought of as a Poisson-gamma mixture; that is, the random variable follows a Poisson distribution where the Poisson parameter is drawn from a gamma distribution. The parameter k can be used as a measure of the degree of aggregation, with values below 1 describing observations that are highly aggregated (Mangel 2006, Mangel and Smith 1985, White and Bennetts 1996). As $k \to \infty$, the NBD converges to the Poisson distribution, and as $k \to 0$ it converges to a logarithmic series distribution. The variance is

$$Var[N] = m + \frac{m^2}{k} \qquad (3.4)$$

so that the method of moments estimator for k is

$$\hat{k} = \frac{\bar{N}^2}{S^2 - \bar{N}} \qquad (3.5)$$

where $\bar{N}$ is the sample mean and S^2 is the sample variance. Using the mean and variance of krill concentrations, I calculated $\hat{k}$ for mid and/or late summer in each habitat in each year.

For mapping, I gridded the survey area into 1000 km^2 cells and calculated spatial mean and standard deviation of krill biomass density (g m^{-2}) in each cell in each year, using the Raster package (Hijmans 2014). In years when surveys were done in both mid summer and late summer, I gridded the data for each leg separately. I also calculated mean krill biomass in each cell across years to examine overall trends and intra-seasonal variability.

SAM and ENSO indices

I examined several metrics of climate variability in the Southern Ocean to explore potential relationships between environmental forcing and krill abundance and distribution. The Southern Annular Mode (SAM) describes the north-south movement of westerly winds around Antarctica. The El Niño Southern Oscillation (ENSO) affects sea ice dynamics around the Antarctica and is connected to krill recruitment success around the NAP (Loeb et al. 2009b). I used two measures of ENSO: the Niño 3.4 Index, a measure of sea-surface temperature anomalies in the equatorial Pacific, and the Southern Oscillation Index (SOI), a measure of large-scale air pressure fluctuations that coincide with El Niño and La Niña events. I obtained

SAM data from the British Antarctic Survey's Ice and Climate Division (http://www.nerc-bas.ac.uk/icd/gjma/sam.html). Data on the El Niño 3.4 Index and SOI were obtained from the NOAA Climate Prediction Center (http://www.cpc.ncep.noaa.gov/). For all analyses, I used 3-month rolling average values of climate variables in order to construct seasonal indices of climate conditions. I calculated correlations (Pearson) between krill time series (mean density, standard deviation of density, Moran's *I*, and $\hat{k}$) and climate indices lagged up to 36 months. I chose this range because krill are long-lived with a 6-7 year lifespan (Siegel 1987), and their reproduction is closely tied to ice extent, duration, and timing of retreat (Siegel and Loeb 1995, Quetin and Ross 2001). Thus, ice conditions that promote preconditioning and enable early and multiple spawning events may show signatures in krill abundance and demography several years in the future.

Results

Interannual variability

Mean krill density varied greatly during 1997-2011, from a high of 171.9 g m^{-2} in 1997 to a low of 9.4 g m^{-2} in 2002 (Figure 3.2). Anomalies of krill abundance indicate relatively high overall krill abundance in years 1997, 1998, 2000, 2007, 2008, and 2009; lower abundance appeared in years 1999, 2001, 2002, 2004, 2005, and 2006 (Figure 3.3). In some years, there was considerable variation across

habitats and within the summer season. For example, in 2011, the on shelf anomaly was 0.27 in midsummer, but -0.12 in late summer, and 1997, the off shelf anomaly was nearly three times that on shelf.

Moran's *I* was consistently positive, indicating some spatial autocorrelation in acoustic observations, but showed considerable variation across time (Figure 3.4). It ranged from -0.0099 in 1999 to 0.50 in 2007, indicating that the degree of spatial aggregation varied by over an order of magnitude across years. However, Moran's *I* was generally less than 0.2, indicating modest to weak spatial autocorrelation in most years and habitats. The NBD dispersal parameter $\hat{k}$ showed a similar degree of variation, ranging 0.2 in 2002 from to 0.65 in 2008 (Figure 3.5). Estimates of Moran's *I* and $\hat{k}$ were uncorrelated, suggesting that these two indices characterize patchiness in different ways (Figure 3.6).

Seasonal variability

Mean biomass concentration values in midsummer and late summer across all years combined were significantly different (Welch two-sample t-test, $p<0.001$), indicating that the overall abundance and/or detectability of krill in the study area tended to decrease as summer progressed. However, this pattern was not consistent across years. In 9 of the 10 years in which the area was surveyed in both mid- and late summer, mean krill biomass concentration declined across surveys, but the decrease

was significant in only 4 of these years (Table 3.2). In one year (2005), there was a significant increase in mean density across the season. In Figure 3.7, I show mean biomass in midsummer versus late summer, with values falling below the identity line indicating years with declining mean biomass across the season.

On average, the greatest krill abundance measures were found north and west of Elephant Island, the southern part of the Bransfield Strait, and along the north side of the South Shetland Islands (Figure 3.8). Average distributions of krill abundance appear to contract across the season, with larger areas with low biomass concentration values and a few areas with very high biomass concentration (Figure 3.8).

Relationships between patchiness and abundance

I found significant linear relationships between Moran's *I* and mean biomass density in midsummer in the shelf slope habitat (p=0.016); however, there was no significant relationship in the shelf slope of on shelf habitats in midsummer or in any habitat in late summer (Figure 3.9). In contrast, $\hat{k}$ and density were positively correlated in the off shelf habitat in both mid and late summer (Figure 3.10).

Correlations with environmental indices

I found that some features of krill abundance were linked with measures of ENSO (Niño 3.4 anomaly and SOI) at approximately 2-2.5 year lags. In particular, I found that mean krill biomass was significantly (p<0.05) negatively correlated with SOI lagged 26-27 and 29-32 months, and that the standard deviation of krill biomass was negatively correlated with SOI lagged 22-32 months (Figure 3.11). Niño 3.4 was significantly positively correlated with krill biomass at a 32 month lag, and standard deviation of biomass at 21-32 month lags. I found a significant correlation between SAM and mean biomass at a 5 and 25-26 month lags, and standard deviation of biomass at a 26 month lag. There was no significant correlation between Moran's I or $\hat{k}$ and Niño 3.4, SOI, or SAM.

The large number of correlations tested raises the possibility of spurious correlations. However, the consistent direction and magnitude of correlations between krill abundance and ENSO indices (SOI and Niño 3.4) lagged 24-32 months indicate that these relationships are unlikely to be the result of chance.

Discussion

Intra-annual variability

Krill distributions near the Antarctic Peninsula show marked changes across seasons, suggesting the possibility of differential habitat use across time (Lascara et al 1999). In summer, krill in the West Antarctic Peninsula are abundant, found in dense aggregations, and located high in the water column, while in the fall and winter abundance and density decrease and krill move deeper in the water column (Lascara et al. 1999b, Ashjian et al. 2004, Lawson et al. 2004). Though the two legs of the data only cover a small part of the entire year, the late summer data may capture the beginning of an autumnal change in habitat. Krill abundance was on average lower in late summer than in midsummer, indicating either fewer krill in the area, or fewer krill in the upper 200 m of the water column where they are detectable by acoustics. Benthic foraging has been observed in krill (Gutt and Siegel 1994, Schmidt et al. 2011), and there is evidence that adult krill may overwinter closer to the sea floor (Gutt and Siegel 1994, Lawson et al. 2004). Thus, the decrease in abundance in late summer may be due to krill utilizing deeper habitat out of reach of acoustics; or alternately leaving the study area entirely through advection, mortality, or migration. However, this decrease was not consistent across years, indicating that other factors are influencing intra-seasonal movement of krill in the study area. Krill spawn in the summer, with spawning aggregations concentrated in off shelf and oceanic waters,

and the particular environmental conditions of a particular year may influence when these aggregations form and disperse.

The relationship between spatial autocorrelation and mean density also varied across mid- and late summer, with a significant positive correlation between global Moran's *I* and mean density in midsummer shelf slop habitat, but not late summer. However, the relationship between $\hat{k}$ and abundance was consistent across mid- and late summer in the off-shelf habitat. This indicates that the relationship between some measures patchiness and abundance at the habitat scale may change across the summer season; however this is only true for patchiness as measured by spatial autocorrelation (Moran's *I*).

Interannual variability

My results show strong interannual variability in both krill abundance and patchiness, consistent with other studies in this area (Reiss et al. 2008, Santora et al. 2009). When only considering data from leg 1, the years with the largest mean anomaly occurred in 1997-8, 2003, and 2007-8, generally consistent with the 5-6 year cycles of krill populations in the West Antarctic Peninsula suggested by Quetin and Ross (2003) (note that the area was only surveyed in late summer in 2000). However, averaging over both legs presents a less clear picture, with positive anomalies in 1997-8, 2000, 2003, and 2007, 2008, and 2009. Though survey effort was not always consistent across years or across legs, making comparisons difficult, it may be that seasonal changes in habitat use (as suggested by Lascara et al. 1999) may alter

abundance of krill measurable by these surveys across the mid- to late-summer season.

Spatial Variability

Spatial organization (*ie* the degree of aggregation) of krill also varied across years. In years with higher krill abundance, there was a tendency towards a patchier spatial distribution (high Moran's *I* and low negative binomial $\hat{k}$), but this relationship was not consistent across habitats, season, or measure of patchiness. This indicates that under some conditions, krill abundance and patchiness are linked, with important consequences for krill-dependent predators. The apparent lack of a relationship between Moran's *I* and $\hat{k}$, and the difference between the patchiness-abundance relationships calculated with these two statistics indicate that they describe spatial aggregation differently. This is unsurprising because Moran's *I* uses a spatial weights matrix to describe how observations near in space relate to each other relative to more distant observations. In contrast, $\hat{k}$ an estimator for the shape parameter of the NBD, which can arise when organisms are distributed over a landscape according to a Poisson distribution with a mean drawn from a gamma distribution (Anscombe 1950). Thus, the NBD offers a convenient model for the distribution of krill swarms across space. Predator foraging success depends on both abundance and distribution of krill (Mangel and Switzer 1998), and in years with low krill abundance, less-aggregated krill may make foraging more expensive, compounding the consequences of low-krill years for predators. Estimates of $\hat{k}$ could be used to inform models of

predator foraging under differing krill conditions. For example, one could generate a number of krill landscapes representing the range of conditions (from low abundance-low patchiness to high abundance-high patchiness) and explore foraging behavior and consequences for predators (e.g. Cresswell et al. 2008). This has the advantage of incorporating the effects of both krill abundance and spatial distribution on predator performance.

Climate variability

Environmental forcing is theorized to affect krill abundances by influencing winter sea ice (Wiedenmann et al. 2009). Negative phases of the SOI (which may be amplified by increasing SAM) are associated with an earlier advance and longer duration of sea ice, which results in greater primary production and better larval krill survival (Quetin et al. 2007). At the Palmer LTER in the West Antarctic Peninsula, strong recruitment events observed in 1991–1992, 1995–1997, and 2000–2003, 2006–2007, and 2010–2011 have been linked to positive chlorophyll *a* anomalies the previous year, which in turn were linked to a negative SAM phase the preceding spring (Ducklow et al. 2013, Saba et al. 2014). These peaks at least roughly correspond to the pattern of positive krill anomalies observed in the data, with peaks in 1997-1998, 2000, 2003, and 2007-8-9. However, I found that SOI appears to have a more extensive influence on krill than SAM. In the north Antarctic Peninsula, Loeb et al (2009) found a significant relationship between 1-year lagged El Niño 3.4 anomaly and krill abundance taken from net hauls. In contrast, I found suggestion of

links between mean krill and standard deviation of krill abundance and ENSO indices lagged approximately 2-2.5 years. This is the first study to our knowledge to link acoustic indices of krill in the NAP and large-scale environmental forcing, indicating that data from predator stomach samples (Saba et al. 2014), nets (Loeb et al. 2009) and acoustics (this study) may provide different information about climate and krill. In addition, the effects of ENSO on krill are not consistent across the Southern Ocean, with SAM dominating further south off the peninsula (Saba et al. 2014) and no apparent effect of ENSO at South Georgia (Fielding et al. 2014).

Conclusions

Both the abundance and spatial organization of krill are important to krill-dependent predators (Santora et al. 2009). Krill are patchily distributed at multiple scales (Murphy et al. 1988, Siegel 2005), and krill recruitment, abundance, and population structure vary across years (Quetin and Ross 2003). Understanding the processes underlying krill variability across space and time are crucial to our conception and management of the Southern Ocean ecosystem. This unique long-term data set provides a window into some of the patterns underlying krill variability in an ecologically- and commercially-important area of the Southern Ocean. Knowledge of the complex interactions between environmental conditions (both local-scale and broad-scale) and krill abundance and distribution highlighted by this study will be important in our understanding and management of the NAP. Future work should further explore the forces that underlie interannual changes in krill

abundance and distribution and this area and its relationships with dynamics both further south along the Antarctic Peninsula as well as across the Scotia Sea. In addition, much work remains in quantifying and explaining seasonal changes in krill abundance and distribution, and potential connections to behavior, species interactions, and advection.

Acknowledgements

Many thanks to the US AMLR Program for creating and sharing this data set.

Tables and Figures

Table 3.1. Details of US AMLR surveys. EI=Elephant Island, S=South, W=West, J=Joinville Island

Year	Leg 1 dates	Leg 2 dates	Strata surveyed, leg 1	Strata surveyed, leg 2
1996	1/25-2/04	2/24-3/05	EI	EI
1997	1/27-2/10	-	EI, S, W	-
1998	1/08-1/25	2/08-2/25	EI, S, W	EI, S, W
1999	1/15-1/28	2/10-2/23	EI, S, W	EI, W
2000	-	2/22-3/06	-	EI, S, W
2001	1/16-1/30	2/12-3/02	EI, S, W	EI, S, W
2002	1/16-1/29	2/24-3/08	EI, S, W, J	EI, S, W, J
2003	1/14-1/26	2/10-2/25	EI, S, W	EI, S, W
2004	1/16-1/31	2/20-3/06	EI, S, W	EI, S, W, J
2005	1/17-1/31	2/22-3/08	EI, S, W, J	EI, S, W, J
2006	1/16-2/01	-	E, S, W	-
2007	1/11-1/26	-	E, S, W	-
2008	1/18-2/03	2/27-3/07	EI, S, W, J	EI, S

2009	1/13-1/29	-	EI, S, W, J	-
2010	1/28-2/03	2/22-3/06	EI	S, W, J
2011	1/17-2/04	2/26-3/03	EI, S, W	S, J

Table 3.2. Mean biomass concentration (g m^{-2}) of krill in mid and late summer for years with two surveys. Years with similar spatial coverage are highlighted in gray.

Year	Mid summer	Late summer	Percent change
1998	92.7	73.1	-21.1 (<**0.001**)
1999	29.8	27.3	-8.4 (0.57)
2001	29.3	10.0	-66.0 (<**0.001**)
2002	9.3	7.7	-16.7 (0.35)
2003	59.0	55.2	-6.5 (0.37)
2004	14.8	14.3	-3.4 (0.78)
2005	25.9	37.0	42.7 (**0.048**)
2008	123.7	118.8	-4.0 (0.71)
2010	71.7	27.6	-61.5 (<**0.001**)
2011	67.8	34.6	-49.0 (<**0.001**)

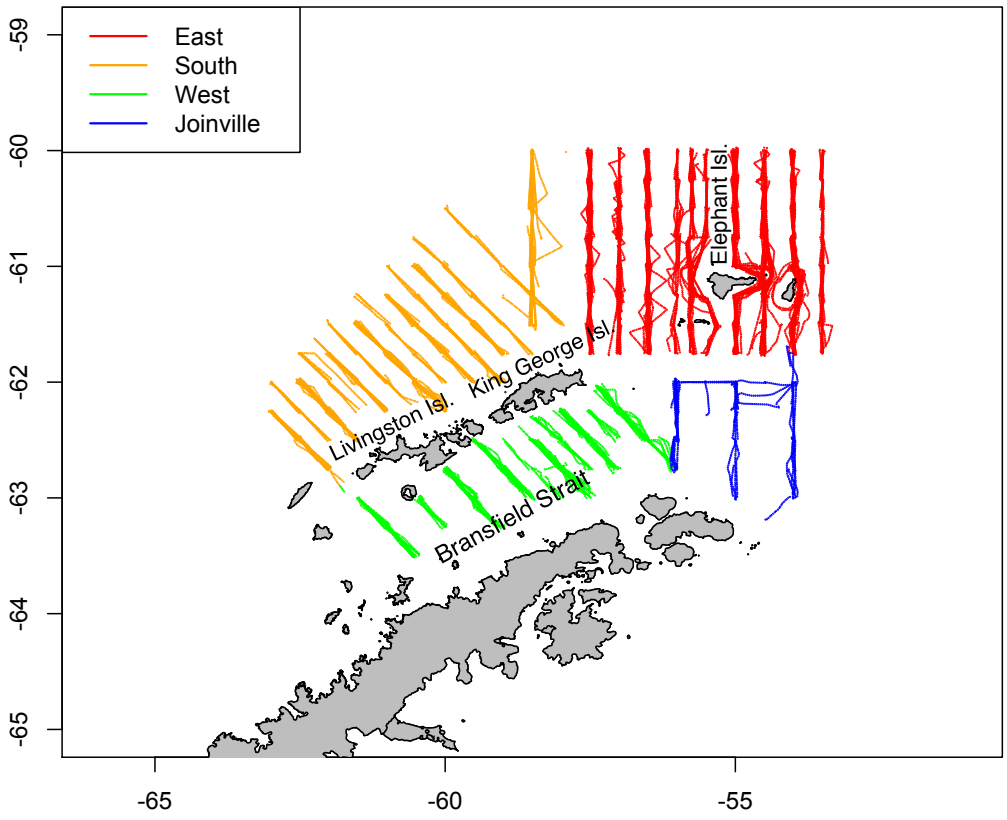

Figure 3.1. All acoustic transects lines completed 1997-2011.

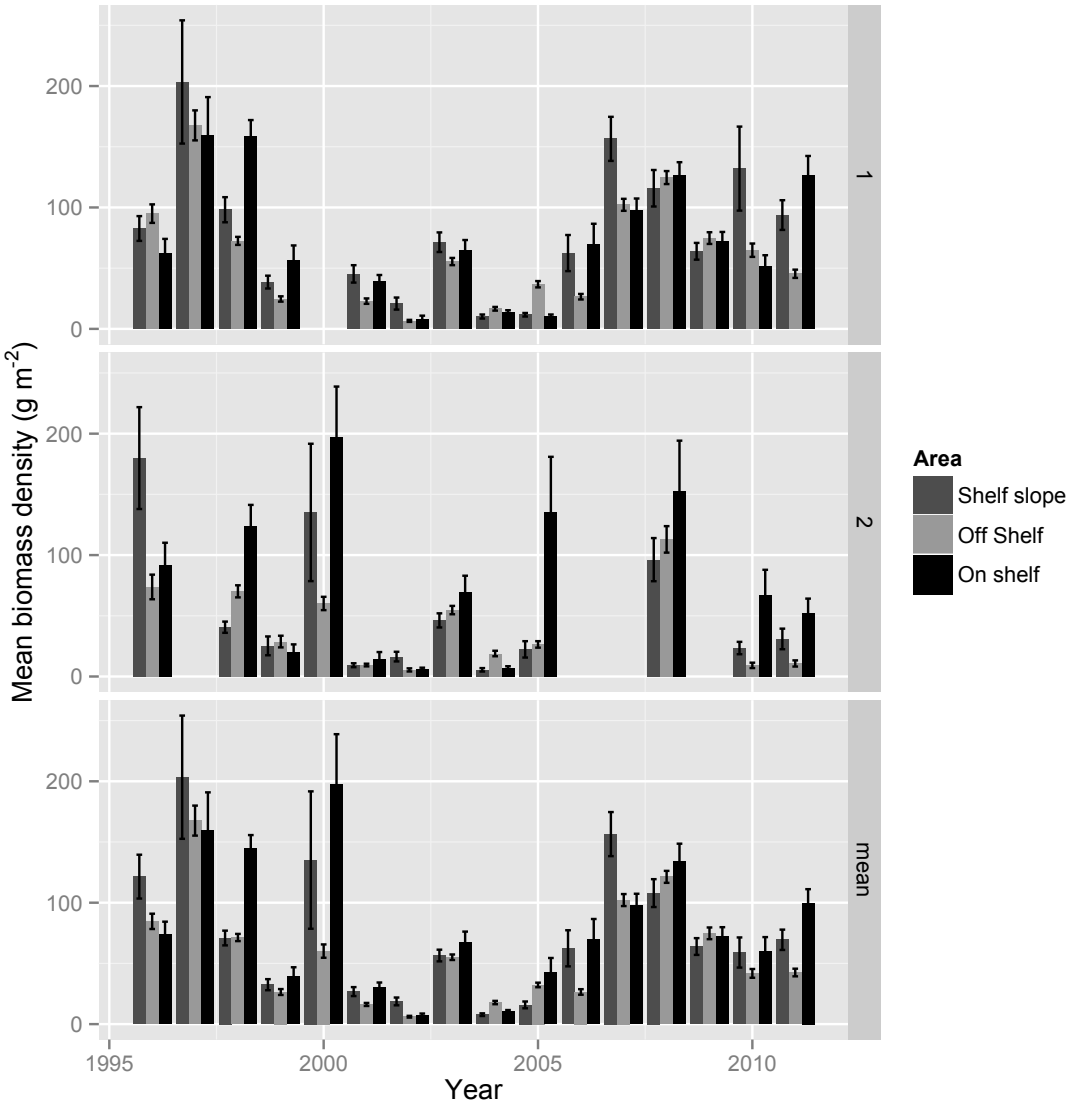

Figure 3.2. Mean biomass in midsummer (top), late summer (center) and averaged across both legs (bottom). Vertical bars represent standard error.

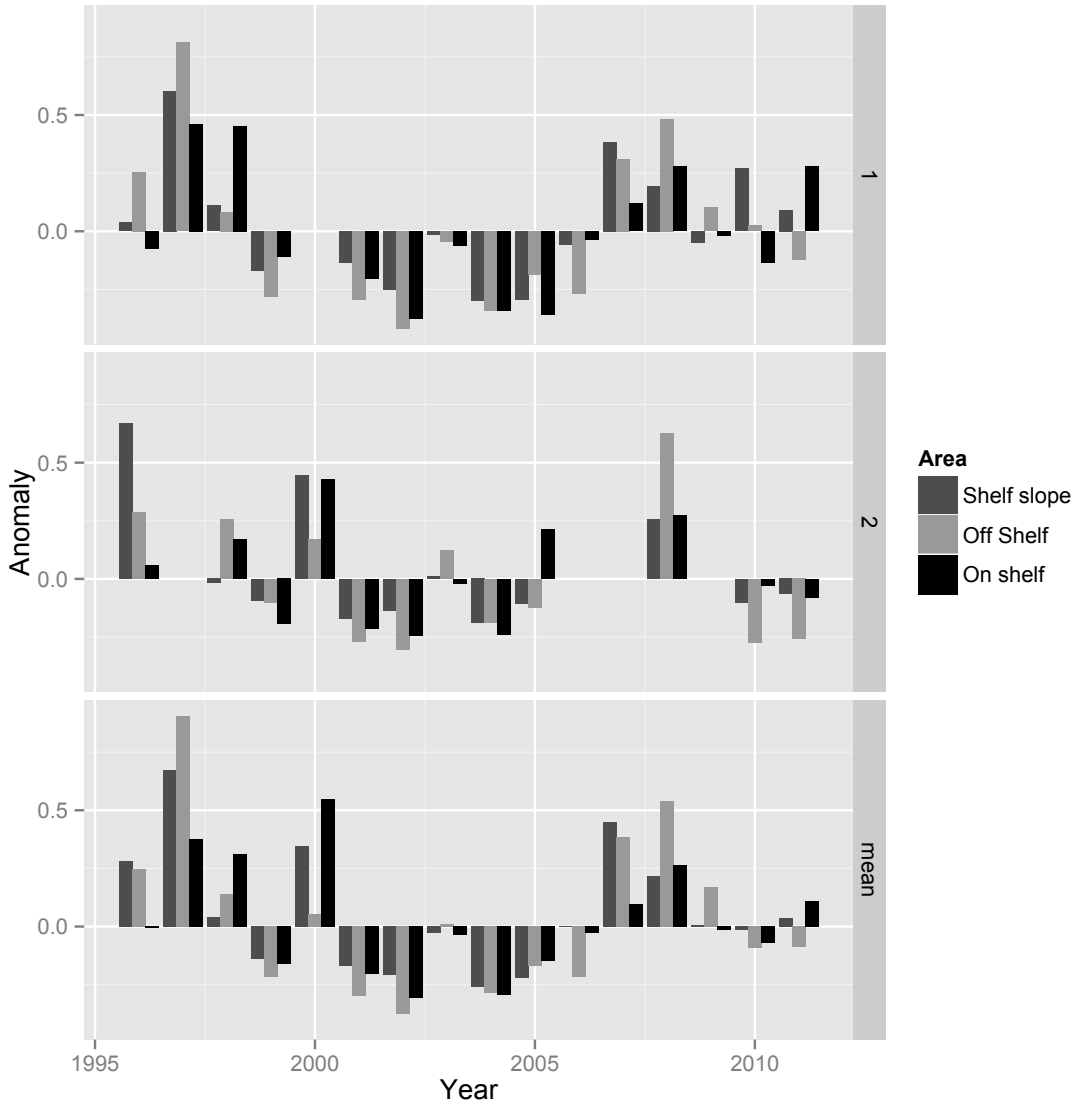

Figure 3.3. Krill anomaly in midsummer (top), late summer (center) and averaged across both legs (bottom).

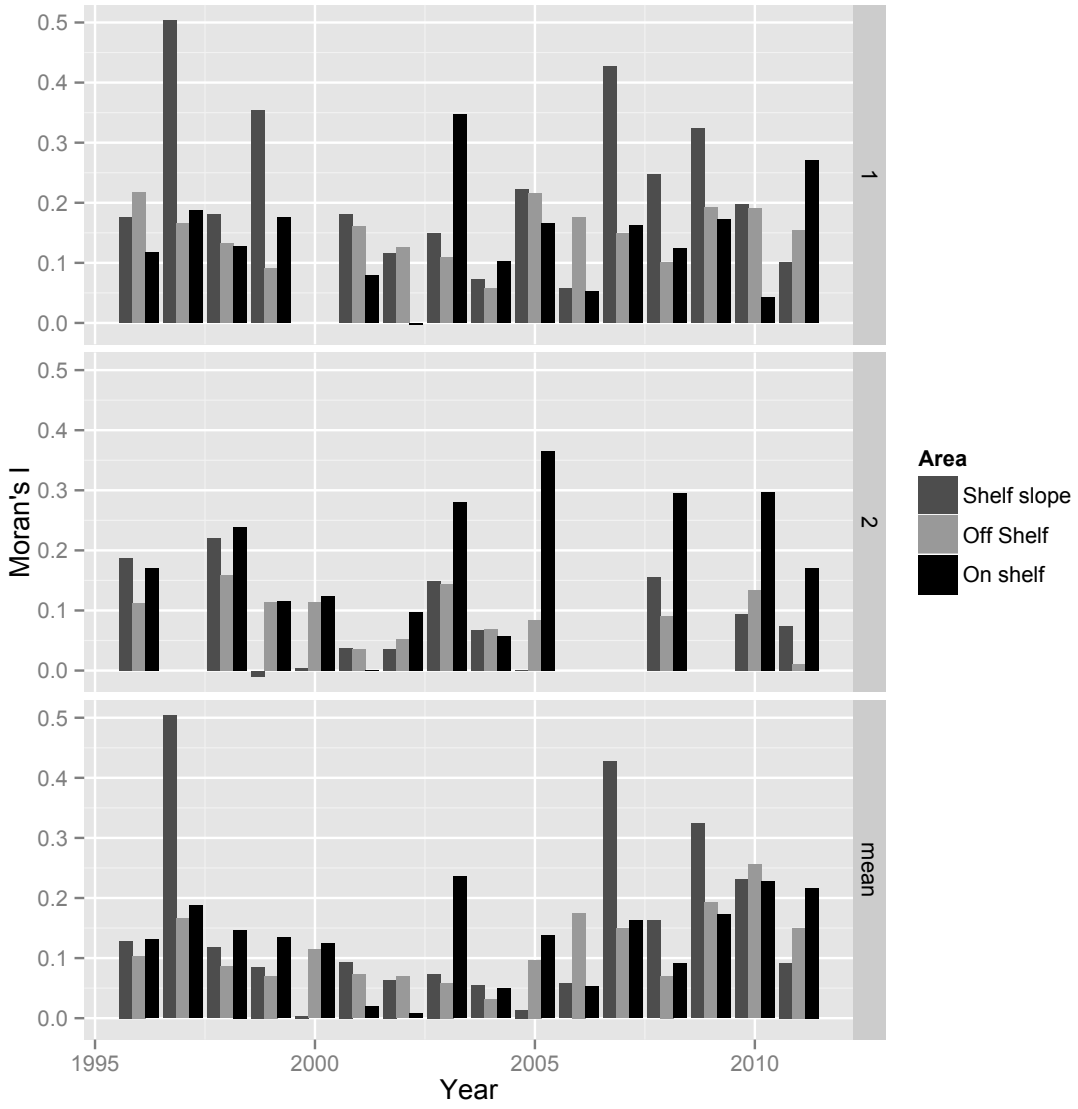

Figure 3.4. Moran's *I* in midsummer (top), late summer (center) and averaged across both legs (bottom).

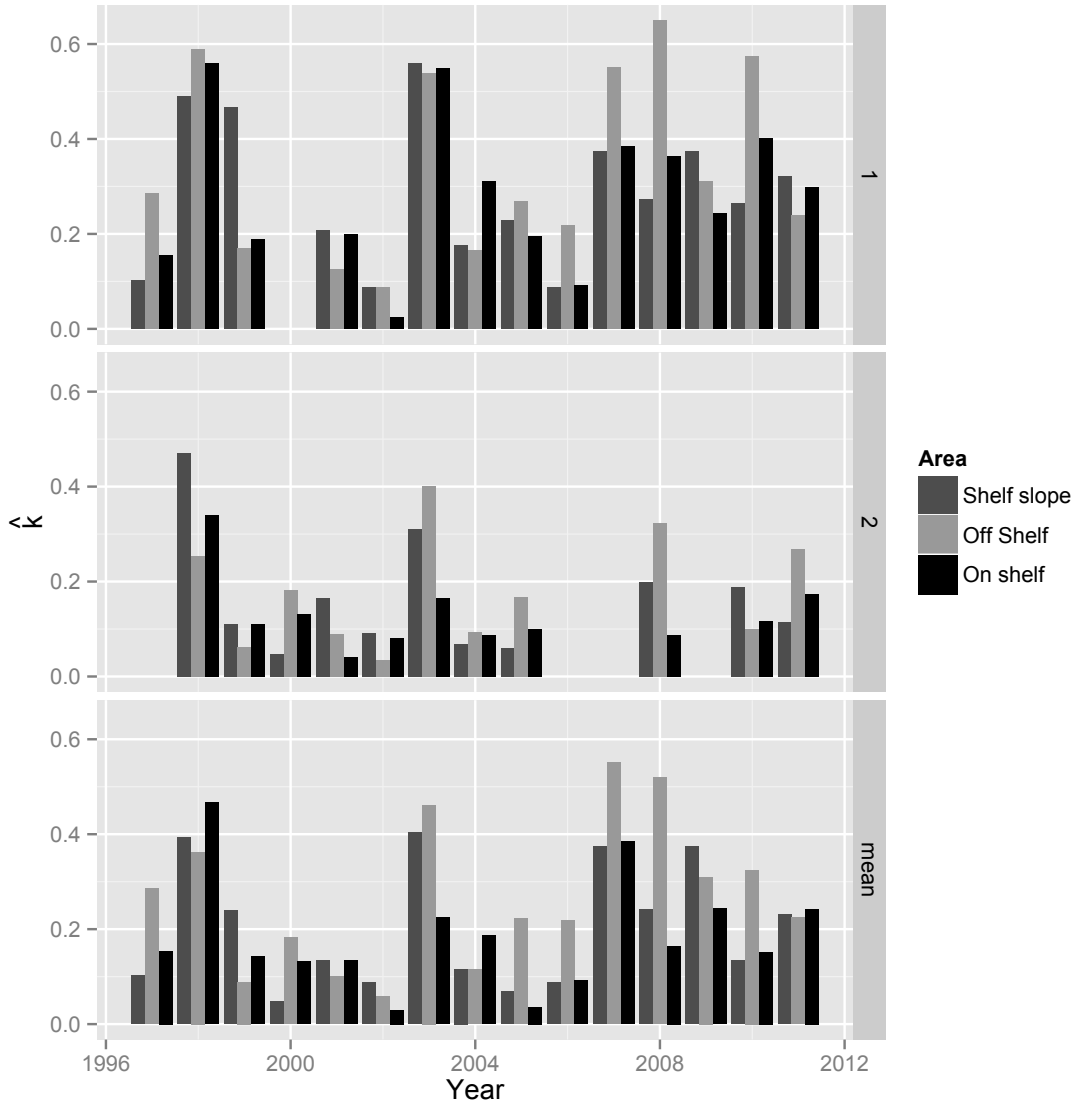

Figure 3.5. Negative binomial distribution $\hat{k}$ in midsummer (top), late summer (center) and averaged across both legs (bottom).

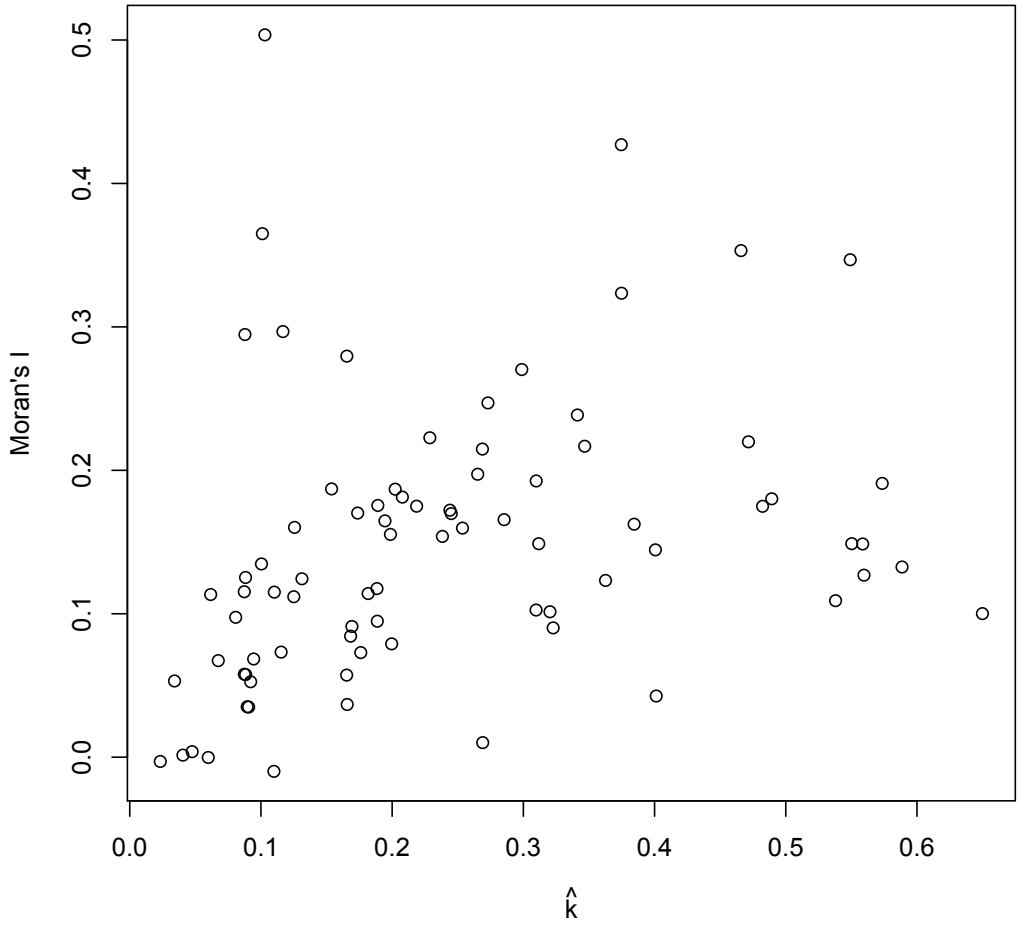

Figure 3.6. Relationship between the negative binomial distribution $\hat{k}$ and Moran's *I* across all habitats, seasons, and years.

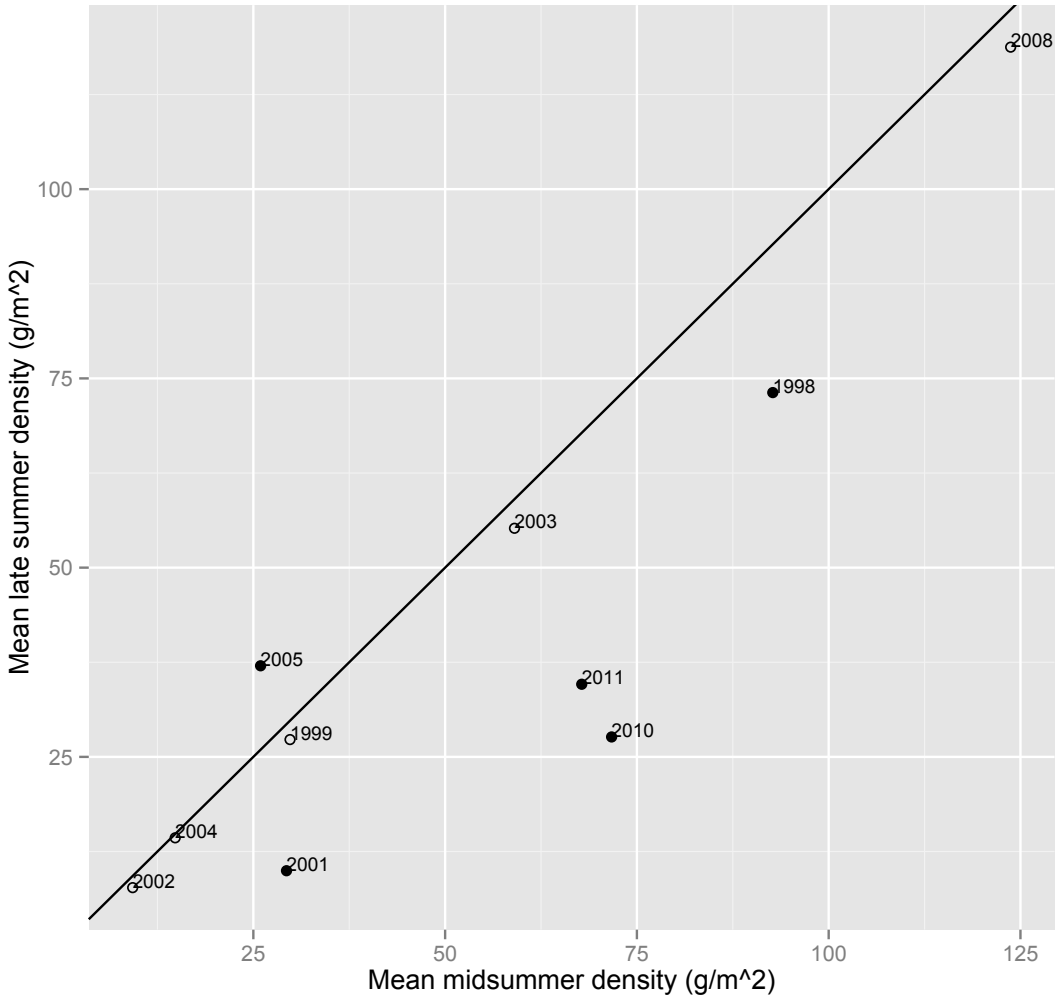

Figure 3.7. Mean krill biomass in mid and late summer, with observations falling below the identity line indicating years with lower mean density later in the summer. Filled circles represent statistically-significant differences across a season (Welch two-sample t-test, $p<0.05$).

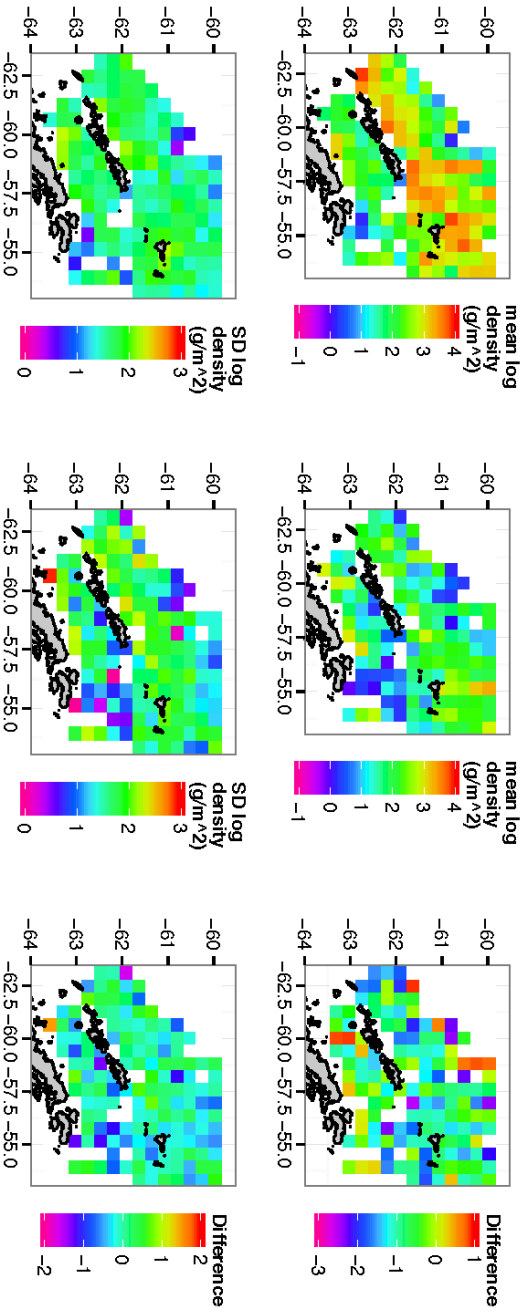

Figure 3.8. Mean and standard deviation of krill density, averaged over available years 1997-2011 in midsummer (left) and late summer (center). The difference between mid- and late summer is shown on the right.

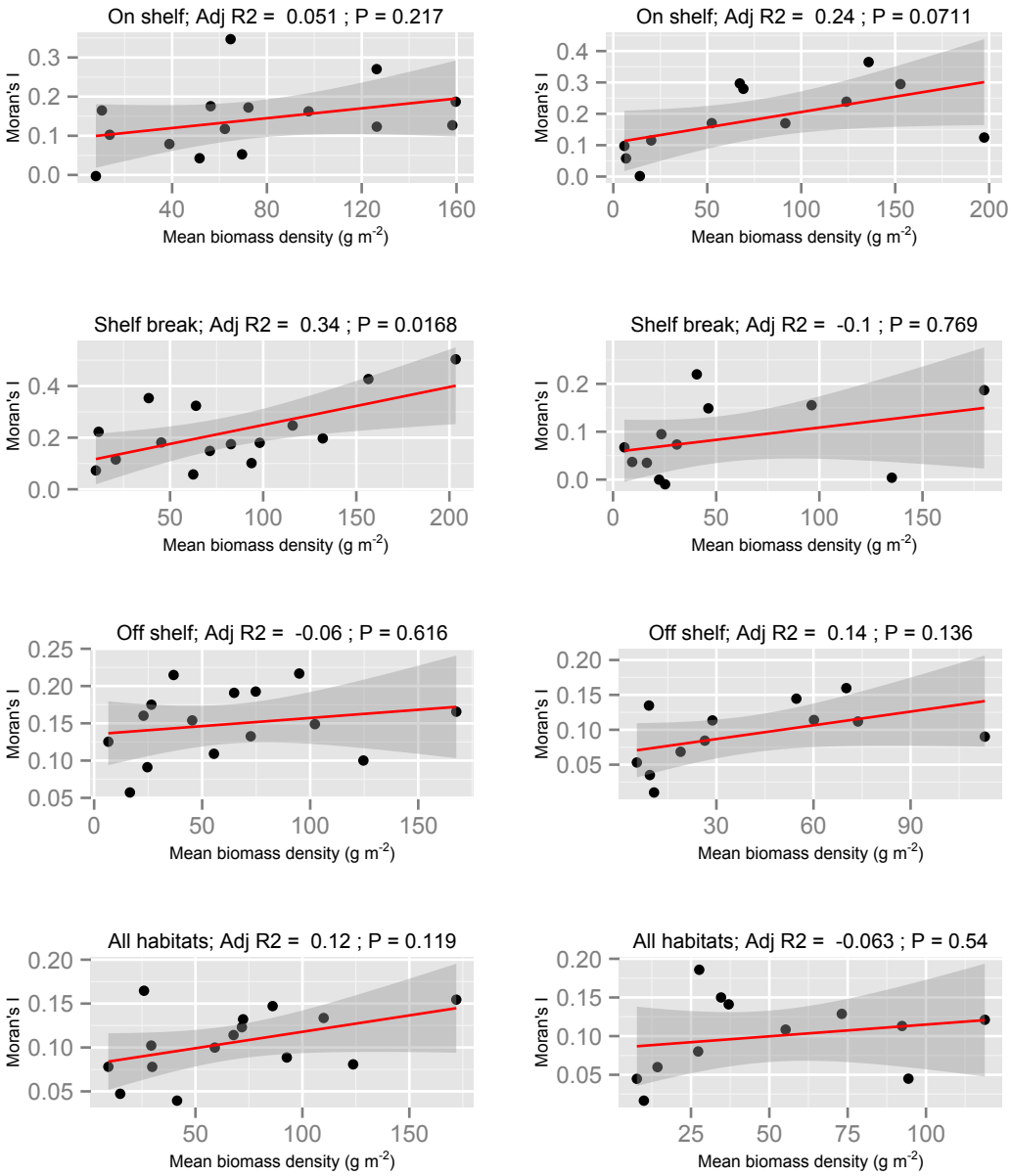

Figure 3.9. Relationships between mean biomass and Moran's *I* across areas in midsummer (left column) and late summer (right column).

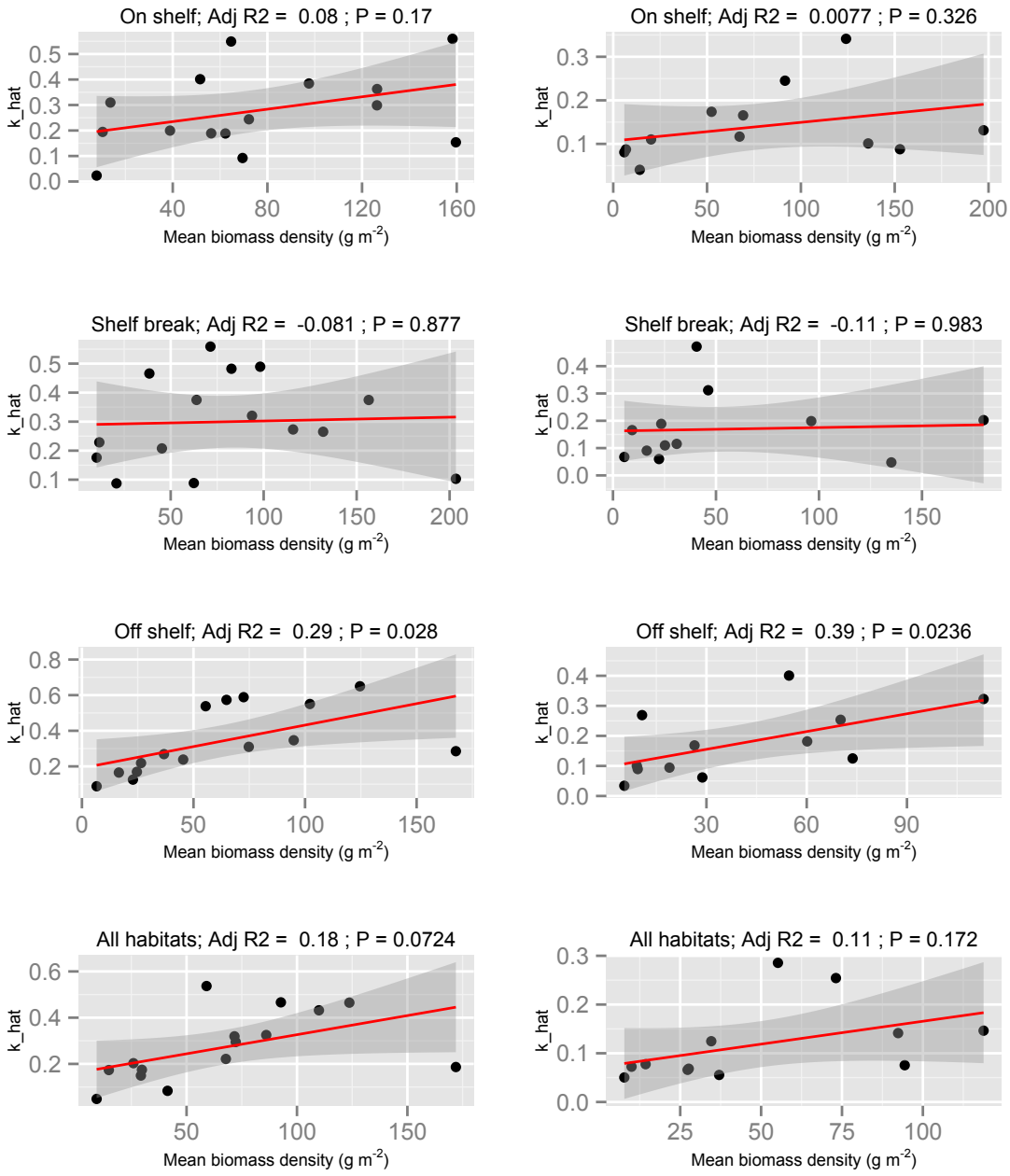

Figure 3.10. Relationships between mean biomass and $\hat{k}$ across areas in midsummer (left column) and late summer (right column).

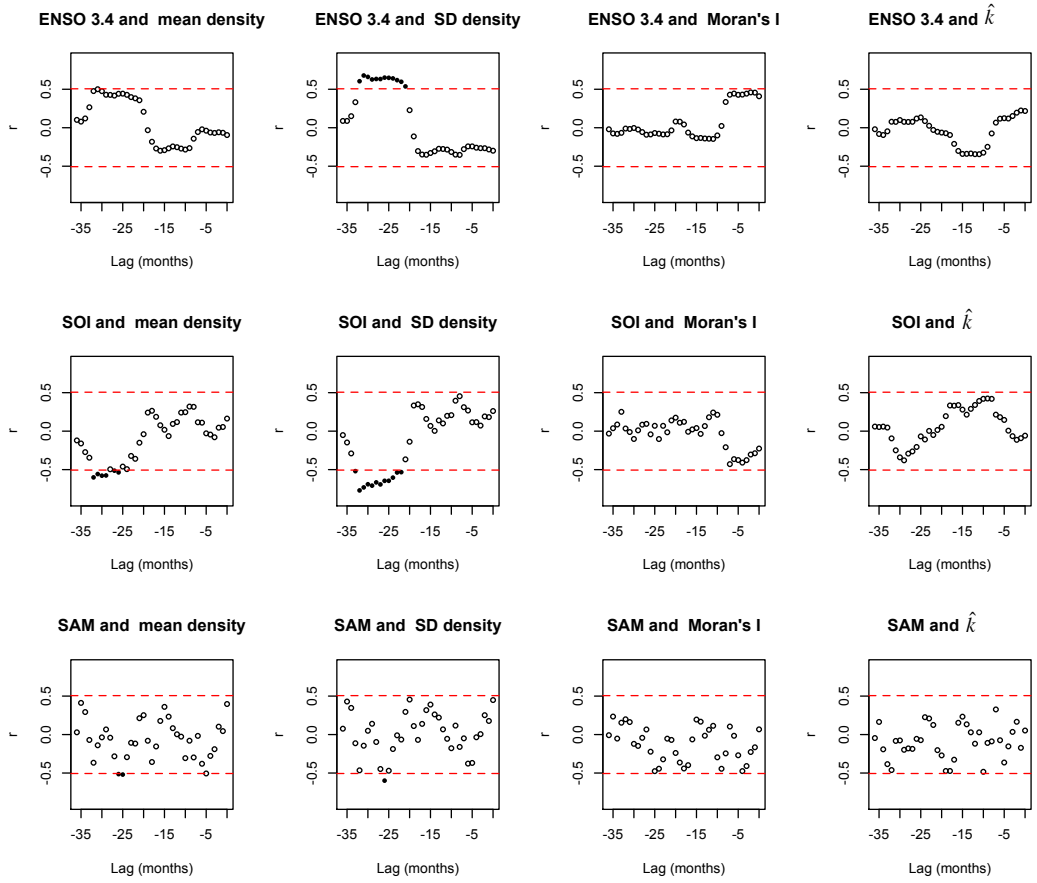

Figure 3.11. Pearson correlations between climate indices, mean krill density (g/m^2), standard deviation of krill density, global Moran's *I* and $\hat{k}$. Dashed lines represent 95% confidence intervals; filled points that fall above or below them are significant at the 0.05 level.

Chapter 4. Life history and temperature-dependent growth in *Thysanossa macrura* in comparison with *Euphausia superba* in future scenarios with a changing ocean

Abstract

Climate change is predicted to affect Southern Ocean biota in complex ways. Euphausiids play a crucial role in the trophodynamics of the ecosystem, and their status under future climate scenarios is the subject of much concern. *Thysanoessa macrura* is the most widely-distributed, numerically abundant and ubiquitous euphausiid south of the Polar Front. Its large and widespread biomass suggests that its trophic importance may be underappreciated. In addition, since it is eurythermic *T. macrura* may be better able to tolerate warming ocean temperatures in comparison to the more stenothermic Antarctic krill *Euphausia superba*. I use a biomass per recruit approach to investigate how the availability of this euphausiid to predators may change as ocean temperatures increase. I contrast this to predictions about the future of *E. superba*, and find that under some ranges of temperature change, increasing *T. macrura* growth may be able to compensate for decreasing *E. superba* growth in terms of biomass available for predators. However, in spite of its considerable

biomass, other aspects of this species such as its size and habitat may limit its potential to replace *E. superba* in the diet of many predators.

Introduction

The ongoing effects of climate change on the Southern Ocean are numerous and varied. Over the past decades, notable changes include a reduction in stratospheric ozone (reviewed in Thompson et al. 2011) and associated change in wind patterns (Marshall et al. 2006), with consequences for ocean circulation and sea ice dynamics (Stammerjohn et al. 2008a). Ocean waters have been warming (Turner et al. 2009, Schmidtko et al. 2014) and freshening (Rintoul 2007, Hellmer et al. 2011). Sea ice has been declining in some areas and the total sea ice extent is projected to decrease by a third over the twenty-first century (Bracegirdle et al. 2008). The Southwest Atlantic region has seen particularly rapid warming over the twentieth century, with sea surface temperatures increasing by ~1.3 ºC around the Antarctic Peninsula since the 1950s (Meredith and King 2005) and ~2.3ºC near South Georgia since the 1920s (Whitehouse et al. 2008a). Such rapid environmental changes have led to concerns over the future of Antarctic krill (*Euphausia superba*) populations, particularly in the Southwest Atlantic region (reviewed in Flores et al. 2012a). *E. superba* is a major prey source for many species of fish, squid, seabirds, and marine mammals, forming a crucial link between primary production and higher tropic levels (Smetacek and Nicol 2005). Antarctic krill recruitment is correlated with the extent and duration of winter sea ice, and the long-term decline in krill abundance in the

Southwest Atlantic has been linked to changes in sea ice extent and duration (Siegel and Loeb 1995, Atkinson et al. 2004, Wiedenmann et al. 2009). In addition, changing ocean temperatures may affect the biomass and population structure of *E. superba*, and consequently its availability to predators (Wiedenmann et al. 2008). Thus, the future of *E. superba* and its predators remains uncertain.

Though *E. superba* is widely considered the most important euphasiid in the Southern Ocean, there are six euphausiid species found south of the Polar Front that may also make important contributions to predator diets (Cuzin-Roudy et al. 2014). Of these, *Thysanoessa macrura* is the most abundant, common, and widespread, with a larger geographic range than *E. superba* and populations that frequently outnumber *E. superba* in some locations and seasons (Nordhausen 1992, Dietrich et al. 2011, Marrari et al. 2011a, Steinberg et al. 2015). Few studies have attempted to quantify the population dynamics of *T. macrura*, but its numbers appear to be increasing in at least some parts of the Antarctic Peninsula (Steinberg et al. 2015). At this time, *T. macrura* forms a significant component of the diets of a number of predator species, including seabirds (Bocher et al. 2000, Connan et al. 2008), penguins (Deagle et al. 2007), fish (Williams 1985), and whales (Nemoto and Nasu 1958). For some predators, *T. macrura* is an important alternate food source in years when *E. superba* is scarce (Kock et al. 1994). In addition, *T. macrura* is a relatively high-quality prey item in terms of lipid content and energy density (Ruck et al. 2014). In light of its abundance and broad distribution, the importance of this species for the ecosystem may have been underestimated (Nordhausen 1992).

The little we know about the life history of *T. macrura* indicates that its life history clearly differs from that of *E. superba*. In contrast to the large and long-lived *E. superba*, *T. macrua* reaches a smaller asymptotic size of 38-45 mm (versus 60 mm in E. superba; Siegel 1987, Driscoll 2013, Haraldsson and Siegel 2014), and it has a shorter lifespan of ~4 years (versus up to 9 years in E. superba; Siegel 1987), a more carnivorous diet (Kattner et al. 1996, Hagen et al. 2001), and earlier spawning season in the late winter and early spring (Makarov 1979). Because *T. macrura* is eurythermic, with the widest latitudinal range of all Southern Ocean euphausiids (Cuzin-Roudy et al. 2014), there is speculation that it may be less affected by warming ocean temperatures in comparison to the stenothermic *E. superba*. This differential response to changing thermal conditions may affect the availability of euphausiids to predators in the future.

Over the twenty-first century, summer Sea Surface Temperatures (SSTs) south of 60ºS are projected to rise between 0.5ºC and 1.25º, while winter SSTs are predicted to change between -0.25ºC and 0.1ºC (Turner et al. 2009). Regardless of season, bottom waters on the shelf at 200 m are expected to rise 0.5ºC and 0.75ºC in most areas, and temperatures of waters from the surface down to 4,000 m along the continental margin are predicted to rise 0.25-0.5ºC. Because euphausiids are ectotherms, changes in the thermal habitat are likely to have important consequences for growth, maturation, and mortality (Pörtner 2010). In addition, Antarctic marine organisms are particularly sensitive to changes in temperature (Peck et al. 2010). Wiedenmann et al. (2008) found that increased ocean temperatures may have

profound effects on the biomass of *E. superba* available to predators. Here, I explore how changing temperatures may affect the growth and biomass of *T. macrura* and contrast it to the possible fate of *E. superba*. In particular, I focus on the biomass per recruit expected to be available to predators for each of these two species under different temperature scenarios.

Methods

Overview

I use a biomass per recruit (BPR) approach to explore how changing temperatures may affect the biomass of *T. macrura* available to predators may change with changing temperatures, and contrast this with that of *E. superba.* BPR is defined as the expected lifetime biomass of a recruit and can be used as a measure of the biomass available to predators. The BPR approach requires a 1) an estimate of natural mortality and 2) a temperature-dependent growth model. Because these processes have not been fully described for *T. macrura*, below I describe approaches for estimating mortality and temperature-dependent growth in this species.

1. Estimating model parameters

Mortality and maturity

The Growth-Maturity-Longevity (GML) theory of (Beverton 1992) relates the optimal size/age at maturity, growth (in terms of the von Bertalanffy *k*) and natural mortality of fishes. I use this approach to obtain an estimate of mortality for *T. macrura*. According to the GML theory, the expected fecundity ϕ of an individual that matures at age *a* is

$$\phi(a) = e^{-Ma} cL(a)^b \qquad (4.1)$$

where *k* is the von Bertalanffy growth coefficient, *M* is natural mortality, and *b* is the scaling exponent that characterizes the relationship between length and fecundity. Length at age *L(a)* is given by the von Bertalanffy equation

$$L(a) = L_\infty (1 - e^{-ka}) \qquad (4.2)$$

where L_∞ is asymptotic size. The optimal age at maturity a^* is commonly understood to be the age at which 50% of individuals in a cohort would be expected to be mature and is thus

$$a^* = \frac{1}{k} \ln\left(1 + \frac{bk}{M}\right) \qquad (4.3)$$

The length at the optimal age of maturity is then

$$L(a^*) = L_\infty \left(\frac{b}{b + M/k} \right) \qquad (4.4)$$

where L_∞ is the asymptotic length. If M is unknown, and a^*, b, L_∞ and k are known this can be rearranged to solve for M

$$M = kb\left(\frac{L_\infty - L(a^*)}{L(a^*)} \right) \qquad (4.5)$$

Because the reproductive ecology of *T. macrura* has not been fully described, I used empirical measurements to estimate *L(a*)* assuming that it is equivalent to the length at which 50% of females are mature during the spawning season.

Along with collaborator R. Driscoll, I measured and staged 2,006 *T. macrura* specimens obtained during the United States Antarctic Marine Living Resources (US AMLR) Program cruise performed August-September 2014 around the South Shetland and Elephant Islands. The goal of this work was twofold: to develop a staging metric and baseline for *T. macrura* winter reproductive status for use in future projects, and to estimate the size at maturity that can be used with the GML theory to provide an estimate of natural mortality.

Samples were preserved in 5% buffered formalin and examined using a standard dissecting scope. A standardized method for staging the maturity of *T. macrura* has not been developed; however, the method of Makarov and Denys (1981)

developed for *E. supberba* has been used to stage *T. macrura* (Färber-Lorda 1994). Because some characteristics (partially developed petasmas and the color of thelycum or ejaculatory duct) were not easily distinguishable in our preserved samples, we developed a slightly simplified version of the classification method used by Makarov and Denys (1981). Note that while in theory stage IV (spent females) should exist, we concluded that our samples were taken early enough in the breeding season that this stage was not present in our samples. We also recorded the presence of internal (males) and external (females) spermatophores. In Table 4.1, I show the staging classifications.

Length frequencies of juveniles and adults appear to indicate near knife-edge maturity, with little size overlap between immature and reproductive individuals and maturation occurring between 10-12 mm (Figure 4.1). Less than 1% of juveniles were larger than 11 mm; thus, I set $L(a^*)$=11.

As fecundity scales linearly with length in *E. superba* (Nicol et al. 1995) I assume the fecundity-length relationship in *T. macrura* takes a similar form and set b=1. A range of von Bertalanffy growth parameters for *T. macrura* have been reported in the literature, possibly due to variation in environmental conditions and sampling season. I use these sets of parameters and Eqn 4.5 to generate a plausible range of natural mortality rates (Table 4.2).

Growth

Method I: Quadratic growth curve

Driscoll et al. (2015) found that daily growth rate (DGR) in *T. macrura* was strongly positively correlated with water temperature over the range sampled (0.7-2.4 °C). However, though the authors found a linear relationship between growth and temperature, over a wider range of temperatures we would expect to see a dome-shaped temperature-growth curve, as is typical of other ectotherms including *E. superba* (Atkinson et al. 2006). Driscoll et al. (2015) measured *T. macrura* living in waters near the lower end of their broad thermal range (-1.8-8 °C, Cuzin-Roudy et al. 2014), indicating that peak growth rates likely occur above of the range measured. Thus, I use a modified version of the growth model developed by Atkinson et al. (2006) for *E. superba* to estimate growth in *T. macrura* over a range of temperatures. The model of Atkinson et al. (2006) models the DGR (mm d^{-1}) of *E. superba* as a function of length *L* (mm), chlorophyll *a* concentration (a proxy for food availability; mg m^{-3}) *F* and temperature *T* (°C) as

$$DGR_s(L,F,T) = a + bL + cL^2 + d\frac{F}{e+F} + fT + gT^2 \qquad (4.6)$$

Though Atkinson et al. (2006) found that food availability had the strongest influence on *E. superba* growth, Driscoll et al. (2015) found that *T. macrura* growth was not correlated with either copepod or phytoplankton availability. Thus, I do not

include food in the model for *T. macrura* growth, and allow DGR to depend on length and temperature as

$$DGR_m(L,F,T) = a + bL - cL^2 + fT - gT^2 \tag{4.7}$$

Because *T. macrura* is distributed across a wider range of thermal environments than *E. superba* (-1.8-8 °C in contrast to -1.8-5 °C; Cuzin-Roudy et al. 2014), it is reasonable to assume that the growth of *T. macrura* will be positive at a correspondingly wide range of temperatures. Though Driscoll et al. (2015) found negative growth at temperatures <1°C, Haraldsson and Siegel (2014) inferred positive growth rates in the Lazarev Sea, where temperatures are commonly <1°C even during summer (Lal 2008). In addition, the temperature range of *T. macrura* extends into waters well below 1°C (Cuzin-Roudy et al. 2014). Thus, I explore two parameterizations of the growth curve: one where DGR is negative below 1°C (model 1), and one where it is negative below 0°C (model 2). I assume that at a given temperature, DGR is maximized at 9 mm, or about 25% of maximum size, following the pattern found for *E. superba* in the model of Atkinson et al. (2006). I further assume that DGR at this size reaches zero at 7 °C, close to the maximum temperature range of *T. macrura.* I set maximum possible to DGR to 0.12 mm/day, the maximum growth rate observed by Driscoll et al. (2015). Thus, I can solve algebraically for the coefficients in Eqn 4.7 (see Appendix 1 for details), assuming that *T. macrura* does not grow larger than 40 mm. These coefficients, along with those for *E. superba* (all age and size classes combined; Atkinson et al. 2006) can be found in Table 4.3. In

Figure 4.2 I show the relationship between DGR and temperature for model 1 and 2 at a variety of lengths, with the relationship found by Driscoll et al. for the 50th size percentile.

Wiedenmann et al. (2008) noted that when using satellite estimates of sea surface temperature and chlorophyll *a*, the growth model of Atkinson et al (2006) produces unrealistic growth curves over time, with krill in some areas growing to near asymptotic size in a year and others shrinking by >10 mm. Thus, I follow Wiedenmann et al. (2008) in assuming minimal growth in May-September for both species. While the extent to which *E. superba* alters its metabolism and feeding in the winter is debated, several authors (Torres et al. 1994, Atkinson et al. 2002) suggest that this species follows a "compromise" winter strategy, with reduced metabolism and limited, opportunistic feeding. This results in little to no growth, or even shrinkage in the winter. While there are limited data on *T. macrura* overwintering strategies, there is some evidence of depletion in the winter (Torres et al. 1994), and their winter excretion rates are low compared to other omnivorous zooplankton (Huntley and Nordhausen 1995). Taking a different approach, Haraldsson and Siegel (2014) fit an oscillating von Bertalanaffy growth curve to *T. macrura* and conclude that there is evidence of reduced growth in the winter and accelerated growth in the summer. However, it appears that *T. macrura* growth is less affected by seasonality in comparison to *E. superba* (Haraldsson and Siegel 2014, Siegel 1987). Thus, for the purposes of this model, I assume that *E. superba* growth is 0 in the non-growing season (May-September), while *T. macrura* growth is 10% of the rate calculated from

Eqn 4.7. I assume that chlorophyll *a* varies across the growing season and use concentrations approximating those found in the Polar Front by Moore and Abbott (2002; Table 4.4).

Method II: von Bertalanffy growth

The von Bertalanffy (VB; von Bertalanffy 1938) growth equation is a classic and commonly-used growth model based on simple physiological principles. It describes growth as a function of the growth coefficient *k*, the asymptotic size L_∞ such that size at time *t* is

$$L_t = L_\infty \left(1 - e^{-k(t-t_0))}\right) \qquad (4.8)$$

where t_0 is the theoretical age at which the organism has a length of zero. Note that this is equivalent to Eqn 42, with time replacing age. Because many fish populations show seasonal patterns in growth, Pauly and Gaschütz (1979) developed the oscillating VB equation

$$L_t = L_\infty \left(1 - e^{-(k(t-t_0)+Ck/2\pi)\cdot \sin 2\pi(t-t_0-t_s)}\right) \qquad (4.9)$$

where *C* describes the magnitude of seasonality and t_s describes the timing of the seasonal oscillation. Haraldsson and Siegel (2014) fit an oscillating VB model to *T. macrura* length frequencies and concluded that there was evidence of seasonal growth in this species.

Driscoll (2013) estimated the length at age for *T. macrura* sampled near the Antarctic Peninsula over four years, and found a significant positive linear relationship between mean body size and temperature at 10 m for age class 1 and age class 2 (Figure 4.3).

In order to estimate the VB growth coefficient k at different temperatures, I use these data in combination with the Ford-Walford plot (Ford 1933, Walford 1946). This method uses a rearrangement of the Von Bertalanffy growth equation to predict k using a regression of length at age $L(t+1)$ against size at age $L(t)$. Specifically, it the slope of the regression line s is related to k by

$$k = -\ln(s) \qquad (4.10)$$

I created Ford-Walford plots at a range of temperatures, using the mean size at age for classes 1, 2, and 3 predicted by the relationships found by Driscoll (2013) and assuming that size in age class 4 is 35 across all temperatures. The relationship between k (year $^{-1}$) and temperature T (C) is then

$$k(T) = 0.123T + 0.294 \qquad (4.11)$$

This is consistent with an approximation of the Metabolic Theory of Ecology (Brown et al. 2004), which describes how metabolic rates increase with temperature (see Appendix 2 for further explanation). I then use the values of C, t_0, L_∞, and t_s described by Haraldsson and Siegel (2014) to generate the oscillating VB growth trajectories of *T. macrura* at different temperatures (Table 4.5).

2. Biomass per recruit

To estimate the biomass available to predators per recruit of a particular cohort, it is necessary to follow a cohort through time, calculating its growth and mortality at each time step. I begin with R recruits at the initial timestep t=1, such that the number of individuals in the cohort N is

$$N(t)=R \text{ for } t=1 \qquad (4.12)$$

$$N(t)=N(t-1)e^{-M} \text{ for } t>1$$

The number of individuals in the cohort dying N_D is thus

$$N_D(t)=N(t-1)(1-e^{-M}) \qquad (4.13)$$

For *E. superba,* I set M=0.91 year^{-1} (0.0025 d^{-1}), an intermediate value from the range reported by Siegel and Nicol (2000). For *T. macrura*, I set M=1.08 year^{-1} (0.0030 d^{-1}), using the mean of the three mortality rates estimated above. This translates to an annual survival of about 40% for *E. superba* and 34% for *T. macrura.*

The biomass per recruit (BPR) of the cohort at time t is

$$BPR(t) = \frac{1}{R} N_D(t) \cdot \alpha L(t)^{\beta} \qquad (4.14)$$

where α and β are scaling parameters that convert length to weight (see 4.6 for

values). For sizes outside the reported length rage, I use the relationship for the nearest length. In the case of *T. macrura*, before converting to weight I convert length in terms of standard length 1 (S1; Mauchline 1980) to standard length 3 (S3; the measurement used by Färber-Lorda 1994), using the relationship described by Miller (1983):

$$S3 = \frac{S1 - 1.661}{1.16} \qquad (4.15)$$

Over the lifetime of a cohort, the total BPR is

$$BPR_{total} = \frac{1}{R} \sum_{t=1}^{t=t_{\max}} N_D(t) \cdot \alpha L(t)^{\beta} \qquad (4.16)$$

where t_{max} is the maximum age. I set R=1000 and use a timestep of one day, and assume that the *T. macrura* cohort is born on September 1, while the *E. superba* cohort is born on February 1 (Siegel 1987). I then explore BPR for each model at temperatures ranging from 0 to 5 ^{o}C, approximating the range of temperatures found in the Southwest Atlantic during summer (see Atkinson et al. 2008).

Results

Size at maturity

Of the 2,006 individuals in the sample, 22% were juveniles, 38% were males, and 40% were females. Juveniles ranged in size from 6-12 mm, mature males from 9-19 mm and mature females from 10-24 mm (4.1). Nearly all individuals appeared to be mature by 11 mm, indicating near knife-edge maturity. Average male size of 13.6 ±1.4 mm was significantly smaller the average female size of 15.7 ± 2.1 mm (Welch two-sample t-test, $p<0.01$), indicating that males may grow faster than females but reach a smaller mean size. Alternately, this pattern may be explained by higher mortality in males. Of the mature males, 96.5% had internal spermatophores visible, while 60.5% of females had unspent spermatophores and 10.6% had spent spermatophores. The vast majority (93.0%) of females were stage 2, while 4.8% were stage 1, 0.25% stage 3, and the remainder unknown. This indicates that spawning had yet to reach full intensity during the time these samples were collected.

Comparison of growth trajectories across models.

As expected, size at age for *T. macrura* increases with temperature up to 4 °C (quadratic model 1) or 3.5 °C (quadratic model 2), and declines thereafter (Figure

4.2). In contrast, VB size at age increases consistently with temperature. *E. superba* size at age decreases at temperatures over ~0.5 °C, as determined by the model of Atkinson et al. (2006) (Figure 4.3). For *T. macrura*, the effects of temperature are more pronounced at lower temperatures in the quadratic models relative to the VB model, with large differences between size at age across relatively small differences in temperature. In contrast, near the peak growth temperature differences are relatively small. The effect of seasonal differences in growth is more pronounced in the quadratic models, with faster growth in the summer and slower growth in the middle in comparison to the oscillating VB. Overall, the quadratic model shows a stronger effect of temperature on growth, with a greater range of size at age at most temperatures relative to the VB model.

Biomass per recruit

Temperature has a strong effect on BPR for all models. Between 0 and 1°C, *E. superba* BPR is at least an order of magnitude larger than *T. macrura* BPR across the lifetime of the cohort (Figure 4.5). However, at 2°C, maximum daily *T. macrura* BPR (model 1) begins to approach *E. superba* BPR, and by 3°C both model 1 and model 2 *T. macrura* BPRs are generally greater than *E. superba*, while VB *T. macrura* BPR is similar to *E. superba.* The interplay of mortality and growth is apparent in the dips in BPR during winter, as growth slows but predation remains constant. *E. superba* BPR is maximized around age 2+ (the third summer after birth), while *T. macrura* BPR is

maximized around age 1+ (the second summer after birth), suggesting the age class most available to predators may vary across these species.

Though total *T. macrura* BPR is greater than total *E. superba* BPR at higher temperatures, it does not approach the maximum total *E. superba* BPR at any temperature (Figure 4.6a). At its maximum, total *T. macrura* BPR is 36.9% (VB) or 60.3% (models 1 and 2) of maximum total *E. superba* BPR. However, the sum of total biomass available to predators (*ie* total *E. superba* BPR plus total *T. macrura* BPR) remains relatively high over a range of temperatures, while *E. superba* biomass alone drops off rapidly (Figure 4.6b). For example, for model 2, combined total BPR is greater than or equal to *E. superba* BPR up to 1.9°C, while at this temperature *E. superba* BPR alone is about two-thirds of its maximum. Thus, over this range, increasing *T. macrura* BPR can compensate for decreasing *E. superba* BPR. By 4°C, *E. superba* total BPR is virtually zero, while *T. macrura* total BPR is between 29% (VB) and 60% (model 1) of maximum *E. superba* total BPR. As temperature increases, *T. macrura* makes up an increasing fraction of the total available BRP (*i.e.* that of both species combined; Figure 4.6c). Between 2.5 and 3.1 °C *T. macrura* begins to make up the majority of the total BPR, and by 4°C the total BPR is entirely comprised of *T. macrura*.

Discussion

Size at maturity

Very little is known about the reproductive ecology of *T. macura*, perhaps due in part to its early spawning season and the difficulties of performing studies in the austral winter. However, several studies have reported some indicator of maturity at size in *T. macrura.* During summer in the Southwest Indian Ocean, Farber-Lorda (1994) classified *T. macrura* as adult or sub-adult, and defined the sub-adult size range as 8.87-16.92 mm and the adults as 17.2 mm and larger. Similarly, Mayzaud et al. (2003) reported adult specimens starting at a size of ~16 mm in the same region and season. These size ranges would be consistent with the conception of *T. macrura* life history proposed by Siegel (1987), who suggested that *T. macrura* can mature at sizes as small as 14 mm, the size class most consistent with age 2+ individuals. This is supported by Haraldsson and Siegel (2014), who classified mature males and females as age 2+ or older in the Lazarev Sea. However, in this study, I found mature individuals as small as 9 mm (males) and 10 mm (females), with nearly all individuals mature by 12 mm (Figure 4.1), indicating that near the north Antarctic Peninsula *T. macrura* may be reproducing at age 1+. This is generally consistent with the work of Nordhausen (1994), who concluded that *T. macrura* in the Gerlache Strait were likely reproducing at 13 months, though the smallest reported mature females were relatively large at 14 mm. Similarly, Marrari et al. (2011a) found mature adults as small as 12 mm in Marguerite Bay. These studies were both

conducted near the Antarctic Peninsula in the early spring (Nordhausen 1994) and fall (Marrari et al. 2011). These differing views of when *T. macrura* reaches maturity (*i.e.* age 1+ versus 2+) may be due to spatial differences in environmental conditions, with the Southwest Atlantic generally being more productive than the Southwest Indian Ocean. Alternately, reproductive characteristics may regress in the summer, making small males and females difficult to distinguish from juveniles. Age at maturity has important consequences for population dynamics; thus, future work should focus on quantifying the life history traits of *T. macrura* and their potential spatial and temporal variability.

Biomass per recruit analyses

The fate of *E. superba* in a changing ocean has been the subject of much concern. Rising temperatures, acidification, and declining sea ice are all predicted to have negative effects on this species, likely leading to altered food sources, diminished growth potential, reduced habitat, and new competitors (Flores et al. 2012a, Hill et al. 2013). In contrast, little attention has been give to the potential effects of climate change on other euphasiids such as *T. macrura*. However, as a relatively eurythermic species *T. macrura* may be able to tolerate warming better than *E. superba.* In particular, my models suggest that for some ranges of temperature increases, increased growth by *T. macrura* may be able to partially compensate for declining *E. superba* biomass on a per-recruit scale. However, it is important to note

that this increased *T. macrura* biomass may not provide the same net energy gain for many predators, even if the biomass is equivalent or greater to that of *E. superba*. In comparison to *E. superba*, *T. macrura* is smaller (Siegel 1987), less aggregated (Daly and Macaulay 1988), and often distributed deeper in the water column (Marrari et al. 2011b). These differences are relevant to predators, particularly air-breathing predators, as prey characteristics such as depth, patchiness, and density are known to affect foraging behavior (e.g. Alonzo et al. 2003, Santora et al. 2009, Benoit-Bird et al. 2013). Deeper and less-aggregated prey patches are likely to increase search and dive costs, and smaller prey may result in larger handling costs relatively to energetic gain. Thus, *T. macrura* biomass may not be energetically equivalent to equal *E. superba* biomass from the perspective of a predator.

It is also important to consider the potential effects of movement, spatial connectivity and heterogeneity over the lifetime of Antarctic euphausiids when interpreting the results of this study. Ocean currents structure the Southern Ocean and their generally eastward flow may transport krill thousands of kilometers over their lifetimes (Thorpe et al. 2007). This means that krill may experience widely variable temperatures, mortality risks, and other environmental conditions over their lifetime, and thus, the euphasiid biomass available to predators at any one location may be influenced by conditions in distant areas. For example, the large aggregations of krill at South Georgia likely originate from points west, particularly the Antarctic Peninsula area (Atkinson et al. 2001). In addition, *E. superba* is an adept swimmer and is known to migrate in response to environmental cues, with important

consequences for spatial location, growth, survival, and reproduction (Richerson et al. 2015; Chapter 2 here). Though little is known about the swimming behavior of *T. macrura,* its relatively large size suggests it is likely also be capable of directed movement. Such behavioral responses may modulate the effects of temperature on growth and risk of predation mortality.

Though I only focus on temperature in this model, other aspects of the Southern Ocean habitat are being altered by climate change. Food availability is an important predictor of *E. superba* growth, and Hill et al. (2013) note that a 50% change in primary production could have a greater effect on growth than temperature. However, the impact of climate change on primary production in the Southern Ocean remains unclear. Boyce et al. (2010) found significant reductions in phytoplankton in the Southern Ocean over the past century, and Montes-Hugo et al. (2009) reported a 12% decline in phytoplankton near the western Antarctic Peninsula (WAP) over the past 30 years. In contrast, Moreau et al. (2015) argue that climate change is increasing primary production near the WAP, and Whitehouse et al. (2008b) suggest that warming around South Georgia is likely to increase phytoplankton growth in that region. Thus, though altered primary production is likely to influence euphausiid growth, the direction and magnitude of that change remains unclear. As a more omnivorous species, *T. macrura* growth may be less affected by changes in phytoplankton relative to *E. superba.*

This study focuses on growth and does not account for the potential effects of climate change on the recruitment success and population dynamics of *E. superba* and *T. macrura.* Recruitment in *E. superba* is positively correlated with the extent and duration of sea ice the previous winter (Siegel and Loeb 1995, Atkinson et al. 2004), likely due in part to its positive effects on ice algae in the winter and spring phytoplankton blooms. Variation in ice due to El Niño Southern Oscillation (ENSO) cycles may alter spring bloom conditions, influencing *E. superba* reproduction and recruitment (Quetin and Ross 2001). Since *T. macrura* spawns in the winter, its reproductive cycle appears to be less dependent the spring bloom. Both *T. macrura* and *E. superba* abundances are correlated with measures of ENSO near the north Antarctic Peninsula, but their responses differ in some respects (Loeb and Santora 2015). Thus, future changes in climate and ice conditions are likely to affect both species, but their population responses may differ. In addition, *E. superba* is likely to be negatively affected by acidification, with egg development inhibited by decreasing pH (Kawaguchi et al. 2013), while he impact of acidification on *T. macrura* is unknown.

As *E. superba* and *T. macrura* co-occur over much of their geographic ranges, interspecific interactions between may influence the dynamics of these two populations. As an omnivore, *T. macrura* has the potential to be both a competitor with and predator on *E. superba,* particularly the egg and larval stages. Changing conditions may shift the balance between these species and interact with other environmentally-driven changes in complex ways. Like other effects of climate

change, these potential interactions are likely to be spatially variable and multifaceted.

Conclusions

Climate change is expected to have complex effects on Antarctic euphausiids and their predators. This study suggests that the available biomass of eurythermic *T. macrura* may increase as the available biomass of stenothermic *E. superba* declines. However, both species may be affected by changing primary productivity, ocean acidification, and other ecosystem changes. As the most common and widespread euphausiid in the Southern Ocean, more work remains to be done in quantifying the life history and populations dynamics of *T. macrura* and its future in a changing ocean.

Tables and Figures

Table 4.1. Classification method for staging preserved *Thysanoessa macrura.*

Stage	**Description**
Juvenile	No visible sexual characteristics
Male	Petasma visible. Internal spermatophores may be present.
Female I	Theylecum visible. Ovary is visible through carapace but does not fill the thoracic space.
Female II	Theylecum visible. Ovary is fills the carapace.
Female III	Theylecum visible. Ovary fills the carapace and the carapace appears swollen.
Female IV	Theylecum visible. Internal body cavity is empty, indicating eggs have been released.

Table 4.2. von Bertalanffy growth parameters for *Thysanoessa macrura* from the literature and estimated natural mortality from Eqn 4.5.

Source	***k* (year^{-1})**	L_∞ **(mm)**	***M* (year^{-1})**
Driscoll 2013	0.521	40	1.37
Haraldsson and Siegel 2014	0.266	45.2	0.83
Haraldsson and Siegel 2014 (oscillating)	0.312	40.6	0.84
Siegel 1987	0.432	37.5	1.04

Table 4.3. Coefficients for models predicting growth on the basis of temperature and length (*Thysanoessa macrura*) and temperature, length, and food (*Euphausia superba*).

Parameter	***T. macrura, model 1***	***T. macrura, model 2***	***E. superba***
a	-0.103	-0.0101	-0.066
b	0.00225	0.00225	0.002
c	-0.000125	-0.000125	-0.000061
d	-	-	0.385
e	-	-	0.328
f	0.107	0.0686	0.0078
g	-0.0133	-0.00980	-0.0101

Table 4.4. Monthly chlorophyll *a* concentrations across the growing season used in the growth model for *Euphausia superba.*

Month	October	November	December	January	February	March	April
Chlorophyll *a* (mg m^{-3})	0.21	0.35	0.6	0.39	0.3	0.24	0.22

Table 4.5. Parameters for the oscillating von Bertalanffy growth model from Haraldsson and Siegel (2014).

L_∞	t_s	t_0	C
40.8	0.151	0.042	0.181

Table 4.6. Parameters used in length-weight relationships.

Species	Length range	α	β	Source
E. superba	2-5	0.0470	2.121	Ikeda (1984)
E. superba	10-40	0.0072	3.021	Hofmann and Lascara (2000)
E. superba	40-60	0.0016	3.423	Hofmann and Lascara (2000)
T. macrura	8.87-16.92	0.00165	3.705	Farber-Lorda 1994
T. macrura	17.20-21.82	0.00013	4.564	Farber-Lorda 1994

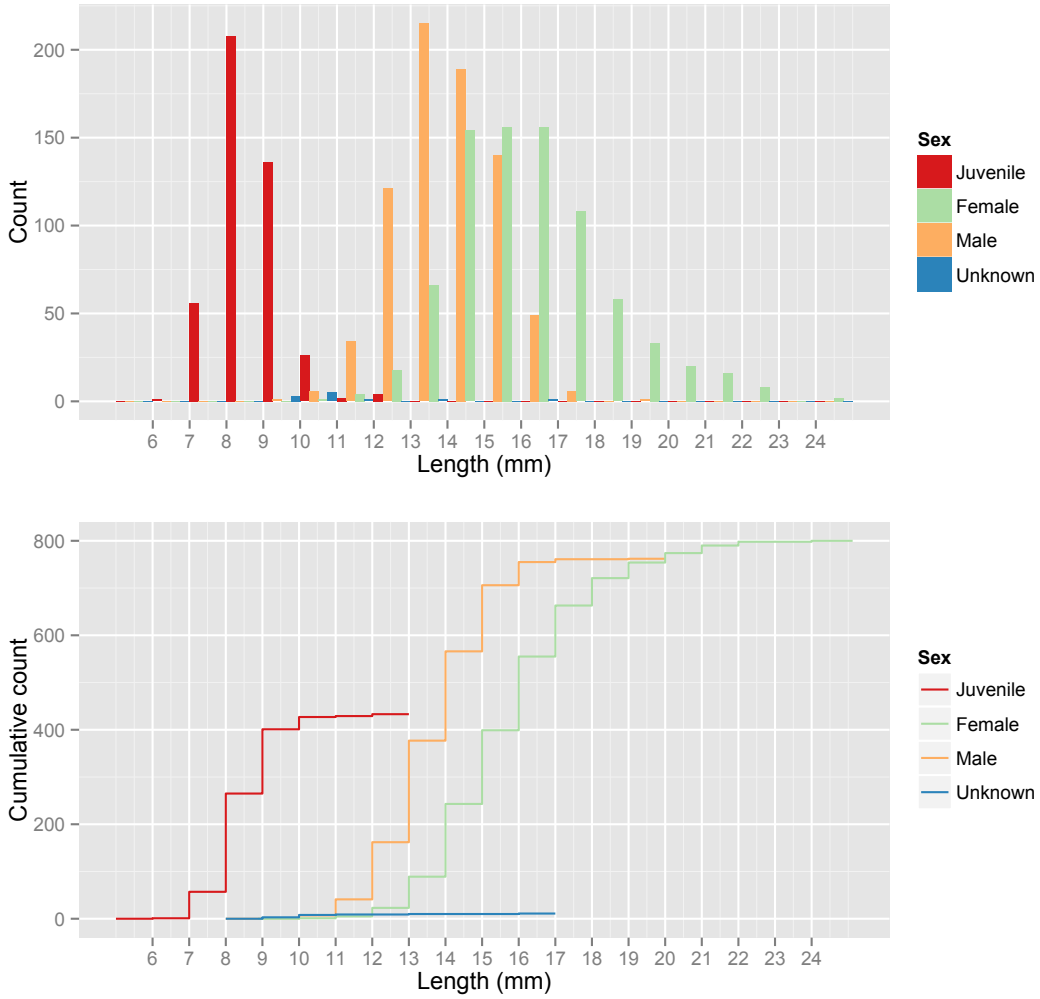

Figure 4.1. *Thysanoessa macrura* length frequencies and maturity stages. Top panel shows counts, bottom panel shows cumulative counts.

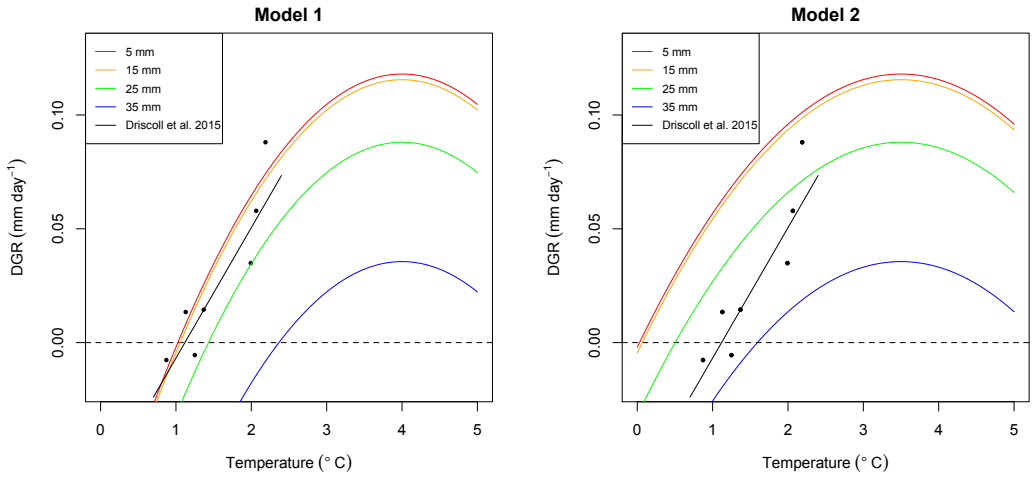

Figure 4.2. Modeled daily growth rates for *Thysanoessa macrura* across temperatures at a variety of sizes for the two quadratic models explored. Data points from Driscoll et al. (2015) show estimated daily growth rates for the 50th size percentile.

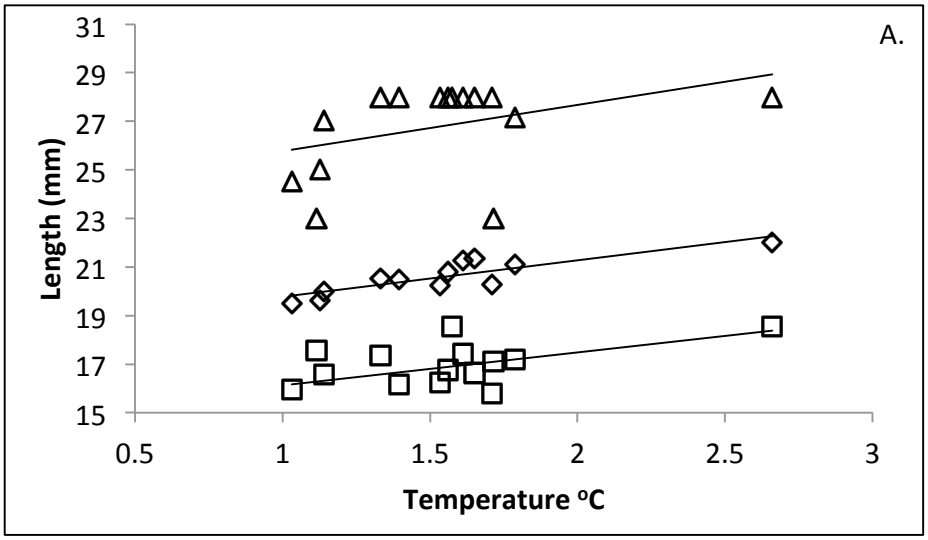

Figure 4.3. Relationships between estimated mean body length of each age and the mean water temperature at 10 m found by Driscoll et al. 2013 (reproduced with permission). Regressions between temperature and size of age class 1 (squares: R^2 = 0.290, p = 0.038, y = 1.3583x + 14.767) and age class 2 (diamonds: R^2 = 0.741, p < 0.001, y = 1.5015x + 18.273) were significant, but age class 3 (triangles: R^2 = 0.160, p = 0.139) was not significant.

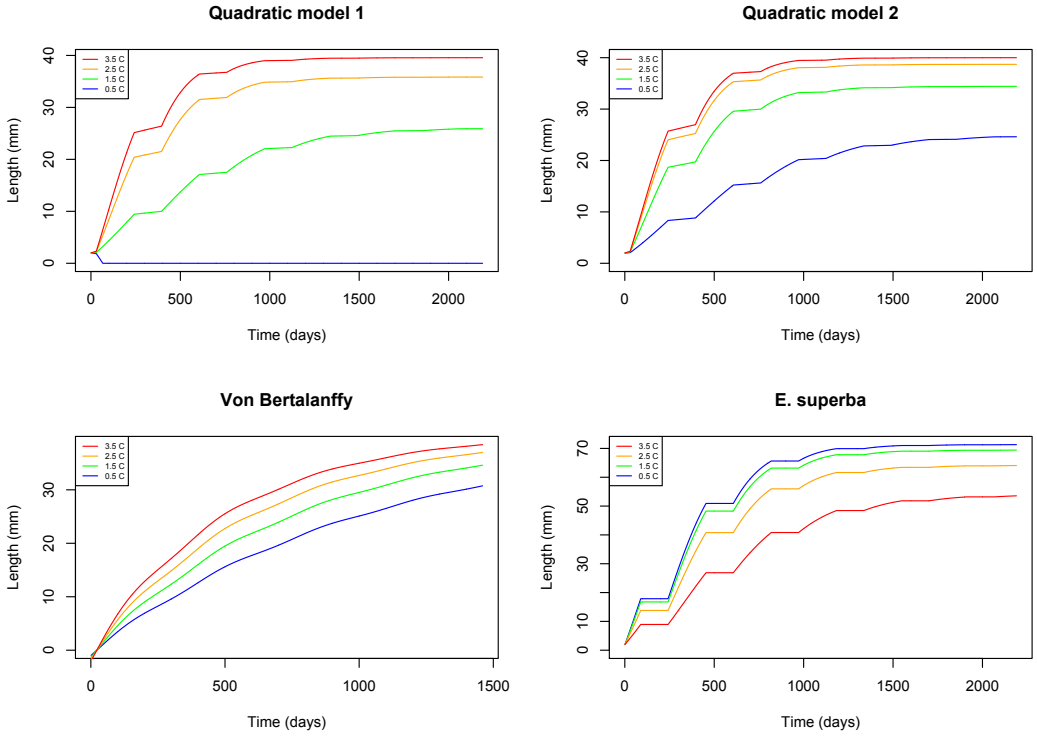

Figure 4.4. Growth trajectories at different temperatures for *Euphausia superba* and *Thysanoessa macrura* using the three different growth models explored.

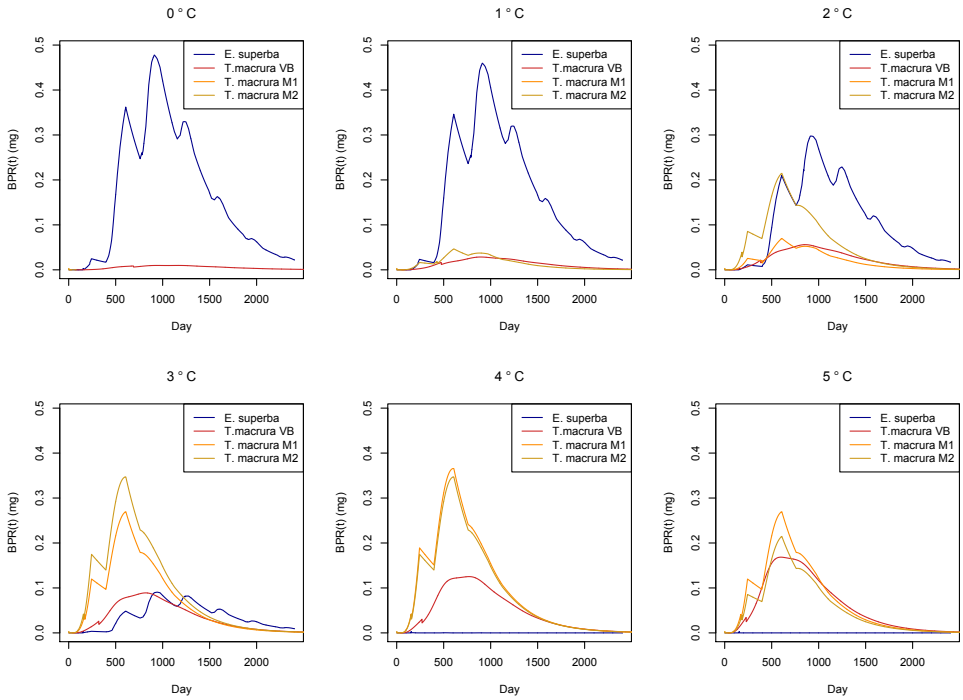

Figure 4.5. Biomass per recruit over time for *Thysanoessa macrura* and *Euphausia superba*.

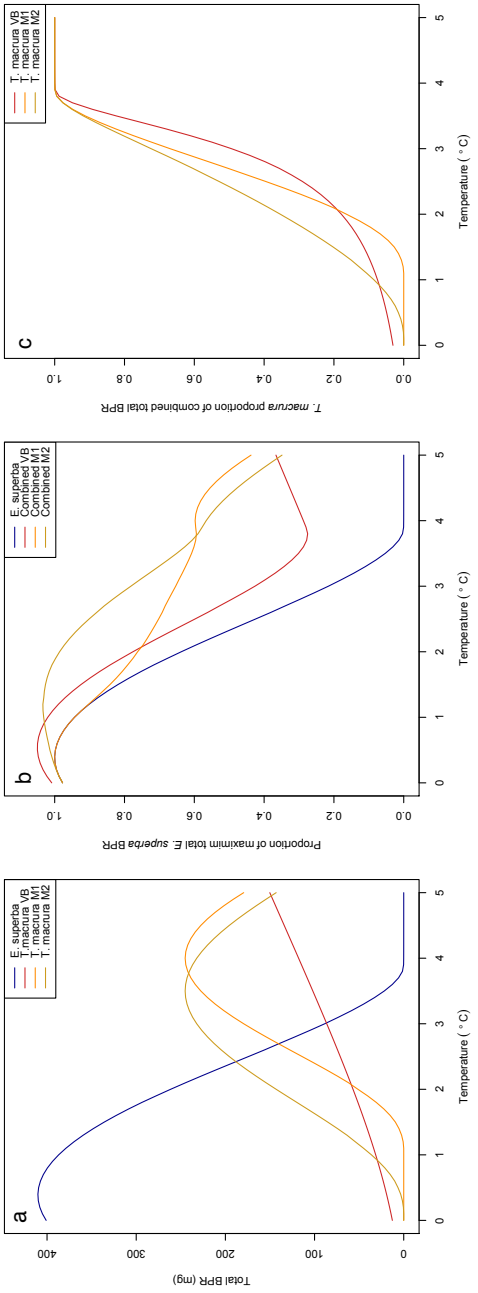

Figure 4.6. a) Total BPR for *Thysanoessa marcura* and *Euphausia superba*; b) proportion of maximum total *E. superba* BPR for both species combined; c) *T. macrura* total BPR as fraction of total BRP for both species combined.

Chapter 5. Conclusions and future directions

Further changes to the Southern Ocean ecosystem are likely inevitable. However, knowledge of the spatial and temporal dynamics of euphausiid populations and their connections to environmental conditions can inform decisionmaking and aid in ecosystem-based management. In Chapter 2, I show that active behavior by *Euphausia superba* can have important consequences for growth, mortality, reproduction, and spatial distribution. Krill movement models have traditionally treated krill as passive drifters, and therefore may not capture an important aspect of krill ecology. My results underscore the importance of accounting for krill behavior; however, before active movement can be incorporated into management models, a more complete model of predicted *E. superba* behavior may be needed. My model focuses on the summer spawning season, when krill must eat, grow, avoid predation, and reproduce under summer conditions. In contrast, krill in other seasons may be facing very different environmental conditions and selection pressures. For example, food abundance and predation may be lower and the potential for growth reduced during the winter. Data suggest that krill may move deeper in the water column and use different habitats across seasons (Lascara et al. 1999a). In addition, because many krill may be transported large distances over their lifetime, an interannual

model that accounts for differing location across years may produce a fuller picture of behavior across the lifetime of a krill. Further behavioral modeling could elucidate these seasonal and interannual movements and explore how behavior may interact with ocean currents to influence krill dynamics across years.

In Chapter 3, I use a long-term data set to explore variability in *E. superba* abundance near the North Antarctic Peninsula, and show a correlations between lagged indices of El Niño Southern Oscillation (ENSO) influence and the mean and standard deviation of krill densities. The 2-2.5 year lags indicated by these data suggest that certain environmental conditions may enhance pre-conditioning of adult krill, allowing increased spawning as well as better larval and juvenile survival. I found that abundance was linked to the degree of spatial aggregation in some habitats, indicating that both the amount and distribution of krill available to predators varies across years, which may have important implications for predator foraging success. In addition, I found that *E. superba* abundance tends decrease across the summer season, indicating that availability to predators may vary over relatively short time scales. It is still unclear whether this reduction in biomass is due to mortality, advection, or other processes. The links between short-term ENSO events, krill, and ecosystem functioning may foreshadow the potential effects of long-term changes to the Southern Ocean system (Trathan et al. 2007). Further studies should combine acoustic indices of krill abundance and spatial distribution with size-frequency data to elucidate how these changes affect predator foraging and reproductive success.

In Chapter 4, I explore how growth of the eurythermic euphausiid *Thysanoessa macrura* may change with temperature, and contrast it with *E. superba.* I find that as the biomass per recruit of *E. superba* available to predators declines with temperature above 0.5 °C, the biomass of *T. macrura* available to predators increases, at least to a point. If, as it is sometimes said, there will climate change "winners and losers", *T. macrura* may in some respects be a winner and *E. superba* a loser. If this is indeed the case, the importance of *T. macrura* in the trophodynamics of the Southern Ocean is likely to increase, but the consequences for the ecosystem are as yet unclear. The life history of *T. macrura* is still not fully described, making predictions about its population trajectory more difficult. Further study of this species, its importance to predators, and its relationship to environmental variability may allow better prediction about future changes to the Southern Ocean food web.

In conclusion, fishing, climate change and other anthropogenic forces are impacting the Southern Ocean ecosystem. As a crucial part of the food web, understanding of euphausiid dynamics and their dependence on the environment is crucial to making effective management decisions. Both modeling and data can make important contributions to our understanding of the behavior, growth, and variability of euphausiids.

Appendix 1: Results from forward simulations

Table A1: Results from forward simulations. Active krill results are in light gray rows, passive krill results are in dark gray rows. Values of Cohen's *d* less than 0.2 are considered small effect sizes, those around 0.5 medium effect sizes, and those larger than 0.8 large effect sizes (Cohen 1988).

Simulation	Start SSMU	Mean distance between passive and active krill (km)	End SSMU	Percent survival	Mean number of viable eggs produced per individual	Cohen's *d*, eggs	Mean length (mm)	Cohen's *d*, length
1	3	89.90	3	91.1	1792.1 (14.0)	176.11	48.92 (0.10)	0.45
			3	80.5	0.0		48.98 (0.17)	
2	3	58.42	3	88.2	1776.7 (18.5)	132.33	48.81 (0.13)	8.13
			1	80.1	0.0		50.04 (0.17)	
3	3	34.19	3	82.9	1868.4 (25.0)	104.89	49.44 (0.17)	5.95
			1	80.3	0.0		50.45 (0.16)	
4	1	45.84	3	88.7	1783.4 (19.7)	125.34	48.86 (0.14)	2.05
			3	80.9	0.0		48.62 (0.09)	
5	1	97.65	4	88.6	1699.9 (41.6)	56.51	48.28 (0.26)	2.80
			3	80.8	0.0		48.84 (0.10)	
6	6	114.79	6	93.6	1702.2 (15.2)	152.66	48.30 (0.11)	5.02
			6	80.9	0.0		49.43 (0.31)	
7	6	118.75	6	93.1	1715.3 (16.2)	144.95	49.39 (0.11)	0.95

			6	81.4	0.0		48.65 (0.39)	
8	6	129.96	6	93.2	1770.7 (15.6)	4.40	48.77 (0.11)	4.40
			6	92.5	1697.3 (17.6)		48.26 (0.12)	
9	6	69.57	6	92.9	1779.7 (18.2)	4.24	48.83 (0.13)	4.24
			6	93.8	1712.1 (13.3)		48.37 (0.09)	
10	3	15.97	3	93.3	1783.6 (15.7)	3.45	48.86 (0.11)	3.45
			3	93.3	1737.1 (10.7)		48.54 (0.07)	
11	3	75.97	3	92.8	1771.0 (17.5)	138.37	48.77 (0.12)	1.72
			3	80.3	0.0		49.11 (0.25)	
12	3	71.91	3	93.4	1788.1 (17.3)	141.31	48.89 (0.12)	1.27
			3	81.4	0.0		49.09 (0.19)	
13	3	10.29	3	90.3	1793.2 (15.6)	3.22	48.93 (0.11)	3.22
			3	83.9	1719.8 (28.6)		48.42 (0.20)	
14	4	59.02	4	90.0	1720.0 (17.5)	1.35	48.42 (0.12)	3.84
			4	82.5	973.3 (800.8)		47.90 (0.15)	
15	4	77.67	4	83.3	1716.9 (229.2)	10.51	48.57 (0.69)	1.17
			1	80.8	0.0		49.27 (0.49)	
16	6	136.66	6	92.2	1607.1 (67.9)	32.48	47.66 (0.22)	14.50
			6	81.6	0.0		49.94 (0.00)	
17	6	68.26	6	95.3	1689.6 (21.6)	6.07	48.19 (0.15)	1.70
			4	81.4	90.9 (386.8)		48.77 (0.48)	
18	6	55.92	7	95.1	1737.3	28.57	48.54	1.58

					(16.1)		(0.11)	
			7	87.5	4.4 (86.0)		48.38 (0.08)	
19	3	59.11	4	97.2	1688.3 (17.1)	16.79	48.20 (0.12)	16.79
			1	98.0	1430.2 (13.5)		46.42 (0.09)	
20	3	83.06	4	94.5	1755.1 (36.0)	8.07	48.66 (0.25)	8.07
			1	96.7	1546.3 (7.6)		47.22 (0.05)	
21	3	65.87	4	94.9	1762.1 (34.3)	6.35	48.71 (0.24)	6.35
			4	95.9	1604.4 (8.6)		47.62 (0.06)	
22	3	8.88	4	94.6	1751.7 (15.2)	1.54	48.64 (0.11)	1.54
			4	92.3	1731.7 (10.2)		48.50 (0.07)	
23	4	50.25	4	92.5	1717.0 (18.1)	81.35	48.40 (0.13)	2.80
			4	81.4	0.4 (24.1)		47.97 (0.07)	
24	4	30.89	4	83.0	1736.8 (152.6)	15.97	48.59 (0.66)	1.65
			4	80.3	0.0		47.81 (0.10)	
25	4	7.73	4	86.9	1771.7 (79.5)	10.83	48.79 (0.28)	3.70
			4	80.3	28.1 (217.1)		47.95 (0.16)	
26	3	68.67	4	97.0	1573.9 (14.5)	35.53	47.41 (0.10)	35.53
			1	98.0	1168.4 (7.1)		44.61 (0.05)	
27	3	73.99	4	96.9	1684.4 (20.3)	21.11	48.17 (0.14)	21.11
			1	98.0	1367.3 (6.4)		45.98 (0.04)	
28	3	61.54	4	96.2	1707.2 (20.5)	17.64	48.33 (0.14)	17.64
			1	97.8	1431.7 (8.4)		46.43 (0.06)	

29	4	32.07	4	96.7	1706.6 (28.7)	9.20	48.33 (0.20)	9.20
			1	97.2	1510.4 (9.2)		46.97 (0.06)	
30	4	40.41	4	93.6	1805.1 (57.6)	3.64	49.02 (0.16)	8.34
			4	93.8	1654.0 (11.8)		47.96 (0.08)	
31	4	65.57	4	92.2	1813.6 (104.9)	23.72	49.11 (0.11)	6.30
			4	81.2	0.0		48.14 (0.19)	
32	4	47.58	4	90.4	1808.3 (86.8)	28.65	49.06 (0.12)	7.11
			4	80.7	0.0		47.79 (0.23)	
33	4	13.86	4	89.6	1801.7 (75.6)	1.05	49.00 (0.12)	5.44
			4	82.7	1230.3 (779.5)		48.40 (0.11)	
34	4	112.86	4	90.3	1764.6 (80.1)	1.32	48.75 (0.10)	5.85
			7	86.0	1687.9 (13.6)		48.20 (0.09)	
35	1	126.40	4	97.2	1325.8 (15.1)	21.37	45.70 (0.10)	21.37
			1	97.8	1094.3 (2.5)		44.10 (0.02)	
36	1	107.77	4	97.8	1435.4 (15.6)	23.92	46.45 (0.11)	23.92
			1	97.7	1152.4 (6.2)		44.50 (0.04)	
37	1	70.23	4	97.8	1542.6 (14.4)	21.81	47.20 (0.10)	21.81
			1	97.8	1283.8 (8.6)		45.41 (0.06)	
38	1	46.94	4	97.9	1625.2 (15.5)	19.79	47.77 (0.11)	19.79
			1	97.8	1347.1 (12.5)		45.85 (0.09)	
39	4	34.17	4	97.8	1675.8 (15.7)	18.17	48.11 (0.11)	18.17

			1	97.9	1377.6 (17.1)		46.06 (0.12)	
40	4	61.31	4	93.7	1800.1 (76.0)	5.32	48.99 (0.11)	24.15
			1	98.0	1515.8 (7.4)		47.01 (0.05)	
41	4	56.49	4	93.8	1819.9 (74.6)	3.22	49.13 (0.11)	14.31
			4	95.9	1650.3 (6.4)		47.94 (0.04)	
42	4	63.04	4	92.7	1821.0 (94.1)	1.37	49.15 (0.11)	7.35
			4	91.2	1728.7 (10.2)		48.48 (0.07)	
43	4	156.74	4	93.5	1793.3 (77.8)	2.27	48.95 (0.10)	9.74
			7	91.6	1666.3 (12.7)		48.05 (0.09)	
44	1	43.56	1	98.0	1152.9 (8.7)	8.63	44.50 (0.06)	8.63
			1	97.8	1081.0 (7.9)		44.01 (0.05)	
45	1	34.96	1	98.0	1230.7 (7.0)	15.82	45.04 (0.05)	15.82
			1	97.8	1109.5 (8.3)		44.20 (0.06)	
46	1	124.80	1	98.1	1318.5 (12.2)	18.55	45.65 (0.08)	18.55
			1	97.7	1147.0 (4.7)		44.46 (0.03)	
47	1	71.42	4	97.9	1422.4 (19.0)	13.71	46.36 (0.13)	13.71
			1	97.9	1214.1 (10.1)		44.93 (0.07)	
48	1	60.32	4	97.3	1530.1 (12.1)	21.41	47.11 (0.08)	21.41
			1	98.0	1307.7 (8.4)		45.57 (0.06)	
49	4	59.91	4	97.5	1633.4 (11.2)	31.13	47.82 (0.08)	31.13
			7	97.7	1351.3 (6.2)		45.87 (0.04)	
50	4	119.41	4	95.7	1720.0	8.95	48.42	11.79

					(45.9)		(0.24)	
			7	97.7	1424.9 (9.6)		46.38 (0.07)	
51	4	168.51	4	93.6	1808.9 (78.1)	4.97	49.05 (0.15)	15.24
			7	97.5	1533.1 (13.5)		47.13 (0.09)	
52	4	57.15	7	95.6	1705.0 (15.4)	11.47	48.32 (0.11)	11.47
			1	97.8	1527.5 (15.6)		47.09 (0.11)	
53	1	65.50	1	98.0	1124.2 (11.0)	5.56	44.31 (0.08)	5.56
			1	97.7	1077.3 (4.7)		43.98 (0.03)	
54	1	47.82	1	97.5	1165.8 (13.1)	6.13	44.59 (0.09)	6.13
			1	97.6	1101.4 (7.0)		44.15 (0.05)	
55	1	26.60	1	97.8	1246.5 (9.6)	14.25	45.15 (0.07)	14.25
			1	97.9	1139.0 (4.6)		44.41 (0.07)	
56	1	98.56	1	97.8	1287.8 (15.6)	7.58	45.44 (0.11)	7.58
			1	97.6	1195.1 ()		44.80 (0.05)	
57	1	40.06	1	97.6	1364.6 (9.9)	12.63	45.97 (0.07)	12.63
			1	98.0	1225.4 (12.1)		45.01 (0.08)	
58	1	39.76	7	97.3	1446.8 (17.2)	12.19	46.53 (0.12)	12.19
			7	97.9	1293.0 (4.7)		45.47 (0.03)	
59	1	53.52	7	96.6	1549.6 (14.6)	19.26	47.24 (0.10)	19.26
			7	97.8	1308.5 (10.0)		45.58 (0.07)	
60	1	50.74	7	96.3	1598.0 (15.8)	17.84	47.58 (0.11)	17.84
			1	97.9	1332.1 (14.0)		45.74 (0.10)	

61	1	78.45	7	97.5	1604.8 (16.6)	10.81	47.62 (0.11)	10.81
			1	97.9	1420.4 (17.5)		46.35 (0.12)	

Appendix 2: Derivation of coefficients for T. macrura quadratic growth model

In the growth model of Atkinson et al. (2006), growth of *E. superba* is a quadratic function of length and temperature. I use a similar structure for the growth of *T. macrura.* In deriving coefficients for the temperature- and length-dependent *T. macrura* growth model, I make the following assumptions:

1) Maximum possible growth rate is DGR_{max}=0.12 mm day^{-1}. This is the maximum growth rate observed by Driscoll et al. (2015).
2) L_{inf}=40 mm, the asymptotic size for *T. macrura* proposed by Driscoll (2013).
3) The maximum temperature at which growth is possible (ie DGR is positive) is T_{crit}=7 °C, near the maximum temperature in the range of *T. macrura*. Thus, the temperature T_{max} where growth rate is maximized for a given size is 4 °C (model 1) or 3.5°C (model 2).
4) For a given temperature, peak growth occurs at L_{max}=9 mm, or approximately 25% of maximum size. I chose this value because *E. superba* growth is likewise maximized around 25% of maximum size according to Eqn 4.6.

Recall that a quadratic equation can be written in the form

$$y = j(x-h)^2 + k \qquad \text{(A2.1)}$$

where (h,k) is the vertex. If the intercept $(n,0)$ is known, we solve for j

$$j = \frac{-k}{(p-n)^2} \qquad \text{(A2.2)}$$

and rearrange the quadratic into the form

$$y = jx^2 - 2jhx + jh^2 + k \qquad \text{(A2.3)}$$

To solve for the parameters in Eqn 4.7, I set $T=T_{max}$, so that Eqn 4.7 becomes

$$DGR(L,T_{\max}) = cL^2 + bL + a' \qquad \text{(A2.4)}$$

where the unknown constant $a' = gT_{\max}^2 + fT_{\max} + a$. This can also be represented in vertex form as

$$DGR(L,T_{\max}) = j\left(L - L_{\max}\right)^2 + DGR_{\max} \qquad \text{(A2.5)}$$

Using the intercept $\left(L_{\inf},0\right)$ we see that

$$DGR(L,T_{\max}) = jL^2 - 2jL_{\max}L + jL_{\max}^2 + DGR_{\max} \qquad \text{(A2.6)}$$

where from Eqn A2.2 we have $j = -\dfrac{DGR_{\max}}{\left(L_{\inf} - L_{\max}\right)^2}$.

Thus, for the growth equation

$$DGR_m(L,F,T) = a + bL - cL^2 + fT - gT^2 \qquad \text{(4.5)}$$

we can see that $c = j$ and $b = -2jL_{\max}$.

Setting $L=L_{max}$ we can solve for g and f analogously using the vertex (T_{max}, DGR_{max}) and the intercept (T_{crit}, 0). We find that $g = -\frac{DGR_{\max}}{\left(T_{crit} - T_{\max}\right)^2}$ and $f = \frac{2DGR_{\max}T_{\max}}{\left(T_{crit} - T_{\max}\right)^2}$. Once b, c, f, and g are known, it is then simple to solve for a, as $a = DGR_{\max} - cL_{\max}^2 - bL_{\max} - gT_{\max}^2 - fT_{\max}$.

Appendix 3: The Metabolic Theory of Ecology

According to the Metabolic Theory of Ecology (MTE), metabolic rates depend on both organism size and temperature (Brown et al. 2004). Because metabolic reactions proceed faster at elevated temperatures, the relationship between temperature and metabolic rate is characterized by the Boltzmann factor $e^{\frac{-E_a}{k_B T}}$, where E_a is the mean activation energy of metabolism, k_B is the Boltzmann constant, and T is absolute temperature. According to the von Bertalanffy growth equation, k is a parameter describing catabolic processes. Thus, according to the MTE k may vary with ocean temperature T_C (in °C) as

$$k = k_0 \exp\left(\frac{-E_a}{k_B\left(273 + T_C\right)}\right) \qquad \text{(A3.1)}$$

where k_0 is a constant. This can be rearranged into

$$k = k_0 \exp\left(\frac{-E_a}{k_B} \cdot \frac{1}{273} \cdot \frac{1}{1 + \frac{T_C}{273}}\right) \qquad \text{(A3.4)}$$

Using the Taylor approximation $\frac{1}{1+x} \approx 1 - x$ (when x small), this then becomes

$$k \approx k_0 \exp\left(\frac{-E_a}{k_B}\left(1-\frac{T_C}{273}\right)\right) \qquad \text{(A3.5)}$$

and can be rearranged as

$$k \approx k_0 \exp\left(\frac{-E_a}{273k_B}\right)\left(1+\left(\frac{E_a}{273^2 k_B}T_C\right)\right) \qquad \text{(A3.6)}$$

Thus, k is a linear function of temperature in the same form as Eqn 4.10.

References

Ainley, D. G., C. M. Brooks, J. T. Eastman, and M. Massaro. 2012. Unnatural selection of Antarctic toothfish in the Ross Sea, Antarctica. Pages 53-75 *in* F. Huettmann, editor. Protection of the Three Poles. Springer, Tokyo, Japan.

Ainley, D. G., and D. Pauly. 2014. Fishing down the food web of the Antarctic continental shelf and slope. Polar Record **50**:92-107.

Akima, H., A. Gebhardt, T. Petzoldt, and M. Maechler. 2013. akima: Interpolation of irregularly spaced data.

Alonzo, S., and M. Mangel. 2001. Survival strategies and growth of krill: avoiding predators in space and time. Marine Ecology Progress Series **209**:203-217.

Alonzo, S., P. Switzer, and M. Mangel. 2003. Ecological games in space and time: the distribution and abundance of Antarctic krill and penguins. Ecology **84**:1598-1607.

Anscombe, F. J. 1950. Sampling theory of the negative binomial and logarithmic series distributions. Biometrika:358-382.

Arrigo, K. R., and G. L. van Dijken. 2003. Phytoplankton dynamics within 37 Antarctic coastal polynya systems. Journal of Geophysical Research: Oceans (1978–2012) **108**:3271.

Ashjian, C. J., G. A. Rosenwaks, P. H. Wiebe, C. S. Davis, S. M. Gallager, N. J. Copley, G. L. Lawson, and P. Alatalo. 2004. Distribution of zooplankton on the continental shelf off Marguerite Bay, Antarctic Peninsula, during austral fall and winter, 2001. Deep Sea Research Part II: Topical Studies in Oceanography **51**:2073-2098.

Atkinson, A., B. Meyer, D. Stuϋbing, W. Hagen, K. Schmidt, and U. Bathmann. 2002. Feeding and energy budgets of Antarctic krill Euphausia superba at the onset of winter—II. Juveniles and adults. Limnology and Oceanography **47**:953-966.

Atkinson, A., R. S. Shreeve, A. G. Hirst, P. Rothery, G. A. Tarling, D. W. Pond, R. E. Korb, E. J. Murphy, and J. L. Watkins. 2006. Natural growth rates in Antarctic krill(Euphausia superba): II. Predictive models based on food, temperature, body length, sex, and maturity stage. Limnology and Oceanography **51**:973-987.

Atkinson, A., V. Siegel, E. Pakhomov, M. Jessopp, and V. Loeb. 2009. A re-appraisal of the total biomass and annual production of Antarctic krill. Deep Sea Research Part I: Oceanographic Research Papers **56**:727-740.

Atkinson, A., V. Siegel, E. Pakhomov, and P. Rothery. 2004. Long-term decline in krill stock and increase in salps within the Southern Ocean. Nature **432**:100-103.

Atkinson, A., V. Siegel, E. Pakhomov, P. Rothery, V. Loeb, R. Ross, L. Quetin, K. Schmidt, P. Fretwell, and E. Murphy. 2008. Oceanic circumpolar habitats of Antarctic krill. Marine Ecology Progress Series **362**:1-23.

Atkinson, A., M. Whitehouse, J. Priddle, G. Cripps, P. Ward, and M. Brandon. 2001. South Georgia, Antarctica: a productive, cold water, pelagic ecosystem. Marine Ecology Progress Series **216**:279-308.

Benoit-Bird, K. J., B. C. Battaile, C. A. Nordstrom, and A. W. Trites. 2013. Foraging behavior of northern fur seals closely matches the hierarchical patch scales of prey. Mar Ecol Prog Ser **479**:283-302.

Beverton, R. 1992. Patterns of reproductive strategy parameters in some marine teleost fishes. Journal of Fish Biology **41**:137-160.

Bocher, P., Y. Cherel, and K. A. Hobson. 2000. Complete trophic segregation between South Georgian and common diving petrels during breeding at Iles Kerguelen. Marine Ecology Progress Series **208**:249-264.

Boyce, D. G., M. R. Lewis, and B. Worm. 2010. Global phytoplankton decline over the past century. Nature **466**:591-596.

Boyd, I., and A. Murray. 2001. Monitoring a marine ecosystem using responses of upper trophic level predators. Journal of Animal Ecology **70**:747-760.

Bracegirdle, T. J., W. M. Connolley, and J. Turner. 2008. Antarctic climate change over the twenty first century. Journal of Geophysical Research: Atmospheres (1984–2012) **113**.

Branch, T. A., K. Matsuoka, and T. Miyashita. 2004. Evidence for increases in Antarctic blue whales based on Bayesian modelling. Marine Mammal Science **20**:726-754.

Brierley, A. S., and M. J. Cox. 2010. Shapes of krill swarms and fish schools emerge as aggregation members avoid predators and access oxygen. Current Biology **20**:1758-1762.

Brown, J. H., J. F. Gillooly, A. P. Allen, V. M. Savage, and G. B. West. 2004. Toward a metabolic theory of ecology. Ecology **85**:1771-1789.

Buchholz, F., and R. Saborowski. 2000. Metabolic and enzymatic adaptations in northern krill, Meganyctiphanes norvegica, and Antarctic krill, Euphausia superba. Canadian Journal of Fisheries and Aquatic Sciences **57**:115-129.

CCAMLR. 1982. Text of the Convention for the Conservation of Antarctic Marine Living Resources.

Chastel, O., H. Weimerskirch, and P. Jouventin. 1993. High annual variability in reproductive success and survival of an Antarctic seabird, the snow petrel Pagodroma nivea. Oecologia **94**:278-285.

Clark, C., and M. Mangel. 2000. Dynamic state variable models in ecology. Oxford University Press, USA, New York, NY.

Clarke, A., D. K. A. Barnes, and D. A. Hodgson. 2005. How isolated is Antarctica? Trends in Ecology & Evolution **20**:1-3.

Cohen, J. 1988. Statistical power analysis for the behavioral sciences. Lawrence Erlbaum Associates, Inc., Hillsdale, NJ.

Connan, M., P. Mayzaud, C. Trouvé, C. Barbraud, and Y. Cherel. 2008. Interannual dietary changes and demographic consequences in breeding blue petrels from Kerguelen Islands. Mar Ecol Prog Ser **373**:123-135.

Constable, A., and S. Nicol. 2002. Defining smaller-scale management units to further develop the ecosystem approach in managing large-scale pelagic krill fisheries in Antarctica. Ccamlr Science **9**:117-131.

Constable, A. J. 2011. Lessons from CCAMLR on the implementation of the ecosystem approach to managing fisheries. Fish and Fisheries **12**:138-151.

Constable, A. J., J. Melbourne‐Thomas, S. P. Corney, K. R. Arrigo, C. Barbraud, D. K. Barnes, N. L. Bindoff, P. W. Boyd, A. Brandt, and D. P. Costa. 2014.

Climate change and Southern Ocean ecosystems I: how changes in physical habitats directly affect marine biota. Global change biology **20**:3004-3025.

Cox, M. J., D. A. Demer, J. D. Warren, G. R. Cutter, and A. S. Brierley. 2009. Multibeam echosounder observations reveal interactions between Antarctic krill and air-breathing predators. Marine Ecology Progress Series **378**:199-209.

Crain, C. M., K. Kroeker, and B. S. Halpern. 2008. Interactive and cumulative effects of multiple human stressors in marine systems. Ecology letters **11**:1304-1315.

Cresswell, K., G. Tarling, S. Thorpe, M. Burrows, J. Wiedenmann, and M. Mangel. 2009. Diel vertical migration of Antarctic krill (Euphausia superba) is flexible during advection across the Scotia Sea. Journal of Plankton Research **31**:1265.

Cresswell, K., J. Wiedenmann, and M. Mangel. 2008. Can macaroni penguins keep up with climate-and fishing-induced changes in krill? Polar Biology **31**:641-649.

Cresswell, K. A., G. A. Tarling, and M. T. Burrows. 2007. Behaviour affects local-scale distributions of Antarctic krill around South Georgia. Marine Ecology Progress Series **343**:193-206.

Croll, D., and B. Tershy. 1998. Penguins, fur seals, and fishing: prey requirements and potential competition in the South Shetland Islands, Antarctica. Polar Biology **19**:365-374.

Croxall, J., T. McCann, P. Prince, and P. Rothery. 1988. Reproductive performance of seabirds and seals at South Georgia and Signy Island, South Orkney Islands, 1976ñ1987: implications for Southern Ocean monitoring studies. Antarctic Ocean and resources variability:261ñ285.

Croxall, J., K. Reid, and P. Prince. 1999. Diet, provisioning and productivity responses of marine predators to differences in availability of Antarctic krill. Marine Ecology Progress Series **177**:115-131.

Cuzin-Roudy, J., J.-O. Irisson, F. Penot, S. Kawaguchi, and C. Vallet. 2014. Southern Ocean Euphausiids. Pages 309-320 *in* C. D. Broyer, P. Koubbi, H. Griffiths, B. Raymond, C. d. U. d´Acoz, A. v. d. Putte, and B. Danis, editors. Biogeographic Atlas of the Southern Ocean. The Scientific Committee on Antarctic Research, Cambridge.

Daly, K. L., and M. C. Macaulay. 1988. Abundance and distribution of krill in the ice edge zone of the Weddell Sea, austral spring 1983. Deep Sea Research Part A. Oceanographic Research Papers **35**:21-41.

De Robertis, A. 2002. Size-dependent visual predation risk and the timing of vertical migration: An optimization model. Limnology and Oceanography **47**:925-933.

De Robertis, A., C. Schell, and J. S. Jaffe. 2003. Acoustic observations of the swimming behavior of the euphausiid Euphausia pacifica Hansen. ICES Journal of Marine Science: Journal du Conseil **60**:885-898.

Deagle, B. E., N. J. Gales, K. Evans, S. N. Jarman, S. Robinson, R. Trebilco, and M. A. Hindell. 2007. Studying seabird diet through genetic analysis of faeces: a case study on macaroni penguins (Eudyptes chrysolophus). PLoS One **2**:e831.

Dietrich, K., A. V. Cise, R. Driscoll, J. Maurer, N. Sanchez, I. Bystrom, N. Ferm, G. Lemons, A. Maloney, S. Martin, and S. Romain. 2011. Zooplankton Abundance around the South Shetland Islands, Antarctica.*in* A. M. V. Cise, editor. AMLR 2009/2010 Field Season Report.

Driscoll, R. M. 2013. Inter-annual variability in the growth and life history of the Antarctic euphausiid Thysanoessa macrura. San Diego State University.

Driscoll, R. M., C. S. Reiss, and B. T. Hentschel. 2015. Temperature-dependent growth of Thysanoessa macrura: inter-annual and spatial variability around Elephant Island, Antarctica. Marine Ecology Progress Series **529**:49-61.

Ducklow, H. W., W. Fraser, D. M. Karl, L. B. Quetin, R. M. Ross, R. C. Smith, S. E. Stammerjohn, M. Vernet, and R. M. Daniels. 2006. Water-column processes in the West Antarctic Peninsula and the Ross Sea: Interannual variations and foodweb structure. Deep Sea Research Part II: Topical Studies in Oceanography **53**:834-852.

Ducklow, H. W., W. R. Fraser, M. P. Meredith, S. E. Stammerjohn, S. C. Doney, D. G. Martinson, S. F. Sailley, O. M. Schofield, D. K. Steinberg, and H. J. Venables. 2013. West Antarctic Peninsula: an ice-dependent coastal marine ecosystem in transition. Oceanography **26**:190-203.

Eicken, H. 1993. The role of sea ice in structuring Antarctic ecosystems. Polar Biology **12**:3-13.

El-Sayed, S. Z. 1978. Primary productivity and estimates of potential yields of the Southern Ocean. Pages 141-160 *in* M. McWhinnie, editor. Polar Research to the Present and Future. Westview Press, Colorado.

Falk-Petersen, S., W. Hagen, G. Kattner, A. Clarke, and J. Sargent. 2000. Lipids, trophic relationships, and biodiversity in Arctic and Antarctic krill. Canadian Journal of Fisheries and Aquatic Sciences **57**:178-191.

Färber-Lorda, J. 1994. Length-weight relationships and coefficient of condition of Euphausia superba and Thysanoessa macrura (Crustacea: Euphausiacea) in southwest Indian Ocean during summer. Marine Biology **118**:645-650.

Fielding, S., J. L. Watkins, P. N. Trathan, P. Enderlein, C. M. Waluda, G. Stowasser, G. A. Tarling, and E. J. Murphy. 2014. Interannual variability in Antarctic krill (Euphausia superba) density at South Georgia, Southern Ocean: 1997–2013. ICES Journal of Marine Science: Journal du Conseil **71**:2578-2588.

Flores, H., A. Atkinson, S. Kawaguchi, B. A. Krafft, G. Milinevsky, S. Nicol, C. Reiss, G. A. Tarling, R. Werner, and E. B. Rebolledo. 2012a. Impact of climate change on Antarctic krill.

Flores, H., J. A. Van Franeker, V. Siegel, M. Haraldsson, V. Strass, E. H. Meesters, U. Bathmann, and W. J. Wolff. 2012b. The association of Antarctic krill Euphausia superba with the under-ice habitat.

Forcada, J., P. Trathan, K. Reid, and E. Murphy. 2005. The effects of global climate variability in pup production of Antarctic fur seals. Ecology **86**:2408-2417.

Forcada, J., P. Trathan, K. Reid, E. Murphy, and J. Croxall. 2006. Contrasting population changes in sympatric penguin species in association with climate warming. Global change biology **12**:411-423.

Ford, E. 1933. An account of the herring investigations conducted at Plymouth during the years from 1924 to 1933. Journal of the Marine Biological Association of the United Kingdom (New Series) **19**:305-384.

Godlewska, M. 1996. Vertical migrations of krill (Euphausia superba Dana). Polskie Archiwum Hydrobiologii **43**:9-63.

Griffiths, H. J. 2010. Antarctic marine biodiversity–what do we know about the distribution of life in the Southern Ocean. PLoS One **5**:e11683.

Gutt, J., and V. Siegel. 1994. Benthopelagic aggregations of krill (Euphausia superba) on the deeper shelf of the Weddell Sea (Antarctic). Deep Sea Research Part I: Oceanographic Research Papers **41**:169-178.

Hagen, W., G. Kattner, A. Terbrüggen, and E. Van Vleet. 2001. Lipid metabolism of the Antarctic krill Euphausia superba and its ecological implications. Marine Biology **139**:95-104.

Hamner, W. M., and P. P. Hamner. 2000. Behavior of Antarctic krill (Euphausia superba): schooling, foraging, and antipredatory behavior. Canadian Journal of Fisheries and Aquatic Sciences **57**:192-202.

Haraldsson, M., and V. Siegel. 2014. Seasonal distribution and life history of Thysanoessa macrura (Euphausiacea, Crustacea) in high latitude waters of the Lazarev Sea, Antarctica. Marine ecology. Progress series **495**:105-118.

Hellmer, H. H., O. Huhn, D. Gomis, and R. Timmermann. 2011. On the freshening of the northwestern Weddell Sea continental shelf. Ocean Science **7**:305-316.

Hernández-León, S., A. Portillo-Hahnefeld, C. Almeida, P. Bécognée, and I. Moreno. 2001. Diel feeding behaviour of krill in the Gerlache Strait, Antarctica. Marine Ecology Progress Series **223**:235-242.

Hewitt, R., D. Demer, and J. Emery. 2003. An 8-year cycle in krill biomass density inferred from acoustic surveys conducted in the vicinity of the South Shetland Islands during the austral summers of 1991-1992 through 2001-2002. Aquatic Living Resources **16**:205-214.

Hewitt, R., G. Watters, P. Trathan, J. Croxall, M. Goebel, D. Ramm, K. Reid, W. Trivelpiece, and J. Watkins. 2004. Options for allocating the precautionary catch limit of krill among small-scale management units in the Scotia Sea. Ccamlr Science **11**:81-97.

Hijmans, R. J. 2014. raster: Geographic data analysis and modeling.

Hilborn, R., and M. Mangel. 1997. The ecological detective: confronting models with data. Princeton University Press, Princeton, NJ.

Hill, S., K. Reid, S. Thorpe, J. Hinke, and N. Fisheries. 2007. A compilation of parameters for ecosystem dynamics models of the Scotia SeañAntarctic Peninsula region. Ccamlr Science **14**:1-25.

Hill, S. L., T. Phillips, and A. Atkinson. 2013. Potential climate change effects on the habitat of Antarctic krill in the Weddell quadrant of the Southern Ocean. PLoS One **8**:e72246.

Hofmann, E. E., and Y. S. Hüsrevoğlu. 2003. A circumpolar modeling study of habitat control of Antarctic krill (Euphausia superba) reproductive success. Deep Sea Research Part II: Topical Studies in Oceanography **50**:3121-3142.

Hofmann, E. E., and C. M. Lascara. 2000. Modeling the growth dynamics oi Antarctic krill Euphausia superba. Marine Ecology Progress Series **194**:219-231.

Hofmann, E. E., and E. J. Murphy. 2004. Advection, krill, and Antarctic marine ecosystems. Antarctic Science **16**:487-499.

Houston, A., C. Clark, J. McNamara, and M. Mangel. 1988. Dynamic models in behavioural and evolutionary ecology. Nature **332**:29-34.

Hucke-Gaete, R., L. Osman, C. Moreno, and D. Torres. 2004. Examining natural population growth from near extinction: the case of the Antarctic fur seal at the South Shetlands, Antarctica. Polar Biology **27**:304-311.

Huntley, M., and W. Nordhausen. 1995. Ammonium cycling by Antarctic zooplankton in winter. Marine Biology **121**:457-467.

Ichii, T., and I. Everson. 2000. Krill harvesting. Pages 228-262 *in* I. Everson, editor. Krill: Biology, Ecology and Fisheries. Blackwell Science Ltd, Oxford.

Ikeda, T. 1984. Sequences in metabolic rates and elemental composition (C, N, P) during the development of Euphausia superba Dana and estimated food requirements during its life span. Journal of Crustacean Biology **4**:273-284.

Jiang, M., M. A. Charette, C. I. Measures, Y. Zhu, and M. Zhou. 2013. Seasonal cycle of circulation in the Antarctic Peninsula and the off-shelf transport of shelf waters into southern Drake Passage and Scotia Sea. Deep Sea Research Part II: Topical Studies in Oceanography **90**:15-30.

Jones, C. D., and D. C. Ramm. 2004. The commercial harvest of krill in the southwest Atlantic before and during the CCAMLR 2000 Survey. Deep Sea Research Part II: Topical Studies in Oceanography **51**:1421-1434.

Kanda, K., K. Takagi, and Y. Seki. 1982. Movement of the larger swarms of Antarctic krill Euphausia superba population off Enderby Land during 1976–1977 season. Journal of the Tokyo University of Fisheries **68**:25-42.

Kattner, G., W. Hagen, S. Falk-Petersen, J. Sargent, and R. Henderson. 1996. Antarctic krill Thysanoessa macrura fills a major gap in marine lipogenic pathways. Marine Ecology Progress Series **134**:295-298.

Kawaguchi, S., A. Ishida, R. King, B. Raymond, N. Waller, A. Constable, S. Nicol, M. Wakita, and A. Ishimatsu. 2013. Risk maps for Antarctic krill under projected Southern Ocean acidification. Nature Climate Change **3**:843-847.

Kawaguchi, S., R. King, R. Meijers, J. E. Osborn, K. M. Swadling, D. A. Ritz, and S. Nicol. 2010. An experimental aquarium for observing the schooling behaviour of Antarctic krill (Euphausia superba). Deep Sea Research Part II: Topical Studies in Oceanography **57**:683-692.

Kils, U. 1982. Swimming behavior, Swimming Performance and Energy Balance of Antarctic Krill Euphausia superba.

Kinzey, D., G. M. Watters, and C. S. Reiss. 2015. Selectivity and two biomass measures in an age-based assessment of Antarctic krill (Euphausia superba). Fisheries Research **168**:72-84.

Klevjer, T. A., and S. Kaartvedt. 2006. In situ target strength and behaviour of northern krill (Meganyctiphanes norvegica). ICES Journal of Marine Science: Journal du Conseil **63**:1726-1735.

Knox, G. A. 2006. Biology of the Southern Ocean. CRC Press, Taylor & Francis Group, Boca Raton, Florida, USA.

Kock, K., S. Wilhelms, I. Everson, and J. Groger. 1994. Variations in the diet composition and feeding intensity of mackerel icefish Champsocephalus gunnari at South Georgia (Antarctic). Marine Ecology Progress Series **108**:43-58.

Lal, R. 2008. Meteorology of Southern Ocean in Lazarev Sea area as revealed from observations obtained from Indian Antarctic Expeditions. Indian Journal of Marine Sciences **37**:93-98.

Lascara, C. M., E. E. Hofmann, R. M. Ross, and L. B. Quetin. 1999a. Seasonal variability in the distribution of Antarctic krill, Euphausia superba, west of the Antarctic Peninsula. Deep-sea research. Part I, Oceanographic research papers **46**:951-984.

Lascara, C. M., E. E. Hofmann, R. M. Ross, and L. B. Quetin. 1999b. Seasonal variability in the distribution of Antarctic krill, Euphausia superba, west of the Antarctic Peninsula. Deep Sea Research Part I: Oceanographic Research Papers **46**:951-984.

Lawson, G. L., P. H. Wiebe, C. J. Ashjian, S. M. Gallager, C. S. Davis, and J. D. Warren. 2004. Acoustically-inferred zooplankton distribution in relation to hydrography west of the Antarctic Peninsula. Deep Sea Research Part II: Topical Studies in Oceanography **51**:2041-2072.

Loeb, V., K. Dietrich, R. Driscoll, J. Fry, D. Krause, J. Sweeney, N. S. Puerto, M. A. Martinez, A. Ligon, and A. V. Cise. 2009a. Distribution, Abundance and Demography of Zooplankton. Pages 25-33 *in* A. V. Cise, editor. AMLR 2008/2009 Field Season Report.

Loeb, V., V. Siegel, O. Holm-Hansen, R. Hewitt, W. Fraser, W. Trivelplece, and S. Trivelplece. 1997. Effects of sea-ice extent and krill or salp dominance on the Antarctic food web. Nature **387**:897-900.

Loeb, V. J., E. E. Hofmann, J. M. Klinck, O. Holm-Hansen, and W. B. White. 2009b. ENSO and variability of the Antarctic Peninsula pelagic marine ecosystem. Antarctic Science **21**:135-148.

Loeb, V. J., and J. A. Santora. 2015. Climate variability and spatiotemporal dynamics of five Southern Ocean krill species. Progress in Oceanography **134**:93-122.

Lowe, A. T., R. M. Ross, L. B. Quetin, M. Vernet, and C. H. Fritsen. 2012. Simulating larval Antarctic krill growth and condition factor during fall and winter in response to environmental variability. Marine Ecology Progress Series **452**:27-43.

Lynnes, A. S., K. Reid, and J. P. Croxall. 2004. Diet and reproductive success of Adélie and chinstrap penguins: linking response of predators to prey population dynamics. Polar Biology **27**:544-554.

Makarov, R. 1979. Larval distribution and reproductive ecology of Thysanoessa macrura (Crustacea: Euphausiacea) in the Scotia Sea. Marine Biology **52**:377-386.

Makarov, R., and G. Denys. 1981. Stages of sexual maturity of Euphausia superba Dana. SCAR, Cambridge.

Mangel, M. 2015. Stochastic Dynamic Programming Illuminates the Link Between Environment, Physiology, and Evolution. Bulletin of Mathematical Biology **77**:857-877.

Mangel, M., and C. Clark. 1986. Towards a unified foraging theory. Ecology **67**:1127-1138.

Mangel, M., and P. Switzer. 1998. A model at the level of the foraging trip for the indirect effects of krill (Euphausia superba) fisheries on krill predators. Ecological Modelling **105**:235-256.

Marr, J. W. S. 1962. The natural history and geography of the Antarctic krill (Euphausia superba Dana). "Discovery" Reports, **32**:33-464.

Marrari, M., K. L. Daly, and C. Hu. 2008. Spatial and temporal variability of SeaWiFS chlorophyll a distributions west of the Antarctic Peninsula: Implications for krill production. Deep Sea Research Part II: Topical Studies in Oceanography **55**:377-392.

Marrari, M., K. L. Daly, A. Timonin, and T. Semenova. 2011a. The zooplankton of Marguerite Bay, western Antarctic Peninsula—Part I: Abundance, distribution, and population response to variability in environmental

conditions. Deep Sea Research Part II: Topical Studies in Oceanography **58**:1599-1613.

Marrari, M., K. L. Daly, A. Timonin, and T. Semenova. 2011b. The zooplankton of Marguerite Bay, western Antarctic Peninsula—Part II: Vertical distributions and habitat partitioning. Deep Sea Research Part II: Topical Studies in Oceanography **58**:1614-1629.

Marschoff, E. R., E. R. Barrera-Oro, N. S. Alescio, and D. G. Ainley. 2012. Slow recovery of previously depleted demersal fish at the South Shetland Islands, 1983–2010. Fisheries Research **125**:206-213.

Marshall, G. J., A. Orr, N. P. Van Lipzig, and J. C. King. 2006. The impact of a changing Southern Hemisphere Annular Mode on Antarctic Peninsula summer temperatures. Journal of Climate **19**:5388-5404.

Martin, J. H., S. E. Fitzwater, and R. M. Gordon. 1990. Iron deficiency limits phytoplankton growth in Antarctic waters. Global Biogeochemical Cycles **4**:5-12.

Mauchline, J. 1980. The Biology of Mysids and Euphausiids. Academic Press.

Meredith, M. P., and J. C. King. 2005. Rapid climate change in the ocean west of the Antarctic Peninsula during the second half of the 20th century. Geophysical Research Letters **32**:L19604.

Miller, D., and I. Hampton. 1989. Krill aggregation characteristics: spatial distribution patterns from hydroacoustic observations. Polar Biology **10**:125-134.

Miller, D. G. M. 1983. Variation in body length measurement of Euphausia superba Dana. Polar biology **2**:17-20.

Montes-Hugo, M., S. C. Doney, H. W. Ducklow, W. Fraser, D. Martinson, S. E. Stammerjohn, and O. Schofield. 2009. Recent changes in phytoplankton communities associated with rapid regional climate change along the western Antarctic Peninsula. Science **323**:1470-1473.

Moore, J. K., and M. R. Abbott. 2000. Phytoplankton chlorophyll distributions and primary production in the Southern Ocean. Journal of Geophysical Research: Oceans (1978–2012) **105**:28709-28722.

Moore, J. K., and M. R. Abbott. 2002. Surface chlorophyll concentrations in relation to the Antarctic Polar Front: seasonal and spatial patterns from satellite observations. Journal of Marine Systems **37**:69-86.

Moran, P. A. 1950. Notes on continuous stochastic phenomena. Biometrika:17-23.

Moreau, S., B. Mostajir, S. Bélanger, I. R. Schloss, M. Vancoppenolle, S. Demers, and G. A. Ferreyra. 2015. Climate change enhances primary production in the western Antarctic Peninsula. Global change biology **21**:2191-2205.

Mori, M., and D. Butterworth. 2006. A first step towards modelling the krill-predator dynamics of the Antarctic ecosystem. Ccamlr Science **13**:217-277.

Murphy, E., D. Morris, J. Watkins, and J. Priddle. 1988. Scales of interaction between Antarctic krill and the environment. Pages 120-130 *in* D. Sahrhage, editor. Antarctic Ocean and Resources Variability. Springer.

Murphy, E., S. Thorpe, J. Watkins, and R. Hewitt. 2004. Modeling the krill transport pathways in the Scotia Sea: spatial and environmental connections generating the seasonal distribution of krill. Deep Sea Research Part II: Topical Studies in Oceanography **51**:1435-1456.

Murphy, E., J. Watkins, P. Trathan, K. Reid, M. Meredith, S. Thorpe, N. Johnston, A. Clarke, G. Tarling, and M. Collins. 2007. Spatial and temporal operation of the Scotia Sea ecosystem: a review of large-scale links in a krill centred food web. Philosophical Transactions of the Royal Society B: Biological Sciences **362**:113-148.

Nemoto, T., and K. Nasu. 1958. Thysanoessa macrura as a food of baleen whales in the Antarctic. Sci Rep Whales Res Inst **13**:193-199.

Nicol, S. 2000. Understanding krill growth and aging: the contribution of experimental studies. Canadian Journal of Fisheries and Aquatic Sciences **57**:168-177.

Nicol, S. 2006. Krill, currents, and sea ice: Euphausia superba and its changing environment. Bioscience **56**:111-120.

Nicol, S., and W. de La Mare. 1993. Ecosystem management and the Antarctic krill. American Scientist **81**:36-47.

Nicol, S., W. K. De La Mare, and M. Stolp. 1995. The energetic cost of egg production in Antarctic krill (Euphausia superba Dana). Antarctic Science **7**:25-30.

Nicol, S., I. Forster, and J. Spence. 2000. Products derived from krill. Pages 262-283 Krill: Biology, Ecology and Fisheries. Blackwell Science, Oxford.

Nicol, S., and J. Foster. 2003. Recent trends in the fishery for Antarctic krill. Aquatic Living Resources **16**:42-45.

Nicol, S., J. Foster, and S. Kawaguchi. 2012. The fishery for Antarctic krill- recent developments. Fish and Fisheries **13**:30-40.

Nordhausen, W. 1992. Distribution and growth of larval and adult Thysanoessa macrura(Euphausiacea) in the Bransfield Strait Region, Antarctica. Marine ecology progress series. Oldendorf **83**:185-196.

Orr, J. C., V. J. Fabry, O. Aumont, L. Bopp, S. C. Doney, R. A. Feely, A. Gnanadesikan, N. Gruber, A. Ishida, and F. Joos. 2005. Anthropogenic ocean acidification over the twenty-first century and its impact on calcifying organisms. Nature **437**:681-686.

Orsi, A. H., T. Whitworth, and W. D. Nowlin. 1995. On the meridional extent and fronts of the Antarctic Circumpolar Current. Deep Sea Research Part I: Oceanographic Research Papers **42**:641-673.

Paradis, E., J. Claude, and K. Strimmer. 2004. APE: analyses of phylogenetics and evolution in R language. Bioinformatics **20**:289-290.

Parkinson, C., and D. Cavalieri. 2012. Antarctic sea ice variability and trends, 1979–2010. The Cryosphere **6**:871-880.

Pauly, D., and G. Gaschütz. 1979. A simple method for fitting oscillating length growth data, with a program for pocket calculators. ICES CM **6**:24.

Peck, L. S., S. A. Morley, and M. S. Clark. 2010. Poor acclimation capacities in Antarctic marine ectotherms. Marine Biology **157**:2051-2059.

Piñones, A., E. E. Hofmann, K. L. Daly, M. S. Dinniman, and J. M. Klinck. 2013. Modeling the remote and local connectivity of Antarctic krill populations along the western Antarctic Peninsula. Marine Ecology Progress Series **481**:69-92.

Plagányi, É. E., and D. S. Butterworth. 2012. The Scotia Sea krill fishery and its possible impacts on dependent predators: modeling localized depletion of prey. Ecological Applications **22**:748-761.

Pörtner, H.-O. 2010. Oxygen-and capacity-limitation of thermal tolerance: a matrix for integrating climate-related stressor effects in marine ecosystems. The Journal of experimental biology **213**:881-893.

Quetin, L., and R. Ross. 1984. Depth distribution of developing Euphausia superba embryos, predicted from sinking rates. Marine Biology **79**:47-53.

Quetin, L., and R. Ross. 2001. Environmental variability and its impact on the reproductive cycle of Antarctic krill. Integrative and Comparative Biology **41**:74.

Quetin, L., and R. Ross. 2003. Episodic recruitment in Antarctic krill Euphausia superba in the Palmer LTER study region. Marine Ecology Progress Series **259**:185-200.

Quetin, L. B., R. M. Ross, T. K. Frazer, and K. L. Haberman. 1996. Factors affecting distribution and abundance of zooplankton, with an emphasis on Antarctic krill, Euphausia superba. Pages 357-371 *in* R. M. Ross, E. E. Hofmann, and L. Quetin, editors. Foundations for Ecological Research West of the Antarctic Peninsula. American Geophysical Union, Washington.

Quetin, L. B., R. M. Ross, C. H. Fritsen, and M. Vernet. 2007. Ecological responses of Antarctic krill to environmental variability: can we predict the future? Antarctic Science **19**:253-266.

R Development Core Team. 2013. R: a language and environment for statistical computing. R Foundation for Statistical Computing. Vienna.

Reardon, J., K. Barad, J. Metcalf, I. Carbone, M. Kenney, J. L. Ohayon, D. Padilla, M. Olivera, K. Richerson, and T. Wise-West. 2013. Experiments in Collaboration: Interdisciplinary Graduate Education in Science and Justice. PLoS Biology **11**: e1001619.

Reid, K., and J. Croxall. 2001. Environmental response of upper trophic-level predators reveals a system change in an Antarctic marine ecosystem. Proceedings of the Royal Society of London. Series B: Biological Sciences **268**:377.

Reiss, C., A. Cossio, V. Loeb, and D. Demer. 2008. Variations in the biomass of Antarctic krill (Euphausia superba) around the South Shetland Islands, 1996-2006. ICES Journal of Marine Science.

Reynolds, R. W., T. M. Smith, C. Liu, D. B. Chelton, K. S. Casey, and M. G. Schlax. 2007. Daily high-resolution-blended analyses for sea surface temperature. Journal of Climate **20**:5473-5496.

Richerson, K., P. S. Levin, and M. Mangel. 2010. Accounting for indirect effects and non-commensurate values in ecosystem based fishery management (EBFM). Marine Policy **34**:114-119.

Richerson, K., G. Watters, J. Santora, I. Schroeder, and M. Mangel. 2015. More than passive drifters: a stochastic dynamic model for the movement of Antarctic krill. Marine Ecology Progress Series **529**:35-48.

Rintoul, S. R. 2007. Rapid freshening of Antarctic Bottom Water formed in the Indian and Pacific oceans. Geophysical Research Letters **34**:L06606.

Ritz, D. 2000. Is social aggregation in aquatic crustaceans a strategy to conserve energy? Canadian Journal of Fisheries and Aquatic Sciences **57**:59-67.

Ruck, K., D. Steinberg, and E. Canuel. 2014. Regional differences in quality of krill and fish as prey along the Western Antarctic Peninsula. Marine Ecology Progress Series **509**:39-55.

Saba, G. K., W. R. Fraser, V. S. Saba, R. A. Iannuzzi, K. E. Coleman, S. C. Doney, H. W. Ducklow, D. G. Martinson, T. N. Miles, and D. L. Patterson-Fraser. 2014. Winter and spring controls on the summer food web of the coastal West Antarctic Peninsula. Nature communications **5**:1-8.

Santora, J. A., C. S. Reiss, A. M. Cossio, and R. R. Veit. 2009. Interannual spatial variability of krill (Euphausia superba) influences seabird foraging behavior near Elephant Island, Antarctica. Fisheries Oceanography **18**:20-35.

Santora, J. A., W. J. Sydeman, I. D. Schroeder, C. S. Reiss, B. K. Wells, J. C. Field, A. M. Cossio, and V. J. Loeb. 2012. Krill space: a comparative assessment of mesoscale structuring in polar and temperate marine ecosystems. ICES Journal of Marine Science: Journal du Conseil **69**:1317-1327.

Santora, J. A., and R. R. Veit. 2013. Spatio-temporal persistence of top predator hotspots near the Antarctic Peninsula. Marine Ecology Progress Series **487**:287-304.

Schmidt, K., A. Atkinson, S. Steigenberger, S. Fielding, M. Lindsay, D. W. Pond, G. A. Tarling, T. A. Klevjer, C. S. Allen, and S. Nicol. 2011. Seabed foraging by Antarctic krill: Implications for stock assessment, bentho-pelagic coupling, and the vertical transfer of iron. Limnology and Oceanography **56**:1411-1428.

Schmidtko, S., K. J. Heywood, A. F. Thompson, and S. Aoki. 2014. Multidecadal warming of Antarctic waters. Science **346**:1227-1231.

Sedwick, P. N., and G. R. DiTullio. 1997. Regulation of algal blooms in Antarctic shelf waters by the release of iron from melting sea ice. Geophysical Research Letters **24**:2515-2518.

Siegel, V. 1987. Age and growth of Antarctic Euphausiacea (Crustacea) under natural conditions. Marine Biology **96**:483-495.

Siegel, V. 1988. A concept of seasonal variation of krill (Euphausia superba) distribution and abundance west of the Antarctic Peninsula. Pages 219-230 Antarctic Ocean and resources variability. Springer-Verlag, Berlin.

Siegel, V. 1992. Assessment of the krill (Euphausia superba) spawning stock off the Antarctic Peninsula. Archiv fur Fischereiwissenschaft **41**:101-130.

Siegel, V. 2000. Krill (Euphausiacea) demography and variability in abundance and distribution. Canadian Journal of Fisheries and Aquatic Sciences **57**:151-167.

Siegel, V. 2005. Distribution and population dynamics of Euphausia superba: summary of recent findings. Polar Biology **29**:1-22.

Siegel, V., and V. Loeb. 1995. Recruitment of Antarctic krill Euphausia superba and possible causes for its variability. Marine Ecology Progress Series **123**:45-56.

Siegel, V., and S. Nicol. 2000. Population parameters. Pages 103-149 *in* I. Everson, editor. Krill biology, ecology and fisheries. Blackwell Science, Oxford, UK.

Smetacek, V., and S. Nicol. 2005. Polar ocean ecosystems in a changing world. Nature **437**:362-368.

Smith, W. O., and D. M. Nelson. 1985. Phytoplankton bloom produced by a receding ice edge in the Ross Sea: spatial coherence with the density field. Science **227**:163-166.

Stammerjohn, S., D. Martinson, R. Smith, X. Yuan, and D. Rind. 2008a. Trends in Antarctic annual sea ice retreat and advance and their relation to El Niño–Southern Oscillation and Southern Annular Mode variability. Journal of Geophysical Research: Oceans (1978–2012) **113**.

Stammerjohn, S., D. Martinson, R. Smith, X. Yuan, and D. Rind. 2008b. Trends in Antarctic annual sea ice retreat and advance and their relation to El Niño–Southern Oscillation and Southern Annular Mode variability. Journal of Geophysical Research: Oceans (1978–2012) **113**:C03S90.

Steinberg, D. K., K. E. Ruck, M. R. Gleiber, L. M. Garzio, J. S. Cope, K. S. Bernard, S. E. Stammerjohn, O. M. Schofield, L. B. Quetin, and R. M. Ross. 2015. Long-term (1993–2013) changes in macrozooplankton off the Western Antarctic Peninsula. Deep Sea Research Part I: Oceanographic Research Papers **101**:54-70.

Strand, S. W., and W. M. Hamner. 1990. Schooling behavior of Antarctic krill (Euphausia superba) in laboratory aquaria: Reactions to chemical and visual stimuli. Marine Biology **106**:355-359.

Sudre, J., C. Maes, and V. Garçon. 2013. On the global estimates of geostrophic and Ekman surface currents. Limnology and Oceanography: Fluids and Environments **3**:1-20.

Swadling, K., D. Ritz, S. Nicol, J. Osborn, and L. Gurney. 2005. Respiration rate and cost of swimming for Antarctic krill, Euphausia superba, in large groups in the laboratory. Marine Biology **146**:1169-1175.

Tarling, G. A., and S. E. Thorpe. 2014. Instantaneous movement of krill swarms in the Antarctic Circumpolar Current. Limnology and Oceanography **59**:872-886.

Thompson, A. F., K. J. Heywood, S. E. Thorpe, A. H. Renner, and A. Trasvi√¯±a. 2009a. Surface Circulation at the Tip of the Antarctic Peninsula from Drifters. Journal of Physical Oceanography **39**.

Thompson, A. F., K. J. Heywood, S. E. Thorpe, A. H. Renner, and A. Trasvi√¯±a. 2009b. Surface Circulation at the Tip of the Antarctic Peninsula from Drifters. Journal of Physical Oceanography **39**:3-26.

Thompson, D. W., S. Solomon, P. J. Kushner, M. H. England, K. M. Grise, and D. J. Karoly. 2011. Signatures of the Antarctic ozone hole in Southern Hemisphere surface climate change. Nature Geoscience **4**:741-749.

Thorpe, S., K. Heywood, D. Stevens, and M. Brandon. 2004. Tracking passive drifters in a high resolution ocean model: implications for interannual variability of larval krill transport to South Georgia. Deep Sea Research Part I: Oceanographic Research Papers **51**:909-920.

Thorpe, S., E. Murphy, and J. Watkins. 2007. Circumpolar connections between Antarctic krill (Euphausia superba Dana) populations: investigating the roles of ocean and sea ice transport. Deep Sea Research Part I: Oceanographic Research Papers **54**:792-810.

Torres, J. J., J. Donnelly, T. L. Hopkins, T. Lancraft, A. Aarset, and D. Ainley. 1994. Proximate composition and overwintering strategies of Antarctic micronektonic Crustacea. Marine Ecology-Progress Series **113**:221.

Trathan, P., J. Forcada, and E. Murphy. 2007. Environmental forcing and Southern Ocean marine predator populations: effects of climate change and variability.

Philosophical Transactions of the Royal Society B: Biological Sciences **362**:2351-2365.

Trathan, P., J. Priddle, J. Watkins, D. Miller, and A. Murray. 1993. Spatial variability of Antarctic krill in relation to mesoscale hydrography. Marine Ecology Progress Series **98**:61-71.

Trathan, P. N., A. S. Brierley, M. A. Brandon, D. G. Bone, C. Goss, S. A. Grant, E. J. Murphy, and J. L. Watkins. 2003. Oceanographic variability and changes in Antarctic krill (Euphausia superba) abundance at South Georgia. Fisheries Oceanography **12**:569-583.

Trivelpiece, W. Z., J. T. Hinke, A. K. Miller, C. S. Reiss, S. G. Trivelpiece, and G. M. Watters. 2011. Variability in krill biomass links harvesting and climate warming to penguin population changes in Antarctica. Proceedings of the National Academy of Sciences **108**:7625-7628.

Turner, J., R. Bindschadler, P. Convey, G. Di Prisco, E. Fahrbach, J. Gutt, D. Hodgson, P. Mayewski, and C. Summerhayes. 2009. Antarctic climate change and the environment.

von Bertalanffy, L. 1938. A quantitative theory of organic growth (inquiries on growth laws. II). Human biology **10**:181-213.

Walford, L. A. 1946. A new graphic method of describing the growth of animals. Biological Bulletin:141-147.

Watkins, J., F. Buchholz, J. Priddle, D. Morris, and C. Ricketts. 1992. Variation in reproductive status of Antarctic krill swarms; evidence for a size-related sorting mechanisms? Marine Ecology Progress Series **82**:163-174.

Watters, G., S. Hill, J. Hinke, J. Matthews, and K. Reid. 2013. Decision-making for ecosystem-based management: evaluating options for a krill fishery with an ecosystem dynamics model. Ecological Applications **23**:710-725.

Watters, G., J. Hinke, and S. Hill. 2008. A risk assessment to advise on strategies for subdividing a precautionary catch limit among small-scale management units during Stage 1 of the staged development of the krill fishery in Subareas 48.1, 48.2, and 48.3. WG-EMM-08/30. Available from George. Watters@ noaa. gov.

Watters, G. M., S. Hill, J. T. Hinke, and P. Trathan. 2009. The risks of not deciding to allocate the precautionary krill catch limit among SSMUs and allowing uncontrolled expansion of the krill fishery up to the trigger level. . CCAMLR document WG-EMM-09/12.

Watters, G. M., H. J.T., K. Reid, and S. Hill. 2005. A krill-predator-fishery model for evaluating candidate management procedures. CCAMLR document WG-EMM-05/13.16

Watters, G. M., H. J.T., K. Reid, and S. Hill. 2006. KPFM2, be careful what you ask for – you just might get it. CCAMLR document WG-EMM-06/22.18.

White, J. W., A. Rassweiler, J. F. Samhouri, A. C. Stier, and C. White. 2014. Ecologists should not use statistical significance tests to interpret simulation model results. Oikos **123**:385-388.

Whitehouse, M., M. Meredith, P. Rothery, A. Atkinson, P. Ward, and R. Korb. 2008a. Rapid warming of the ocean around South Georgia, Southern Ocean, during the 20th century: forcings, characteristics and implications for lower trophic levels. Deep Sea Research Part I: Oceanographic Research Papers **55**:1218-1228.

Whitehouse, M. J., M. P. Meredith, P. Rothery, A. Atkinson, P. Ward, and R. E. Korb. 2008b. Rapid warming of the ocean around South Georgia, Southern Ocean, during the 20th century: Forcings, characteristics and implications for lower trophic levels. Deep Sea Research Part I: Oceanographic Research Papers **55**:1218-1228.

Wiebe, P. H., C. J. Ashjian, G. L. Lawson, A. Piñones, and N. J. Copley. 2011. Horizontal and vertical distribution of euphausiid species on the Western Antarctic Peninsula US GLOBEC Southern Ocean study site. Deep Sea Research Part II: Topical Studies in Oceanography **58**:1630-1651.

Wiedenmann, J., K. Cresswell, and M. Mangel. 2008. Temperature-dependent growth of Antarctic krill: predictions for a changing climate from a cohort model. Marine Ecology Progress Series **358**:191-202.

Wiedenmann, J., K. Cresswell, and M. Mangelb. 2009. Connecting recruitment of Antarctic krill and sea ice. Limnol. Oceanogr **54**:799-811.

Wiedenmann, J., K. A. Cresswell, J. Goldbogen, J. Potvin, and M. Mangel. 2011. Exploring the effects of reductions in krill biomass in the Southern Ocean on blue whales using a state-dependent foraging model. Ecological Modelling **222**:3366-3379.

Williams, R. 1985. Trophic relationships between pelagic fish and euphausiids in Antarctic waters. Pages 452-459 Antarctic nutrient cycles and food webs. Springer.

Wright, S. W., R. L. van den Enden, I. Pearce, A. T. Davidson, F. J. Scott, and K. J. Westwood. 2010. Phytoplankton community structure and stocks in the Southern Ocean (30–80 E) determined by CHEMTAX analysis of HPLC pigment signatures. Deep Sea Research Part II: Topical Studies in Oceanography **57**:758-778.

Zwally, H. J., J. C. Comiso, C. L. Parkinson, W. J. Campbell, and F. D. Carsey. 1983. Antarctic sea ice, 1973-1976: Satellite passive-microwave observations. NASA, Washington, DC.